

## Durham E-Theses

---

### *Investigation into the strength, toughness and porosity of barium titanate PTC ceramics*

Blamey, Jonathan M.

#### How to cite:

---

Blamey, Jonathan M. (1990) *Investigation into the strength, toughness and porosity of barium titanate PTC ceramics*, Durham theses, Durham University. Available at Durham E-Theses Online:  
<http://etheses.dur.ac.uk/6627/>

#### Use policy

---

The full-text may be used and/or reproduced, and given to third parties in any format or medium, without prior permission or charge, for personal research or study, educational, or not-for-profit purposes provided that:

- a full bibliographic reference is made to the original source
- a [link](#) is made to the metadata record in Durham E-Theses
- the full-text is not changed in any way

The full-text must not be sold in any format or medium without the formal permission of the copyright holders.

Please consult the [full Durham E-Theses policy](#) for further details.

---

Academic Support Office, Durham University, University Office, Old Elvet, Durham DH1 3HP  
e-mail: [e-theses.admin@dur.ac.uk](mailto:e-theses.admin@dur.ac.uk) Tel: +44 0191 334 6107  
<http://etheses.dur.ac.uk>

The copyright of this thesis rests with the author.  
No quotation from it should be published without  
his prior written consent and information derived  
from it should be acknowledged.

## **Title**

**Investigation into the Strength, Toughness & Porosity of Barium Titanate PTC Ceramics.**

## **Sub-Title**

The effect of processing variables on the Strength and Toughness of n-doped Barium Titanate PTC Ceramics has been investigated. Fracture Toughness,  $K_{IC}$ , has been measured using an indentation technique and a more conventional notched beam specimen geometry. Strength, measured by pure bending of a beam and diametral compression of flat circular specimens has been related to material toughness in terms of the material porosity introduced by processing.

A Thesis submitted to the University of Durham  
for the degree of  
Master of Science  
by  
Jonathan M. Blamey

School of Engineering and Applied Science

October 1990



17 OCT 1991

## SUMMARY

The effect of processing conditions on the mechanical and electrical properties of Holmium doped Barium Titanate Positive Temperature Coefficient of Resistance (PTC) Ceramics has been investigated. Strength was evaluated using Diametral Compression of discs of material and Four-Point Bending of beam specimens. Fracture toughness was evaluated by the loading of notched beams under Four-Point Bending. An indentation technique for estimating fracture toughness was also investigated using a Vickers pyramid indenter. It was shown to provide results 50% higher than beam tests for materials with a fracture toughness in the range of 0.6 to 1.0 MPam<sup>1/2</sup>. However, refinements to the technique, by recording the onset of crack growth were made, which resulted in increased correlation.

The processing variables which caused the largest change in material properties was found to be the use of laboratory calcined material which resulted in an increase in mechanical strength from 30 to 70MPa. This was interpreted as being as a result of reduced porosity as fracture toughness values were unchanged at 0.95MPam<sup>1/2</sup>. It also provided a reduction in the PTC effect of 1 decade. The effect of binders and die lubricants was to provide a large increase in both mechanical strength and fracture toughness. Diametral Compression was also conducted on "green" pellets to assess the influence of pellet aspect ratio and powder properties as well as die pressures used. A reduction in the pressing speed showed how the strength of the "green" pellets could be substantially improved by over 100%. Production and research processing routes were compared under mechanical and electrical testing and extensive work was performed using different sintering atmospheres. The most detrimental effect of a non-oxidising atmosphere was a 1 decade reduction in PTC effect and 50% reduction in strength and toughness.

### Acknowledgements

Thanks must go to the following people without whom this work could not have taken place.

Dr. Tom Parry for the overseeing of the project as my supervisor, his advice on all things mechanical and his help in the discussion on the manuscript.

Jenny Illingsworth helped me extensively in the preparation and electrical testing of the ceramics as well as the theory of PTC Devices.

Dr. Haider Al-Allak for his help on the theory of electrical ceramics and encouragement throughout the project.

Also my gratitude must be extended to Peter Thomson and Peter Dodd of Elmwood Sensors Ltd. for their generous funding of the projects, the samples which I required from the production facility and the round table discussions which helped a great deal. Dr. Andy Brinkman and Prof. John Woods also helped by steering me towards the correct areas of research.

## CONTENTS

1.0	Introduction	1
1.1	Project Objectives	6
2.0	Theory	7
2.1	PTC Theory	7
2.2	Thermal Stresses	10
2.2.1	Residual Stresses	11
2.2.2	Temperature Related Studies	11
2.3	Mechanical Strength	14
2.3.1	Porosity	14
2.3.2	Testing Mechanical Strength	15
2.3.3	Testing Fracture Toughness	19
2.4	Preparation Theory	27
2.4.1	Milling Process	27
2.4.2	Pressing Stage	28
2.4.3	Sintering	31
3.0	Materials	35
3.1	Materials : Part I	35
3.2	Lower Purity Material	40
3.3	Materials : Part II	41
3.3.1	Mix 1	41
3.3.2	Mix 2	42
3.3.3	Mixes 3 & 4	42
3.4	Differences in the processing of the Production and Research Facilities	44
3.4.1	Milling	44

3.4.2	Additives	44
3.4.3	Pressing	45
3.4.4	Sintering	45
4.0	Method	47
4.1	Electrical Testing	47
4.2	Mechanical Testing	49
4.2.1	Diametral Compression	49
4.2.2	Loaded Beam Tests	53
4.2.3	The Vickers Indentor	56
4.2.4	Testing of unsintered compacts	59
4.2.5	Scanning Electron Microscopy	59
5.0	Results	61
5.1	Part I : Initial Mechanical Tests	61
5.2	Part II : Mechanical Tests on samples sintered in different gaseous atmospheres	65
5.3	Electrical Characteristics of samples sintered in different gaseous atmospheres	85
5.4	Microstructure	95
6.0	Discussion	100
6.1	Part I of the Study	100
6.2	Mechanical Studies of Part II of the Project	106
6.3	Electrical Studies of Part II of the Project	123
6.4	Future Work	126
7.0	Conclusions	128
	References	131
	Appendix I	134

## List of Figures

- 1 Standard Resistance-Temperature Plot for a Barium Titanate PTC Device
- 2(abc) Resistance-Temperature Plots for different PTC Devices
- 3 The Perovskite Crystal Structure
- 4 The Atomic Positions in Tetragonal  $\text{BaTiO}_3$
- 5 The Dipoles and Domains
- 6 The Resistivities through the granular structure
- 7(ab) The Bending Moments in 3 and 4-Point Bending
- 8 The Diametral Compression Test
- 9 Stresses in the Vicinity of an Elliptical Crack
- 10 The Modes of extension of a Crack
- 11(ab) Schematic Diagram of the Vickers Indentation
- 12 Abnormal Grain Growth in Barium Titanate Ceramics
- 13 The Durham Sintering Temperature Profile
- 14 Sintering Temperature Profiles for Durham and Elmwood
- 15a Resistance-Temperature for an Elmwood Production PTC
- 15b The Effect of Temperature on the Dielectric Constant of Barium Titanate
- 16 Beam Preparation from Sintered Discs
- 17 The Four-Point Bend Test Arrangement
- 18 The Sample Groups used in Part I of the Study
- 19 Values of Porosity for sintered material investigated in Part I of the Study
- 20 Values of UTS obtained by Diametral Compression of sintered material investigated in Part I of the Study



- 21 The Sample Groups used in Part IIa of the Study
- 22 Porosity in the "green" and sintered pellets for the  
Mixes used in Part IIa of the Study
- 23 UTS for the "green" pellets of the Mixes used in  
Part IIa of the Study
- 24 UTS for the sintered pellets of the Mixes used in  
Part IIa of the Study
- 25 A plot of the porosity in the "green" pellet against  
pressing pressure for Mix 4
- 26 The sintering atmospheres used for each of the Mixes
- 27 Values of porosity for the 13mm pellets sintered in  
different sintering atmospheres
- 28 Values of porosity for the 39mm pellets...
- 29 Values of porosity for the 5.1mm pellets...
- 30 Values of UTS obtained from Diametral Compression and  
Bend Tests on specimens sintered in different gaseous  
atmospheres
- 31 Values of Fracture Toughness obtained from notched four-  
point bend tests of beams sintered in different gaseous  
atmospheres
- 32 Values of Fracture Toughness obtained from notched four-  
point bend tests of beams and Vickers indentation  
techniques
- 33 The Vickers indentation test specimens
- 34 Resistance Temperature plots for Mixes 1,2,3 & 4  
sintered in 80% N<sub>2</sub> 20% O<sub>2</sub>
- 35 Resistance-Temperature plots for Mixes 1,2,3 & 4

- sintered in 100% N<sub>2</sub>
- 36 Resistance-Temperature plots for Mixes 1,2,3 & 4  
sintered in 100% N<sub>2</sub> and annealed in air
- 37 Resistance-Temperature plots for Mixes 1,2,3 & 4  
sintered in 60% N<sub>2</sub> 40% O<sub>2</sub>
- 38 Resistance-Temperature plots for Mixes 1,2,3 & 4  
sintered in 40% N<sub>2</sub> 60% O<sub>2</sub>
- 39 Resistance-Temperature plots for Mixes 1,2,3 & 4  
sintered in 20% N<sub>2</sub> 80% O<sub>2</sub>
- 40 Resistance-Temperature plots for Mixes 1,2,3 & 4  
sintered in 100% O<sub>2</sub>
- 41 Resistance-Temperature plots for Mixes 3 & 4 sintered  
in different furnaces
- 42 The effect of sintering atmosphere on grain size & shape
- 43 The microstructure of the Mixes sintered in air
- 44 The microstructure of the Mixes sintered in 100% N<sub>2</sub>
- 45 The microstructure of the Mixes sintered in 100% O<sub>2</sub>
- 45a Cracking within samples, involving Blistering
- 46 The critical defect sizes to cause failure in specimens  
under Diametral Compression and Bend Tests
- 47 The forces to which a compact are subjected
- 48 The shrinkage of Barium Titanate pellets
- 49 The effect of porosity on UTS for Mixes 1-4
- 50 The microstructure of the material made from Cookson  
"low purity" Barium Titanate
- 51 The pre-cracking caused by the act of machining beams

## SYMBOLS

$P$	Load
$a_I$	Distance from beam support to load
$a$	Crack length
$a_c$	Critical crack length
$H$	Vickers hardness
$K$	Stress intensity factor
$K_I$	Stress intensity factor for Mode I crack extension
$K_C$	Critical stress intensity factor
$K_{IC}$	Fracture toughness
$\sigma$	Tensile stress
$\sigma_f$	Failure stress
$\tau$	Shear stress
$E$	Young's modulus
$\phi$	Shape parameter used in Vickers indentation tests
$\psi$	Shape parameter used in notched-beam tests
$b$	Beam width
$d$	Beam depth
$d_I$	Disc diameter
$t$	Disc thickness
$F_R$	Radial force acting on a compact
$F_A$	Axial force acting on a compact
$\nu$	Poisson's ratio

## 1.0 INTRODUCTION

Barium Titanate is currently used both as a dielectric and a PTC device in its doped state. Its applications as a PTC include motor protection devices, heating elements and temperature sensors.

For optimum performance each of these applications requires different electrical properties, which are normally referenced by a Resistivity-Temperature (R-T) plot of the material. The standard resistance-temperature plot for a PTC material such as Barium Titanate often approximates to the Figure 1. The PTC region is often described to be the part of the graph where the resistivity value is increasing with temperature. Points  $T_a$  and  $T_b$  may be estimated as the extents of this region. The point at which the maximum gradient occurs is referred to as  $T_c$ , the Curie Point or Curie Temperature. The maximum gradient of the curve within the PTC region is often used to specify a particular device and is normally expressed as the percentage resistivity change corresponding to a one degree temperature rise. In addition the total resistivity change over the PTC region,  $\Delta R$  is often quoted.

Over-Temperature Protection Devices require an R-T plot with a steep gradient as well as the ability to accurately reproduce a switching temperature on each component (Figure 2a). This form of PTC device is used extensively in electric motors and



**Figure 1 : Standard Resistance-Temperature Plot  
for a Barium Titanate PTC Device**

Resistance (ohm)

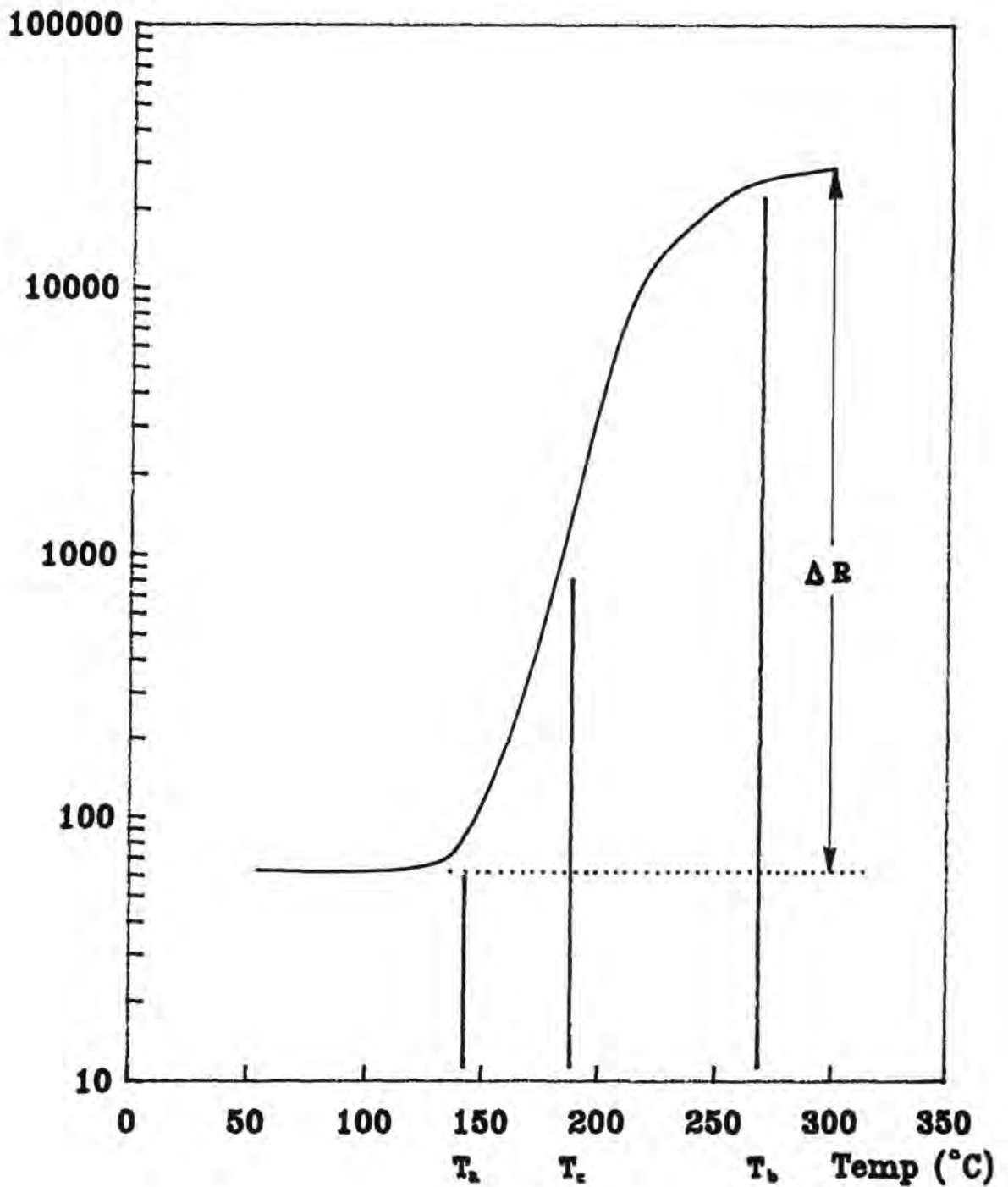
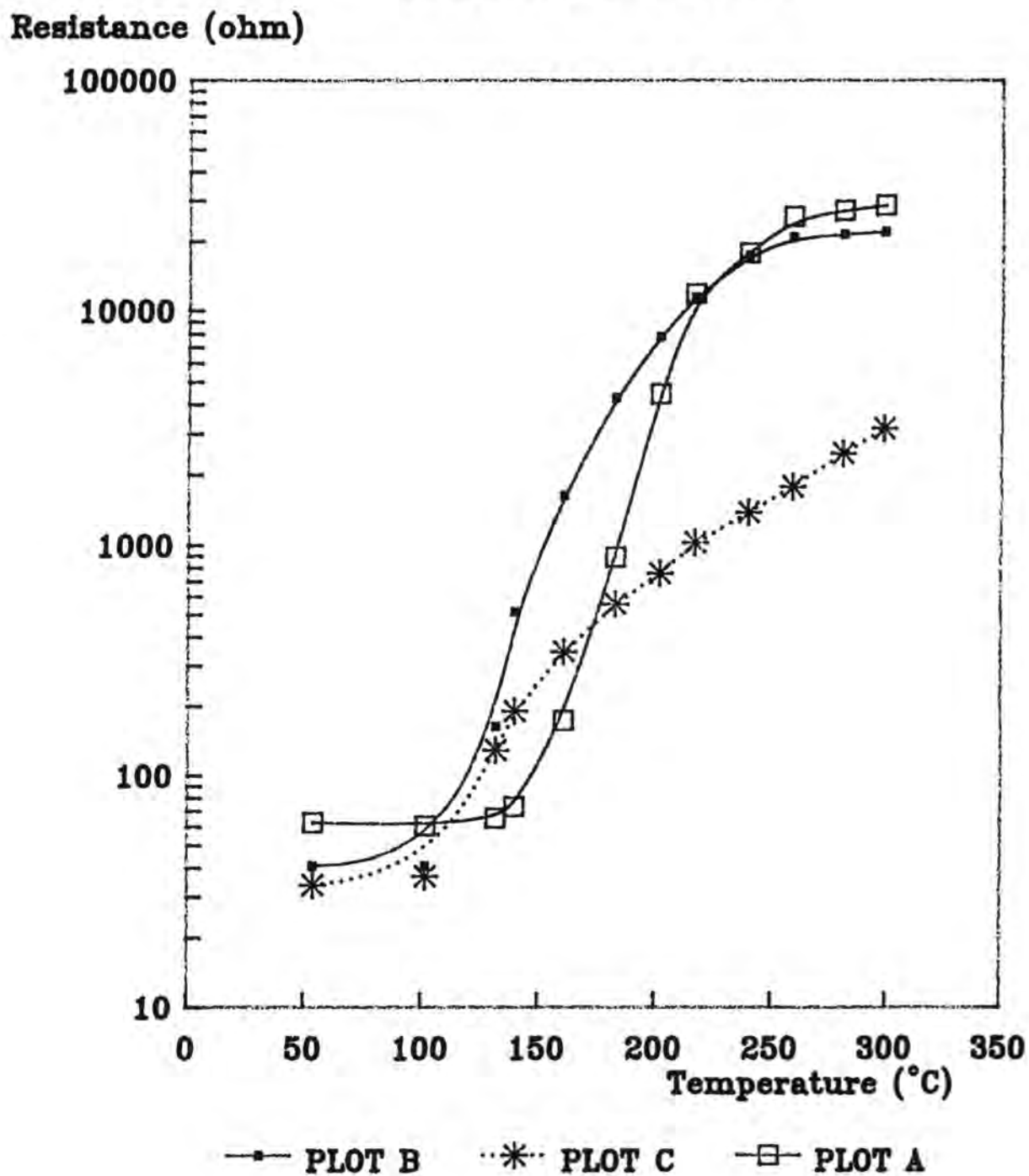


**Figure 2 : Resistance–Temperature Plots for  
Different PTC Devices**



Transformers which often operate at temperatures  $15^{\circ}\text{C}$  below the limits of the winding insulation.

For use as a heating element the actual resistivities of the material above and below the Curie temperature are important, as is the switching temperature. However a more shallow gradient than that used in protection devices is normally specified to reduce current fluctuations (Figure 2b).

The use of Barium Titanate PTC's as temperature sensors has only recently been realised. For this application a reproducible linear relationship between resistance and temperature over a wide temperature range is desirable. A high temperature coefficient of resistance (large resistance change for small temperature changes) is also advantageous (Figure 2c). These characteristics are difficult to obtain with PTC's and at present this application has not been fully explored.

PTC's are used in the protection of vacuum tubes in all forms of radio receivers as current overload protection devices. An R-T plot for this type of device is similar to that shown in Figure 2b for over-temperature protection devices.

Sensing of the level of liquid in a tank can be accomplished by the use of a PTC device which makes use of the differing

conduction properties of fluids. In a similar way the flow of a fluid can also be measured.

The use of PTC's in all of the above applications show that continuity and reproducibility between components are important. In addition for many applications the device should not be adversely affected by its working environment and should show good fatigue properties under temperature cycling. For PTC Thermistors the low temperature resistivity, the position, extent and gradient of the PTC region and the voltage sensitivity are critically dependent on the chemical stoichiometry and composition of the starting materials. The entire preparation process is important, in particular the sintering stage with the times, temperatures and atmosphere used determining the properties of the manufactured component.



### 1.1. Project Objectives

The purpose of research into the mechanical properties of Barium Titanate PTC ceramics was threefold.

The first section of the work involved evaluating mechanical tests which could be performed on inherently brittle materials with minimal preparation requirements and minimal distortion of results. The Brazilian Test was selected as it could be performed on disc samples of various dimensions prepared through normal production routes.

This information led to the second part of the project which involved mechanical testing of various preparations of Barium Titanate in order to produce a material which was mechanically strong, exhibited the electrical characteristics required by PTC devices, and which could be incorporated cheaply into a high volume production process.

The third stage of the work was to look at alterations in material variables with a view to lowering cost and reducing rejection rates during the manufacturing process. New preparation routes and sintering atmospheres were explored to investigate entirely new applications for the product, which would warrant further investigation. It was hoped that all of the work would contribute towards an even greater understanding of this and other ceramic materials.

## 2.0 . . THEORY

### 2.1 . . PTC Theory

Barium Titanate is a ceramic material which, prior to the 1960's had been used extensively as a dielectric owing to its high dielectric constant and insulating properties.

However a positive temperature coefficient of resistance (PTC) effect was described for Barium Titanate containing small quantities of Lanthium in 1956 by Sauer and Flaschen. They reported the effect centred at a temperature of  $120^{\circ}\text{C}$  with a maximum temperature coefficient of  $14\%/^{\circ}\text{C}$

The PTC effect was noticed to occur in polycrystalline materials only and it was subsequently deduced to be a grain boundary effect (Heywang, 1964 & Goodman, 1964). Heywang (1964 & 1971) indicated that a space charge barrier layer at the inter-crystallite boundaries was the cause of the PTC phenomenon (Figure 5). This layer has since been visibly demonstrated by Gerthsen & Hardtl (1963) and Rehme (1966), and is regularly referred to as the Schottky Barrier.

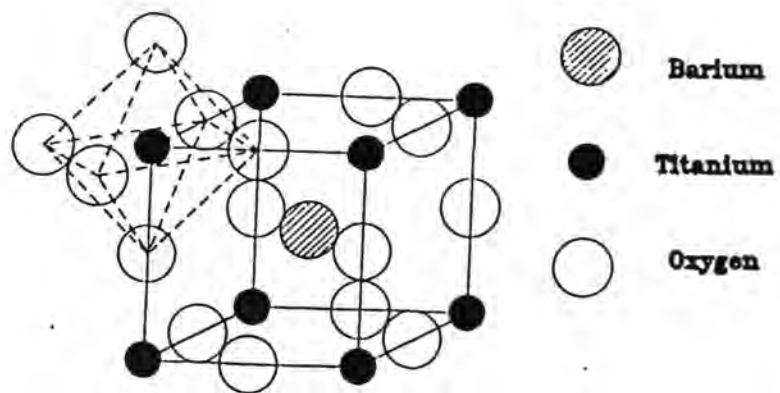


**Figure 3 : The Perovskite Crystal Structure**

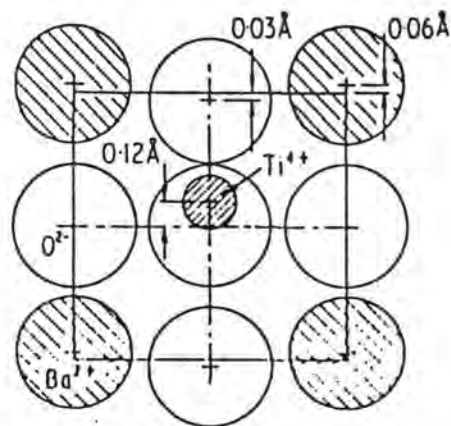


**Figure 4 : The Atomic Positions in Tetragonal  $\text{BaTiO}_3$**

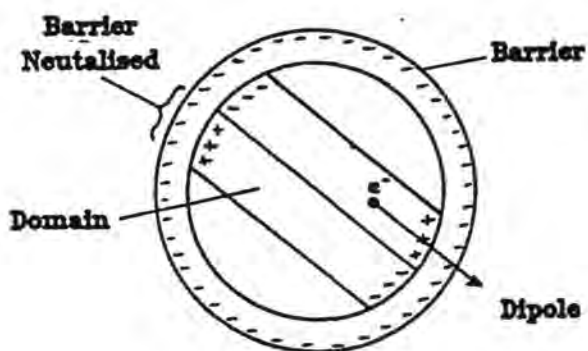


**Figure 5 : The Dipoles and Domains**

Barium Titanate crystallises with a perovskite structure which exhibits a pseudo-cubic rhombic lattice as shown in Figure 3.

The titania cations occupy the corners of a cube, the Barium ions a central position and six oxygen ions surround each Titania site in an octahedral arrangement.

As a crystal of Barium Titanate is progressively cooled its structure changes to tetragonal as  $120^{\circ}\text{C}$  is reached. This is achieved by the Titania atoms in one plane moving closer together in one direction and the other planes moving apart (Figure 4). This temperature is referred to as the Curie or switching temperature

Spontaneous polarisation of the crystal occurs because the reduction in thermal energy below  $120^{\circ}\text{C}$  stops the Titania cation remaining at the central point between the six oxygen ions, a position it occupies at temperatures above  $120^{\circ}\text{C}$ . Because of this shift, which can amount to  $0.15\text{\AA}$ , a dipole is formed (Shirane et al, 1955). These dipoles form regularly orientated areas called domains (Figure 5). It was suggested that the polarisation at the ends of these domains had the effect of neutralising the surface charge over some of the area of the grains thus leading to a greatly reduced resistivity between grains (Jonker, 1964 & Heywang, 1964), and is responsible for the subsequent PTC effect.

## 2.2 Thermal Stresses

The conditions to which Barium Titanate components are subjected often result in a large range of stresses applied during their working life as PTC devices. These are described briefly below:

Swift temperatures changes which may be introduced in protection devices as well as in heating devices under current surge conditions, such as switch on, may result in thermal stresses being produced. These are tensile in nature at the component edges and compressive at the centre under heat up. Stresses of up to 30MPa may be produced from a rapid temperature change of 200°C (Johns, 1965).

Large thermal gradients may also be present within a ceramic component. These are partly because of the poor thermal conductivity between the grains. Research has shown that during heat up the centre of a thermistor has often passed through the Curie Temperature whilst the extremities of the component are 30°C below this point. Because of the cubic-tetragonal crystallographic phase transformation which takes place at the Curie temperature and the corresponding volume changes, mechanical stresses are set up.

In addition, the PTC effect is caused by grain boundary activity with the centres of the grain considered to be

conducting (Heywang, 1964). This leads to discontinuities and further small mechanical stresses because of the differing heating rates of grain centre and boundary (Figure 6).

Work has been done on fracture initiated at soldered contacts of Barium Titanate Ceramics (Van den Avyle et al, 1983) and concluded that thermal/mechanical stresses were the driving force for failure.

#### 2.2.1. Residual Stresses

Residual stresses such as produced during the manufacturing process or fixation of the component have also been measured. Michuie et al (1986) performed work which was successful in measuring internal stresses by the indentation method, values of 10MPa being typical. Measurements of surface stresses following machining operations have been made (de With et al, 1983) and values of 7MPa obtained.

#### 2.2.2. Temperature Related Studies

A number of studies have investigated the temperature dependence of fracture toughness and tensile strength for Barium Titanate Ceramics (Cooke et al, 1983) and concluded that there is an appreciable drop in both quantities, of the order of 40%, during heating from room temperature to the Curie temperature which was 220°C for the material investigated.

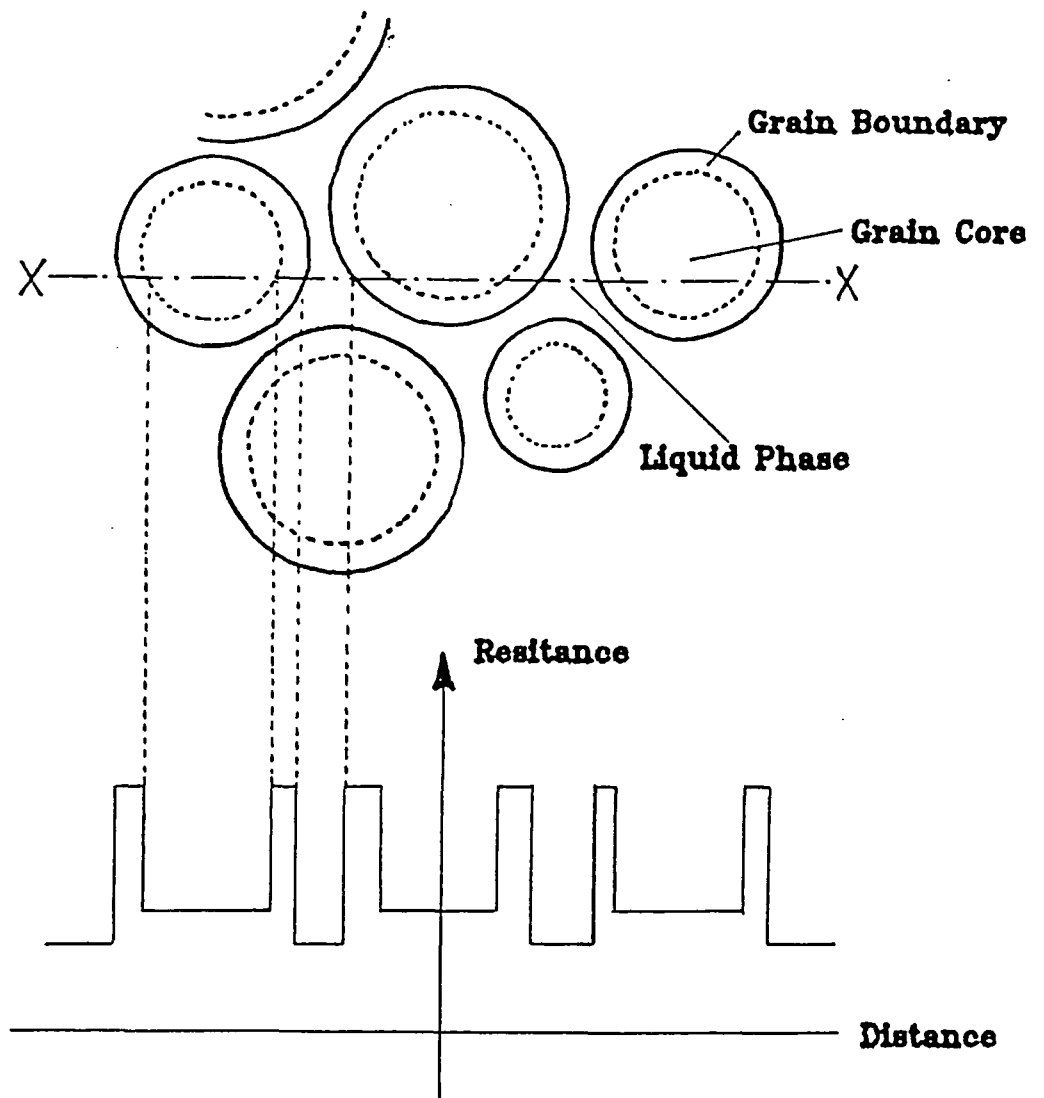


**Figure 6 : The Resistivities through the Granular Structure**

Extensive studies have also been performed on thermal fatigue life when mechanical stresses are also present (Cooke et al, 1983) which have proved the validity of fatigue formulae. In addition recent work in the area of thermal fatigue using slow cooling as opposed to quenching has proved the fatigue formulae to be accurate (Kamiya, 1989).

Previous work on Barium Titanate at Durham has included thermal cycling tests using the self heating capacities of the thermistors. This form of testing is of great importance as it accurately reflects the service conditions of the component. However, much experimental work is required before this method may be used instead of the more commonly employed mechanical testing.

Testing for thermal shock is also important and may be accomplished with a number of cooling rates. Analysis of copper discs (Kamiya & Kamigaita, 1989) showed that water and air blast quenching could both be used depending on the desired rate of heat loss. The experiments need to correspond to the in-service conditions of the devices. For Barium Titanate PTCs this can be closely modelled by air blast quenching.



### 2.3. Mechanical Strength

The mechanical strength of ceramics as a family of materials is becoming much more important as the uses to which they are put diversifies. Modern ceramics are required to withstand not only mechanical loading but also thermal stresses, wear and impact damage in service.

The problems associated with ceramic components normally stem from their brittle nature at most working temperatures. This generally leads to low resistance to crack growth as well as crack initiation from pores, which are normally present to some degree in all ceramic components. Because the failure strength of ceramics can be dependent on one very large pore, a sharp crack or a series of smaller pores close together valid testing is extremely difficult to conduct and quantify with a large results scatter being the norm.

#### 2.3.1. Porosity

To produce a ceramic material with its mechanical strength highly repeatable between components of a batch, requires a low porosity arising from small spherical pores spread uniformly throughout the material. As expected these criteria also lead to a higher overall mechanical strength for the component. For example a ceramic component with pores  $5\mu\text{m}$  in diameter and only  $3\mu\text{m}$  apart represents a porosity of 13% which is a common value

for Barium Titanate produced for commercial purposes at Elmwood Sensors Ltd.

The porosity of a ceramic component can be measured relatively easily by Archimedian or mass and volume techniques. Typical values can be as low as 0.3% in alumina components produced by Hot Isostatic Pressing (HIP) or as high as 85% in some fire bricks. Typical values for Barium Titanate, the material used in this investigation, can range from 3.0% to 28% depending on the preparation route taken and the raw materials employed.

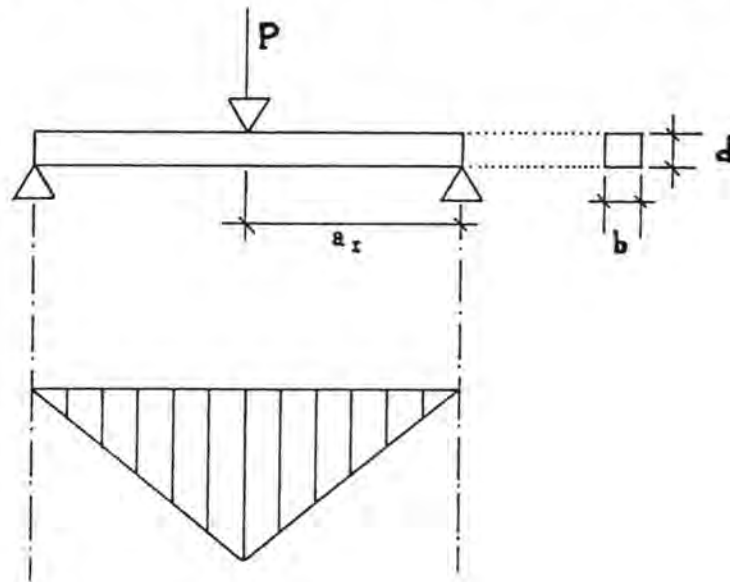
One technique which may be used to "view" the pores within a component involves ultrasonics and use of this technique which is in a highly experimental stage at present may provide important results in the future (Private Communication, NCT)

### 2.3.2. Testing Mechanical Strength

Axial testing of components is desirable to measure mechanical strength however, the machining of the test pieces is extremely difficult and so bend tests are normally employed.

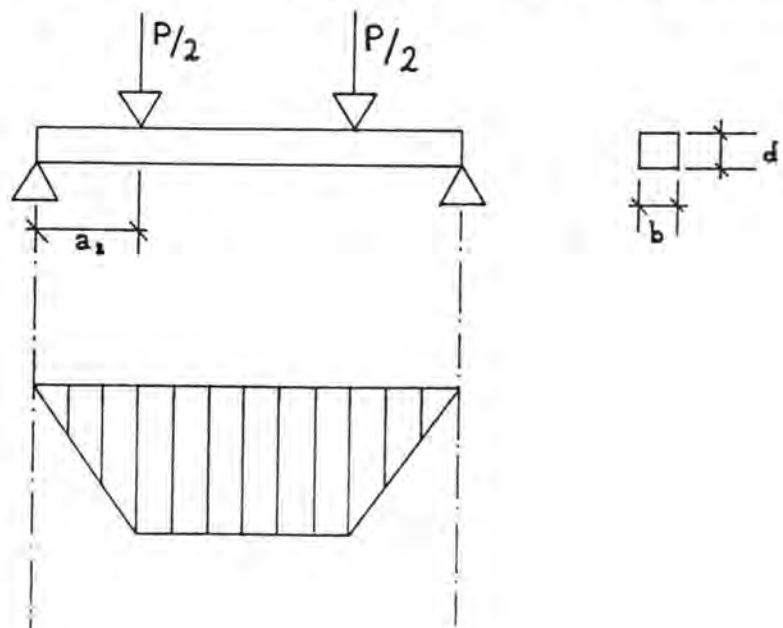
Experimentally, arrangements which place a uniform stress field over as large an area of the component as possible are desirable. It is for this reason that the four-point bend test has largely taken over from the three-point bend test for the measurement of mechanical strength of brittle materials. The Bending Moment Diagrams for both 3 & 4 Point Bending are shown

**Figure 7a: Bending Moment Diagram for Three-Point Bending**



$$\text{Maximum Stress} = 3Pa_r/bd^2$$

**Figure 7b: Bending Moment Diagram for Four-Point Bending**



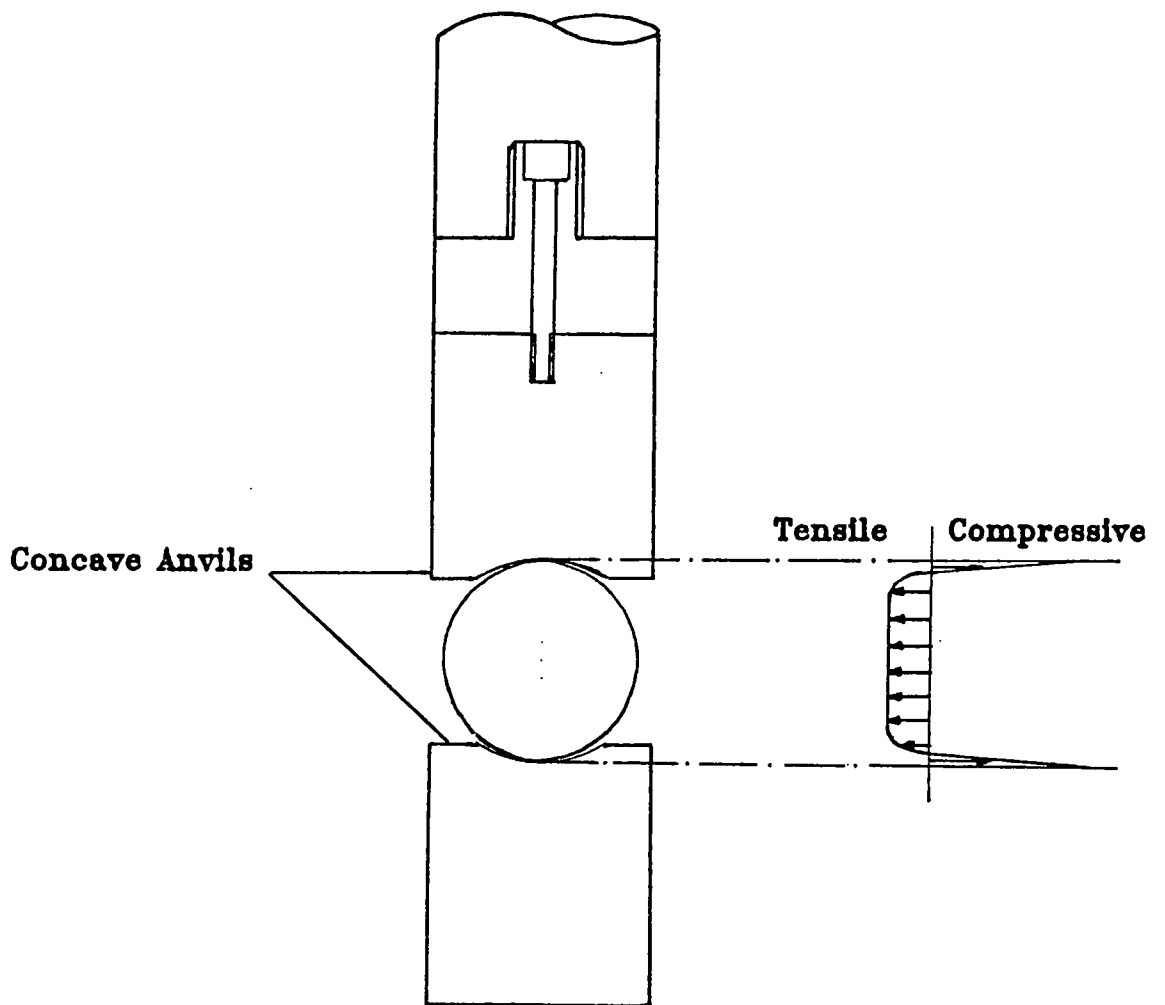
$$\text{Maximum Stress} = 3Pa_r/bd^2$$

in Figures 7a & 7b. The problem with all forms of beam tests is that time consuming and costly sample preparation is required. Additionally these results may not give accurate measurements for the components due to size effects being important in ceramics (Almond et al, 1986) as well as the possibility of surface microcracks produced during the machining operations (de With & Parren, 1984).

It was for these reasons that the Diametral Compression Technique was developed. In terms of sample preparation it is ideal for PTC pellets pressed in a simple die as little or no sample preparation is required. The process has been in use in the Pharmaceutical Industry for a number of years for testing pill/capsule designs and so results have been well documented (Pitt et al, 1988). It has also been in use for many years for the testing of concrete cylinders as it provide a quick measurement of the strength of cores taken from structures (Brewer, 1962). A further advantage of this test is that it may allow measurement of the strength of "green" pellets. This would be useful in the assessment of binder and die lubricant performance, especially for the production process.

The stress field produced by this form of testing is shown in Figure 8. The constant tensile stress extends for a region of approximately 70% of the diameter of the disc and so results from this form of testing tend to show less scatter than for three-point bend tests (G.Moran, 1988).

**Figure 8 : The Diametral Compression Test**



The Maximum Tensile Stresses present in a disc under Diametral Compression may be calculated from the equation below. This equation is prepared from analysis of the stresses in a situation of plane stress.

$$\sigma = \frac{2 P}{\pi d_I t}$$

$\sigma$  = Max. Tensile Stress

P = Load Applied

$d_I$  = Disc Diameter

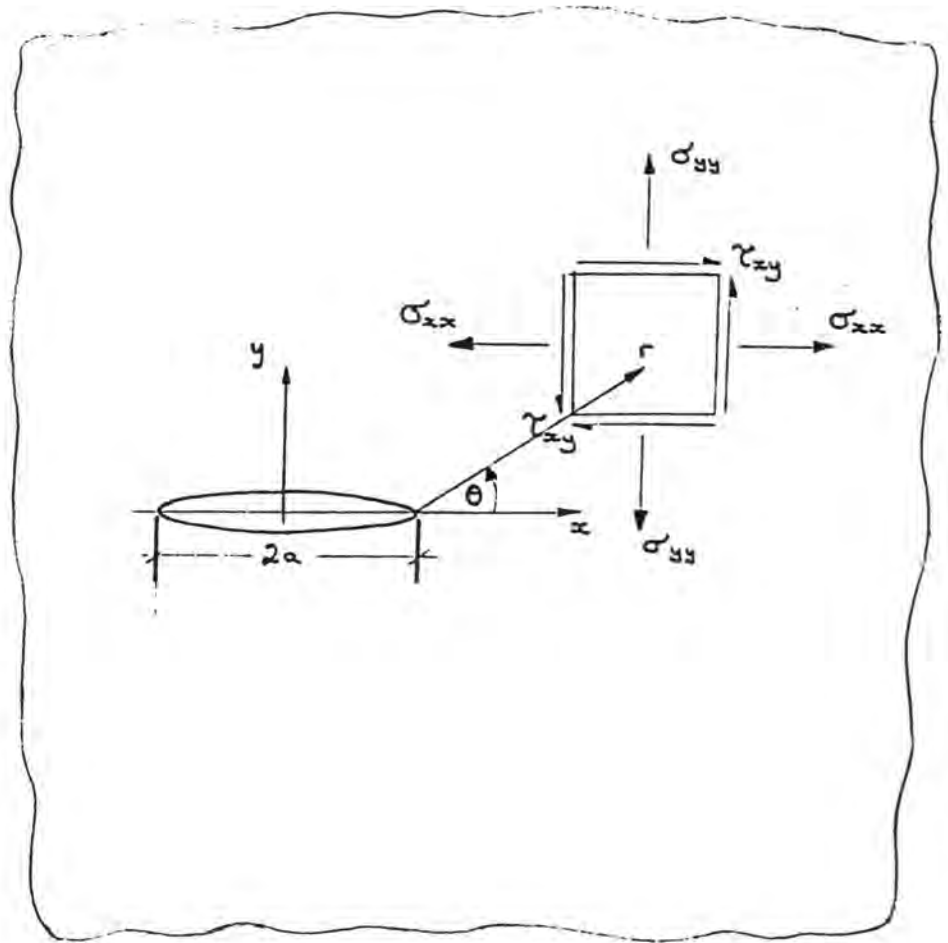
t = Disc Thickness

Problems which were initially encountered with this technique included failure owing to the large contact stresses which developed at the loading points. However, the use of concave loading anvils has eliminated this problem almost entirely (Moran, 1988).

### 2.3.3. Testing Fracture Toughness

Fracture Toughness is a measure of the resistance offered by a material to the growth of pre-existing cracks under an applied load. Two methods are currently in use describing fracture toughness which are either based on an energetic approach and the use of stress intensity factors. The latter approach was adopted for this study.

Irwin (1957) originally developed the technique based on work by Westergaard (1939) and it was noted that the stresses in the



$$\begin{bmatrix} \sigma_{xx} \\ \sigma_{yy} \\ \tau_{xy} \end{bmatrix} = \frac{K \cos\left(\frac{\theta}{2}\right)}{\sqrt{2\pi r}} \begin{bmatrix} 1 - \sin\left(\frac{\theta}{2}\right) \sin\left(\frac{3\theta}{2}\right) \\ 1 + \sin\left(\frac{\theta}{2}\right) \sin\left(\frac{3\theta}{2}\right) \\ \sin\left(\frac{\theta}{2}\right) \cos\left(\frac{3\theta}{2}\right) \end{bmatrix}$$

**Figure 9: Stresses in the vicinity of an Elliptical Crack**

vicinity of a crack could be expressed as shown in Figure 9. The crack shown is often referred to as a thumbnail crack and  $r$  and  $\Theta$  are cylindrical polar coordinates.  $K$  is a measure of the stress intensification due to the crack and its geometry.

There are three modes of crack extension (Figure 10), and for each of these modes a different stress intensity factor is apparent. Opening (Mode I) tends to be the most common mode of failure because the resistance offered by the material to crack extension is a minimum. Mode II which corresponds to edge sliding and Mode III, anti-plane shearing, also operate.

Dimensional analysis of a body containing a crack similar to that in Figure 9 undergoing Mode I opening shows that the stress intensity factor operating will be:

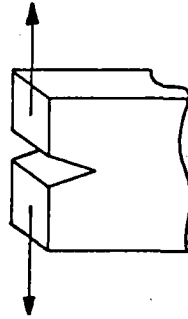
$$K = \psi \sigma \sqrt{\pi a} \quad (a)$$

where  $\psi$  is a dimensionless constant which depends on the loading geometry and crack configuration (Evans & Tappin, 1972). It is normally obtained by numerical or analytical methods such as applied by Cartwright and Rooke (1977) in dealing with many geometrical configurations of engineering interest.

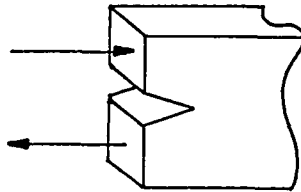
For brittle materials, fracture occurs when the normal stress in the close vicinity of the crack tip reaches a critical value



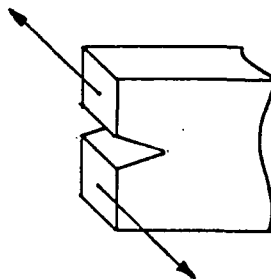
FIGURE 10 : The Modes of Extension of a Crack



Mode I (opening)



Mode II (edge sliding)



Mode III (anti-plane shear)

for bond rupture. Corresponding to this condition will be a critical value for the stress intensity factor  $K_{IC}$ . Therefore the equation above may be rewritten as:

$$K_{IC} = \psi \sigma_f \sqrt{\pi a_c} \quad (b)$$

Measurement of  $K_I$  for fast fracture have confirmed that  $K_{IC}$  is a material parameter when fracture occurs exclusively by Mode I and plane strain conditions operate at the crack tip.

Therefore by measuring failure of samples of known loading and defect characteristics, it is possible to calculate this critical value as  $K_{IC}$ , the fracture toughness.

However, further use may be made of this equation, to assess where fracture of components may have initiated. Ceramics, being of granular construction will have pore sites between grains which may act as fracture initiators. From notched or precracked specimens of the material  $K_{IC}$  may be calculated as may the strength from un-notched specimens. From these two values  $a_c$ , the critical defect size may be calculated and relating this to the microstructure of the material may reveal the initial fracture site, equation (b).

Inherently brittle materials show little resistance to crack growth and hence this property usually specifies the limits of mechanical and/or thermal loading of ceramics.

The measurements of fracture toughness has prompted a great deal of research over recent years. Many of the methods involve measurement of the loading required to extend an artificially prepared crack.

For ceramic materials single-edge notched beam tests have been shown to provide acceptable results without requiring extensive sample preparation (Pabst et al, 1974). The fracture toughness is calculated by considering the bending moment diagram of the beam setup (Figure 7). Relating the stresses in the beam to formulae for fracture toughness reveals:

$$K_{IC} = \psi \frac{P a_I \sqrt{\pi a}}{b d^2}$$

The shape parameter,  $\psi$ , is obtained from tables such as those contained in "The Compendium of Stress Intensity Factors" (HMSO:1977).

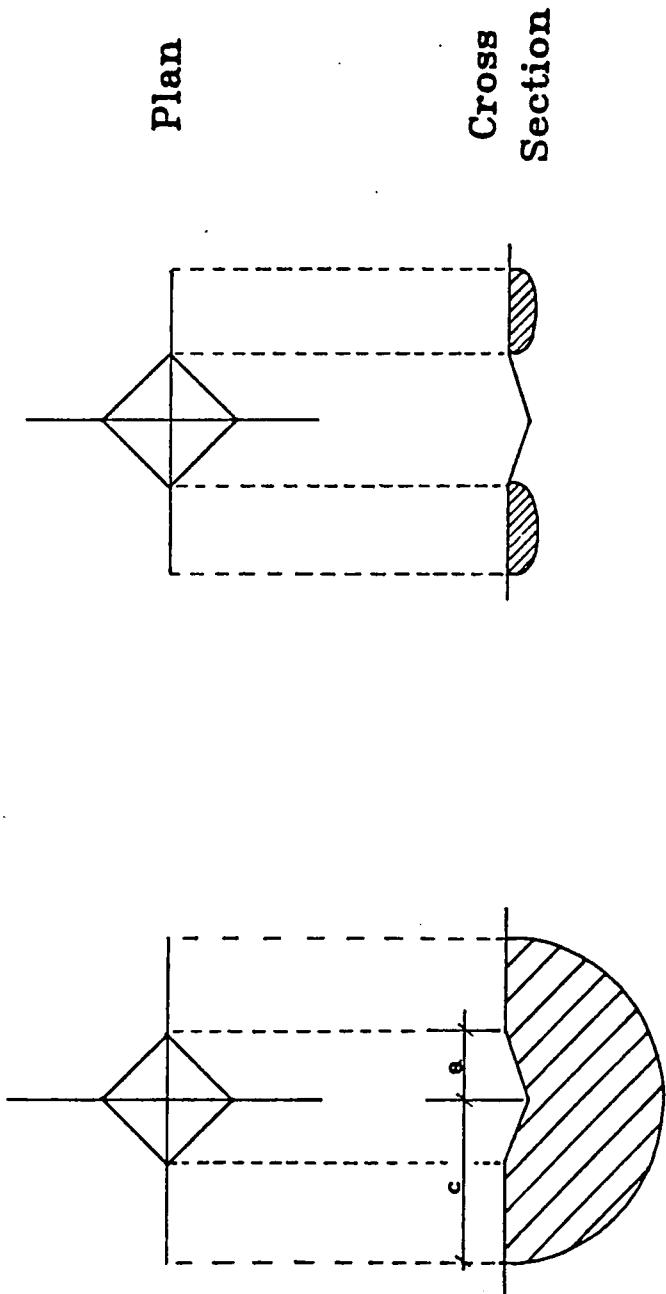
Recently the requirement for a technique to measure fracture toughness ( $K_{IC}$ ) which requires minimal sample preparation has been recognised. Bend tests can be very time consuming and as ceramics exhibit mechanical properties that are size dependent (Morrell, 1988) the reliability of results must be questionable.

The use of sharp indenter to measure fracture toughness ( $K_{IC}$ ) was first realised by Palmqvist (1962). It was discovered that the cracks originating from the corners of a Vickers indent increased in length with applied load. Lawn et al (1975) observed that the crack radius increased with  $(load)^{0.67}$  and the crack length was dependent on indenter profile and the roughness of the material surface. Evans & Charles (1976) prepared a formula for "half-penny" cracks (Figure 11a) and more recently Niihara et al (1982) modified this formula to consider Palmqvist cracks (Figure 11b).

Lankford (1982) has since performed much experimental work and modified Evans & Charles' formula. However, the results obtained from the two formulae are very similar over the range of toughness values for ceramics. Evans & Charles' formula for "half-penny" cracks is most commonly used in experimental work and was used in this study.

$$\left( \frac{K_{Ic}\phi}{Ha^{1/2}} \right) \left( \frac{H}{E\phi} \right)^{0.4} = 0.129 (c/a)^{-3/2}$$

Figure 11 : Schematic Diagram of the Vickers Indentation



a : Half-Penny Crack

b : Palmqvist Crack

## 2.4. Preparation Theory

The modern methods of preparation for all forms of high quality ceramics, including Barium Titanate, has been the subject of extensive research over the past 15 years. The aim of most production processes is to produce a dense ceramic with small evenly distributed pores as cheaply as possible. The fulfilment of these criteria result in components which can exhibit impressive and reproducible mechanical and/or electrical properties.

### 2.4.1. Milling Process

Most Ceramic components consist of a base material with additions of other compounds which improve density or electrical and mechanical properties, density or limit granular changes during the later stages of processing. These constituents are normally mixed using a milling process whereby hard spheres of material which causes as little contamination to the ceramics powders as possible are caused to both crush and mix the ingredients. This is normally performed by the rotation of a drum containing milling balls, ceramic constituents and a liquid milling medium which, for reasons of cost, is normally de-ionised water. Studies have been made to find the optimum milling time, milling ball material and subsequent contamination has been looked at in detail (Nelson et al, 1959). Also the effects of dry and wet milling have

been investigated and it has been shown that much higher green pellet densities are possible when a ceramic powder is milled in a liquid medium (Tsang-Tse Fang et al, 1988).

#### 2.4.2. Pressing Stage

The next stage of the preparation is normally granulation followed by addition of a binder. The pressing of ceramic powders to form "compacts" or "green" pellets has prompted much research. However, the size of particles required for the formation of a ceramic component is very important and often has an effect on the structural integrity of the ceramic. The strength and hardness of the agglomerates is also pertinent. Work performed by Leiser et al, (1970) has concluded that large soft agglomerates containing less eccentric particles produced the strongest "green" pellets following compaction of the powders. The work also showed a higher green density from slower rates of compaction, a result confirmed by Youshaw et al, (1988). Tests made on Alumina powders under shock compaction (which is a process used when processing some metal powders) showed large particle size decreases from 10 to 0.1 $\mu$ m but the presence of cracks in some grains was noted (Akashi & Sawaoka, 1984). Typically pressures of 30GPa may be reached under this form of compaction. Thompson (1981) concluded that the shape of particles was important, with a platelet shape being preferable to spherical particles. It was also showed that agglomerates made of fine sticky particles

were preferable to powders made up of coarse free pouring grains. Fong & Hsieh (1988) showed that the density of a Barium Titanate "green" compact could be improved by pressing of a damp powder owing to the high pressures which could be tolerated within the die. Compacts formed from dry powders exhibited delamination at pressures as low as 180MPa whereas no problems were noted with wet powders subjected to pressures as high as 500MPa.

A further source of cracking in a compact is during the ejection process. High shear and tensile stresses are developed as a result of the high pressures being maintained on the edge of the compact by the walls of the Die (Thompson, 1981).

Successful use of a binder is dependent on a number of important factors; the most important being the ability to wet the individual grains of the powder. Achieving uniform distribution of binder is also very important to reduce the possibility of large voids in the ceramic following binder burnout.

The use of die lubricants to aid the pressing process has become much more widespread in the last twenty years and their advantages have been scientifically confirmed (Macleod et al, 1977). Heinz and his co-workers (1988) showed how the breakdown of clusters of barium titanate powders occurred in



two stages, with a pressure of 100MPa normally being sufficient to crush the clusters of particles. Higher pressures than this caused cracking of the compact with no density increase resulting. Many Research Groups have used the simple single or dual acting cylindrical die. This form of die is often used to form electrical ceramics which are subsequently mounted in metal or plastic casings to form a finished component. The pressures which may be generated within a powder during compaction have been accurately measured (Macleod et al, 1976) and (Leiser et al, 1970), as have powder densities and some startling results have emerged. Localised density variations of up to 6% have been observed as have pressures of double that exerted at the die face. These variations tend to be more pronounced in compacts with high length/diameter ratios.

Long (1960) obtained an expression for the Ratio of Axial to Radial forces acting in a simple die; which for a powder such as Barium Titanate gave a value of 2.1. This inequilibrium of forces is one of the reasons for the variations of density within a powder compact. These density variations can lead to dimensional problems following sintering (Section 6.2), and this is one of the reasons that Hot Isostatic Pressing has gained popularity. If samples with a high ratio of length/diameter are required a double acting die is recommended (Thompson, 1981) as it reduces the effective compact length by 50%.

Work performed by Ueyama et al (1987) has shown that increases in green density can be translated to higher densities in the sintered ceramic (up to 98% of theoretical density), higher mechanical strength and higher dielectric constants for undoped barium titanate. His studies have also shown that a higher compact density can considerably reduce the sintering temperature required.

Studies have also been made into the effect of pressing pressure applied to the compact on the density of the green pellet (Fong et al, 1988). It has also been discovered that pressing of powders can repair some of the pores created during the spray drying of powders if this production route has been used (Agbarakwe et al, 1989).

Investigations into the effects of temperature and moisture content of powders have also been made (Youshaw et al, 1982) with the conclusion that higher temperatures and moisture contents are beneficial to the production of a dense compact.

Youshaw and his co-workers have also investigated the effect of isostatic pressing of compacts with higher green densities being obtained at lower pressures.

#### 2.4.3. Sintering

Sintering of ceramic components is performed to consolidate

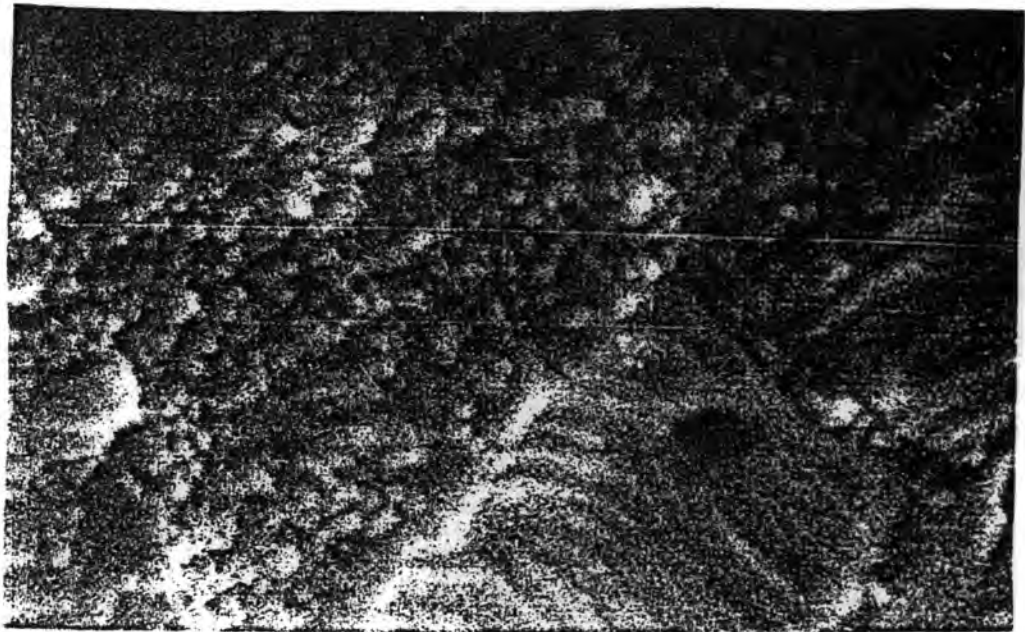
increasing density by reducing the size of pores originally present in the green sample and to bring about controlled growth of grains as well as chemical reaction. Sintering temperatures are normally about 85% of the melting temperature of the base material. However in many cases a liquid phase is employed to fill many of the smaller voids within the grain structure and the melting temperature of the liquid phase is instrumental in the determination of the sintering temperature.

The theories behind densification of ceramic components during sintering have been well documented and many mathematical definitions have been produced which explain the thermodynamic forces behind densification and grain growth (Lange & Kellest, 1989).

Xue & Brook (1989) have made experimental studies on Barium Titanate and have concluded that there is an increase in densification at the onset of abnormal grain growth (Figure 12).

In the case of doped electrical ceramics such as Barium Titanate acting as a PTC, a minimum temperature must be attained to allow the dopant to replace some of the base material in the ceramic lattice. There are many possible changes which can be made to the sintering process, a number of which can affect the product greatly. Studies by Al-Allak et al (1988) have allowed for optimisation of the maximum

Figure 12 : Abnormal Grain Growth



4μ

temperature reached during the sintering profile as well as the rates of heat up and cool down for doped Barium Titanate PTC's, with particular relevance to electrical properties.

Work has been done optimising electrical properties with regard for material density (Kuwabara et al, 1985). Porosities of 20% were found to produce the best PTC effects, with up to seven orders of magnitude resistivity change, for high Curie temperature PTCs. The "best PTC effects" normally correspond to the steepest R-T plot and the largest total resistivity change. Unfortunately follow-up work into the detrimental effects of engineering such porosities, especially on material fracture toughness and fatigue, has not been made by Kuwabara. It is intended that this study will look into porosity and its mechanical implications.

Much work has been performed looking at the microstructural changes on Barium Titanate during sintering. The effects of grain size and shape on both mechanical and electrical properties, as well as the sintering profiles required to give this controlled grain growth have been investigated. It is useful to note that many ceramics behave in similar ways with regard to changes in mechanical strength and so it is possible to obtain useful information from research on different materials.

Some important work on Barium Titanate has shown that as the maximum sintering temperature increases the grain growth rises to a maximum with grain sizes of  $60\mu\text{m}$  at  $1240^{\circ}\text{C}$  but then falls gradually to  $10\mu\text{m}$  at  $1360^{\circ}\text{C}$ . The high values at  $1240^{\circ}\text{C}$  represent abnormal growth and there are many grains under  $1\mu\text{m}$  diameter present (Matsuo et al, 1971). Studies made by Kahn (1971) have concluded that initial particle size has very little effect on the final particle size of the sintered ceramic. However increasing dopant concentration, in this case Niobium (Nb), above 0.4 molar% results in grains of about  $1\mu\text{m}$  diameter being produced compared with a standard grain size of  $60\mu\text{m}$  at lower Niobium concentrations. This represents a massive increase in grain boundary surface area which is where the PTC effect seems to originate (Section 2.1). Work performed by Lubitz (1981) has shown that the use of a slower heating rate near to the maximum temperature results in greater grain growth. However, increases in the time at the peak temperature (from 30 minutes to 50 hours) showed little change in the grain size.

### 3.0. MATERIALS

Over the course of the study a number of preparations of Barium Titanate Ceramics were produced. However, in many cases the base material used was a high purity grade from TAM chemicals, produced by the ignition of Barium Titanyl Oxylate. This method produces an extremely pure product. A chemical analysis of the material revealed the following:

Material	% by mass	molar %
Barium Oxide	65.49	49.45
Titanium Dioxide	34.46	49.97
Alumina	<0.04	<0.034
Ferric Oxide	<0.005	<0.002
Silica	<0.03	<0.041
Total % Impurities	<0.05	<0.42

Mole Ratio of  $\text{BaO/TiO}_2 = 0.990$

### 3.1. Materials: Part I

The standard mix for the first part of the study comprised the following materials which were milled together in 150ml of distilled water for 12 hours.

Material	Mass(g)	No. of Moles
BaTiO <sub>3</sub>	116.62	0.500
CaTiO <sub>3</sub>	11.90	0.087
TiO <sub>2</sub>	0.866	0.0108
Ho <sub>2</sub> O <sub>3</sub>	0.646	0.0018
SiO <sub>2</sub>	0.751	0.0045
Al <sub>2</sub> O <sub>3</sub>	0.281	0.0027
MnCO <sub>3</sub>	0.038	0.0004

Ball Milling was used for this process, a technique which mixes the components as well as reducing the particle diameters to the order of 10 $\mu$ m. The milling balls were of Agate and of three distinct sizes; 10mm, 12mm & 20mm, and the milling vessel was of (UHMW) Polyethylene.

Following milling the mixture was filtered and dried in an oven. Glucose and PVA were then added in an aqueous solution (5% Glucose, 5% PVA) which was mixed by hand to act as a binder for the powder when pressed into pellets. The mixture was again dried and then granulated using a pestle and mortar and sieved to extract the portion of powder which had granule sizes of between 90 & 500 $\mu$ m.

The powder was then pressed into pellets using a hand press. Two cylindrical die were used to produce "green" pellets (pellets prior to firing) of two sizes; 13mm diameter and

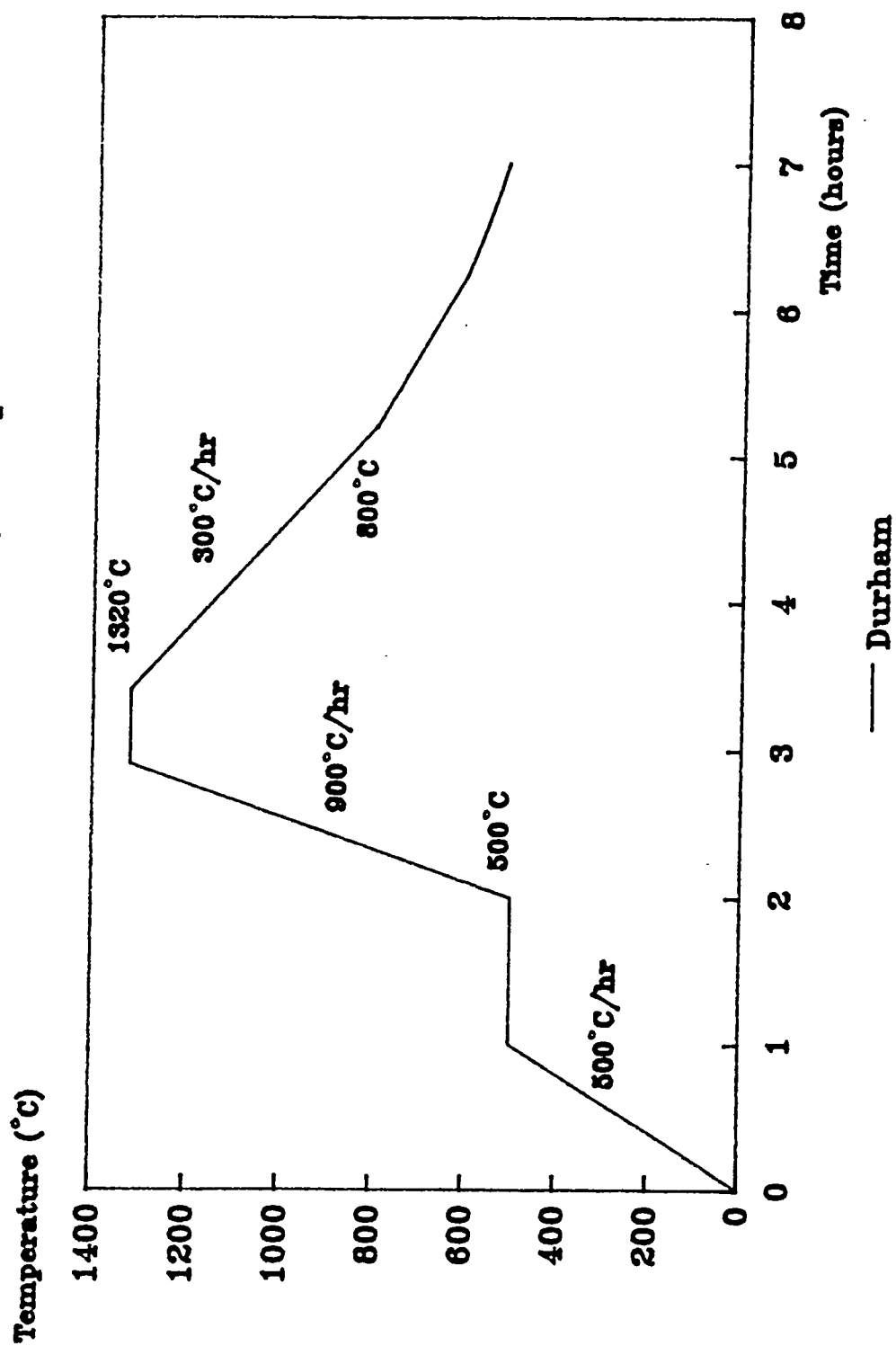


approximately 2.2mm thickness for mechanical testing and microstructural analysis and 5.1mm diameter and 3mm thickness for Resistance-Temperature data collection. The standard loads used during pressing were 1.0 and 0.2 tonnes respectively for the two sizes of die, resulting in compaction pressures of 78 & 100 MPa. The density of these powder compacts was in the region of 55% of theoretical density.

The green pellets were then sintered in air in a tube furnace. The standard sintering profile is shown in Figure 13. The binder was burnt off at 500°C and this temperature was maintained for 60 minutes to ensure complete elimination of the binder. The temperature of the furnace is then raised to 1320°C to allow formation of the liquid phase and densification of the pellet. During the firing process densification and contraction of the pellets took place resulting in pellets attaining typically 85% of their maximum theoretical density.

An alternative to using commercially produced Barium Titanate is to produce the material in the laboratory by a calcining reaction. This was done by wet milling a mixture of Barium Carbonate and Titanium Dioxide for 12 hours, drying and then heating in a muffle furnace, with a peak temperature of 1100°C being maintained for 2 hours. The other chemicals required to complete the mix (in the same proportions as previously) were added at the first milling stage. Following the calcination reaction further milling took place in order to break up the

Figure 13 : Durham Sintering Temperature Profile



agglomerates. Addition of the binder, granulation and screening of particle size were performed in the usual way.

### 3.2 - Lower Purity Material

A short study was made into the possible use of a lower grade of Barium Titanate produced by Cookson Materials. The cost of this material was only 20% of the cost of the purer grade used in current production batches.

A chemical Analysis was performed to indicate the level and nature of impurities:

Material	% by mass	molar %
Barium Oxide	63.7	48.1
Titanium Dioxide	34.2	49.6
Strontium Oxide	0.82	0.92
Alumina	0.10	0.085
Ferric Oxide	0.01	0.005
Silica	0.08	0.110
Sodium Oxide	0.08	0.110
Total % Impurities	2.10	2.30

Mole Ratio of  $\text{BaO/TiO}_2 = 0.971$

Average Particle Size =  $1.30\mu\text{m}$

This material was used in the way as the TAM material with the same additives and identical processing route.

### 3.3. Materials : : Part. II

The second part of the study involved four batches of material which were to undergo preparation in a similar way to that undertaken previously. The main change was at the Sintering stage, during which the sintering atmosphere was to be controlled. In addition sintering was performed in a vacuum.

The constituents of the Mixes were as follows:

#### 3.3.1. Mix. 1

Chemicals	Mass(g)	Molar %
BaTiO <sub>3</sub>	116.50	99.0
Ho <sub>2</sub> O <sub>3</sub>	0.378	0.20
TiO <sub>2</sub>	0.200	0.50
Si <sub>3</sub> N <sub>4</sub>	0.210	0.30

This mix was processed in the normal way, as described in Section 3.1. However, the binder was added prior to the first milling stage, an action which was found to be advantageous during the first stage of the study (Section 5.1).

### 3.3.2..Mix.2

This material was prepared using the calcining reaction described previously and the binder was added prior to the second stage of milling which is discussed above.

Chemicals	Mass(g)	Molar %
BaCO <sub>3</sub>	98.65	49.5
TiO <sub>2</sub>	40.20	50.0
Ho <sub>2</sub> O <sub>3</sub>	0.378	0.20
Si <sub>3</sub> N <sub>4</sub>	0.210	0.30

### 3.3.3..Mixes.3.&.4

These formulations contained the same proportions of constituents, with Mix 3 being made in batches of 150grammes maximum at Durham and Mix 4 being prepared at Elmwood Sensors' production facility in a batch of 25kg. The differences in the production processes are outlined in Section 3.4.

Chemicals	Mass(g)	Molar %
BaTiO <sub>3</sub>	116.50	76.1
PbTiO <sub>3</sub>	21.10	10.6
CaTiO <sub>3</sub>	9.92	11.1
Ho <sub>2</sub> O <sub>3</sub>	0.646	0.26
Si <sub>3</sub> N <sub>4</sub>	0.765	0.83
Al <sub>2</sub> O <sub>3</sub>	0.382	0.57
TiO <sub>2</sub>	0.242	0.46

### 3.4. Differences in Processing of the Production and Research Facilities

#### 3.4.1. Milling:

In the production process at Elmwood Sensors the milling media are silica "stones" of approximately 70mm diameter which rotate in a steel drum. A milling time of 24 hours is used and the materials used total 25kg. The research demands are for much smaller quantities, the mass of the constituents being about 150 grammes. An UHMW polyethylene tub is used together with many agate balls of 10, 12 & 20mm diameters and a milling time of 12 hours is usually employed.

#### 3.4.2. Additives:

The production process demands both a binder and die lubricant being present because of the pressing process employed. The method of addition of the additives is in a semi-dry state using a mechanical mixer; the laboratory additives include only a binder which is added as an aqueous solution by hand. The particle size used for the preparation of compacts in the production process is slightly larger than for the research process and the agglomerates tend to be a great deal softer.

#### 3.4.3. Pressing:

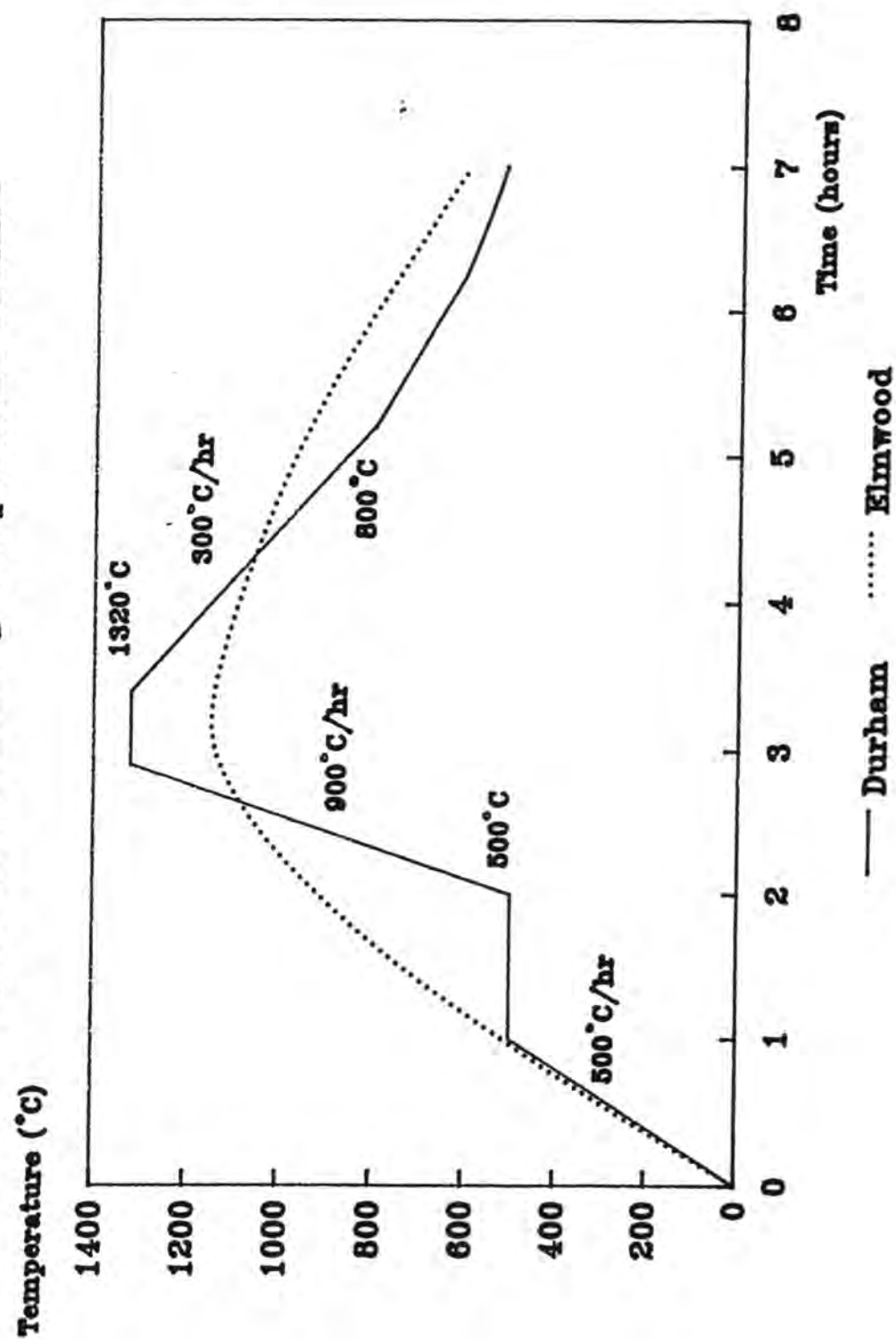
In a production process speed is of great importance and so the time taken to press each pellet has to be very short. A cycle time of 1.5 seconds is used which compares to approximately 60 seconds in the research process. However, the die pressures used are similar with an average pressure of 70MPa for the research press and 48 MPa for the production press.

#### 3.4.4. Sintering:

The sintering profiles used are shown in Figure 14 and the differences can clearly be seen. The production process relies on a moving belt passing through the furnace. The time spent in the furnace is 3 hours longer and the maximum temperature lower in the production process.



Figure 14 : Sintering Temperature Profiles



#### 4.0. .METHOD

##### 4.1. .Electrical Testing

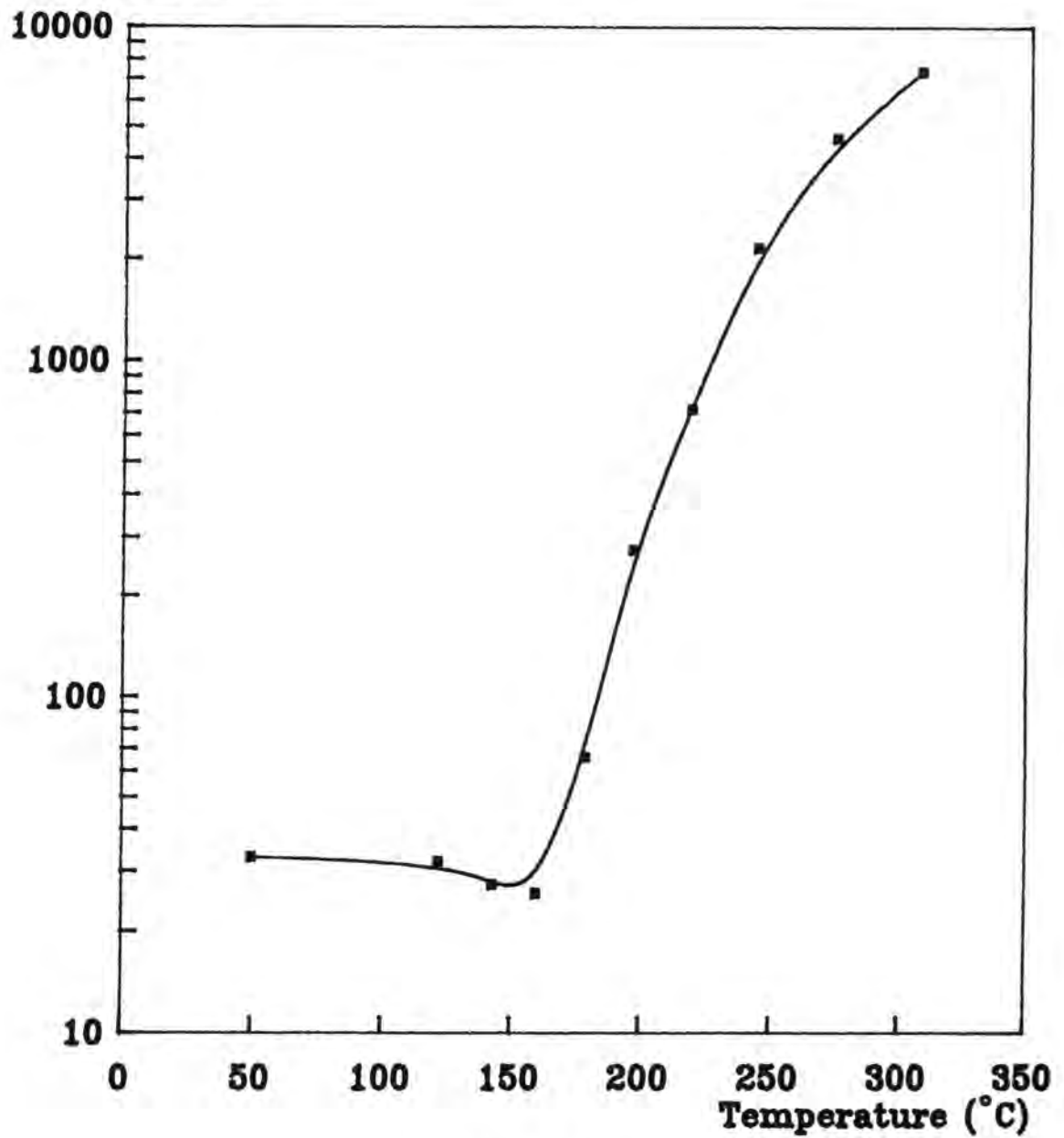
A number of methods are commonly in use to catalogue the electrical properties of PTC ceramics such as Barium Titanate.

Resistance-Temperature (R-T) plots are made to assess the scale of the resistivity changes as well as the maximum rate of resistivity change and the temperature at which this occurs. The rig used for the R-T plots is controlled by a BBC microcomputer and consists of an insulated cabinet with 9 electrical stations to allow comparisons to be made between samples. The importance of a large zone of constant temperature becomes apparant when one considers that samples may be catalogued as having switching temperatures to  $\pm 0.5^{\circ}\text{C}$ . The rate of temperature increase is  $3^{\circ}\text{C}/\text{minute}$  and the temperatures are maintained for 4 minutes prior to resistance measurements. A sample plot for the sensors produced at the Elmwood production facility is shown in Figure 15a and the steep gradient can clearly be seen.

The pellets used for the R-T measurements were pressed in the 5.1mm die and sintered in the normal way. The upper and lower faces of the discs were ground flat and polished with 240 grit paper and coated with Indium-Gallium eutectic in order to provide an electrical contact. Production samples from Elmwood

**Figure 15a : Resistance-Temperature Plot for  
an Elmwood Production PTC**

**Resistance (ohm)**



—■— MIX 4 Elmwood

were also tested and these had to be cut to size in order to fit within the measurement apparatus. In this case the edge of the pellet had also to be polished in order to allow for accurate measurements of sample cross-sectional area and density.

The Voltage dependence of resistance is often measured to assess the behavior of the PTC at high voltages (for example 240V) and how the resistivity changes when a fluctuating voltage supply is to be used. As this study was mainly concerned with the mechanical properties of the PTCs this form of electrical measurement was not used.

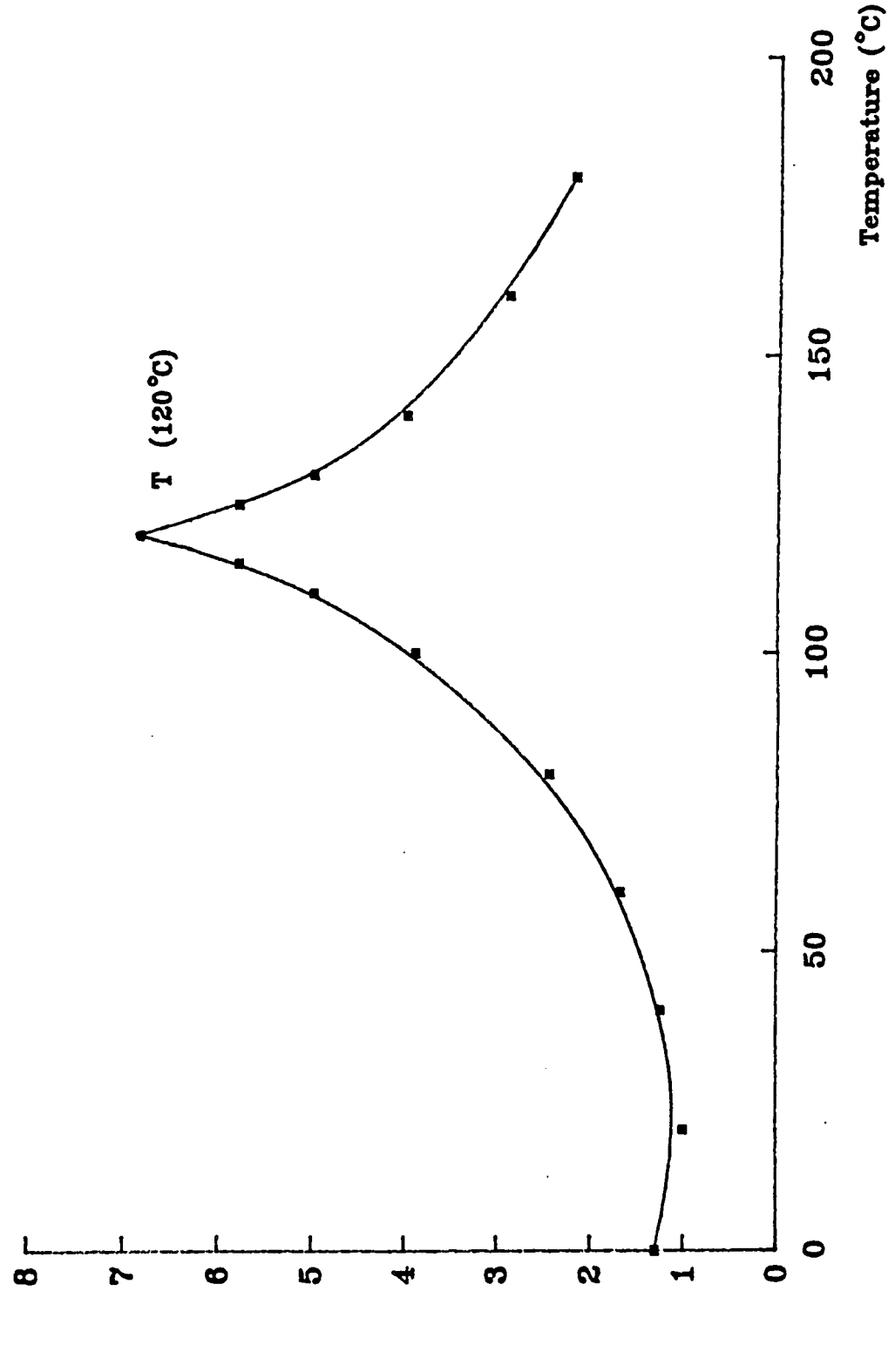
The dependence of dielectric capacitance with temperature is also used in the assessment of a commercial PTC device. Plots of this nature were not made in this study, however a sample plot is shown in Figure 15b.

## 4.2. Mechanical Testing

### 4.2.1. Diametral Compression

The diametral compression technique was chosen as the method used to assess the maximum tensile stress carried by the Barium Titanate discs. The major advantage of this form of testing was that minimal sample preparation was required, as the ceramic was in the form of a circular disc.

Figure 15b: The Effect of Temperature on the Dielectric Constant of BaTiO<sub>3</sub>



The sample preparation involved making sure that the loading surfaces were parallel and free from large defects. This was found to be more critical with the smaller pellets with the smaller aspect (diameter/thickness) ratios. This was due to the change in shape of the pellet during the sintering process because of the non uniform densities in the "green" pellets. The larger diameter pellets pressed using 13mm & 22mm diameter dies had much higher aspect ratios and hence were not subject to the same degree of non uniform shrinkage. Therefore polishing was not normally necessary. The dimensional changes which were encountered with the pellets following sintering were investigated and details are included in Section 5.3.

The large faces of the pellets were ground flat to enable accurate density calculations to be made. The density measurements were made using the mass/volume method. This method was compared with the Archimedian method which uses a density bottle, and is a standard density measurement technique. The correlation between the results was excellent and the mass/volume method chosen for subsequent use as it was much easier to perform.

Measurement of the density, and relating this to the maximum theoretical density of the material gives an indication of the porosity of the pellets. As failure of ceramics is usually initiated from pores or cracks within the component, the

porosity is a very important quantity which should be kept to a minimum, to ensure a long service life.

The loading anvils used for the diametral testing of the mechanical specimens were concave with radii of curvature of 6.25mm. The diameter of the sintered pellets ranged from 10.5mm to 11.2 mm, and this combination resulted in a working ratio of approximately 1.18. This value has previously been found to be within the range necessary for accurate and repeatable testing (Moran, 1988).

A number of pellets which underwent mechanical testing were from the production at Elmwood Sensors Ltd, the project sponsors, and these were of approximately 9.5mm radius. Thus a second set of loading anvils were produced with radii of curvature of 11.5mm.

The machine used to provide the loading was an Instron 1000 Tensile Testing Machine. A five kN load cell was used, together with a loading speed of 2mm/minute. The pellets were examined prior to testing and positioned in such a way as to eliminate erroneous results through using an obviously damaged region as one of the loaded contacts.

The machine calibration was confirmed on each occasion that tests were carried out and the load ranges on the machine were not altered at any time, an action which may have resulted in

discrepancies. In addition the loading speed was checked manually at regular intervals throughout the duration of the testing. The machine was connected to an X-Y plotter which provided load-time curves, which could be analysed. Analysis of these plots allowed estimation of the changes in the gradient of the graph to be made, which gave an indication of the load carried at initial crack propagation.

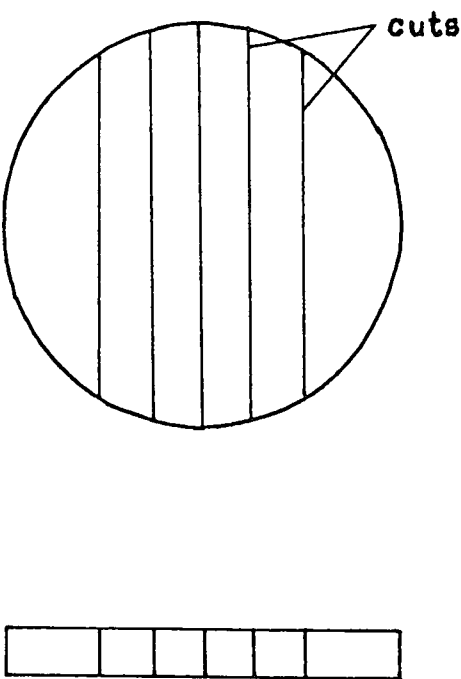
Following testing, the specimens were examined and the position of the diametral crack noted. This was to allow the stresses to be accurately calculated with regard to the crack position. Many of the specimens were viewed under the scanning electron microscope (SEM) to establish the points of initiation of failure, and to assess whether trans- or inter- granular failure had occurred.

#### 4.2.2 Loaded Beam Tests

In order to provide a back-up to the diametral compression results, four point bend tests were performed, on rectangular sectioned beams of Barium Titanate. To allow a reasonable size of beam to be used, discs of typically 32mm diameter and 4mm thickness were produced (post-sintered dimensions). These discs were sectioned using a rotating diamond saw in such a way as to produce four beams from each disc (Figure 16).



**Figure 16 : Beam Preparation from Sintered Discs**



Following the cutting stage, the faces of the beams were ground with 240 and 600 grit paper, and the surfaces lapped using alumina paste. A cloth polishing wheel was used to finish the surfaces which were to act as the loaded contacts.

At this stage, three beams were set aside from each batch of eight. These were to be used for four-point testing to assess the tensile stress carried by the material at failure. The remainder of the beams were notched to a depth of about 1.4 mm (approximately 40% of the depth) in order that notched four-point beam testing could be conducted. A Diamond coated saw of 0.75mm width was used to produce the notch. This form of testing was used to assess the fracture toughness of the beam material. Pre-cracking was not required on these specimens as previous investigations (Okada & Sines, 1986) had concluded that the act of machining is sufficient to form small cracks along the machined edge. Scanning Electron Microscopy and the use of a Toolmakers microscope with both Barium Titanate and brittle polymer beams of Polymethyl-Methacrylate (PMMA) confirmed this.

To ensure that accurate measurement of the length of the notch and crack could be made red dye was sprayed onto the base of the notch to decorate the extent of machining cracks.

The tests were performed on a Lloyd 6000R testing machine. The machine was modified by the addition of linear bearings on

the upper loading anvil which provided lateral stability in compression which the machine ordinarily lacked. A loading rate of 0.10mm/minute was used. The beams were all tested under four-point bending.

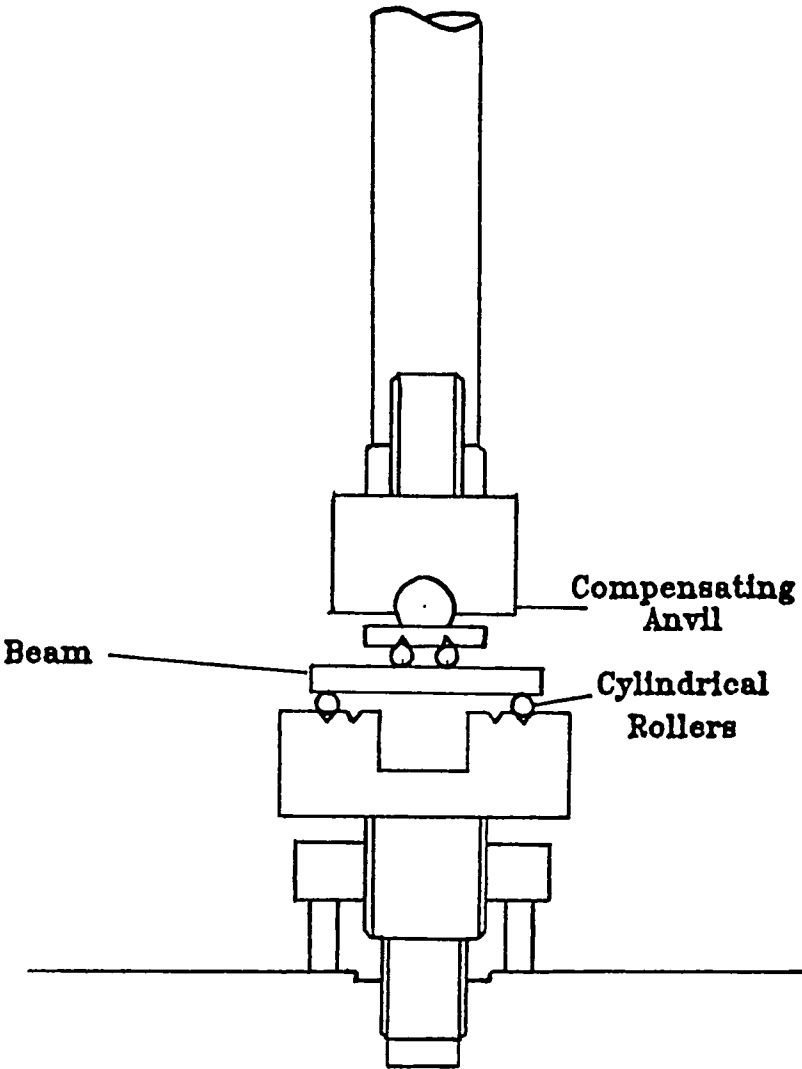
This form of bend test was used because it provides a pure bending of constant magnitude to the central portion of the beam with no shear force, and the position of the notch in the beam is not critical due to the constantly applied stress to the central portion (Figure 7b). Three point bending was not used owing to the shear forces that are brought to bear on the tip of the crack and the requirement for accurate notch placement leading to possible inaccuracies.

The rig used for the beam testing is shown in Figure 17. The loading platform was able to rotate to ensure that the loads applied at the two points of contact on the upper surface were equal in magnitude. The steel cylinders used to provide contact were coated with a PTFE spray to minimise friction under loading.

#### 4.2.3 The Vickers Indenter

The use of a Vickers Diamond indenter was in two capacities. In the conventional manner the device was used in conjunction with an Eseway testing facility to assess the hardness of the samples. For Barium Titanate used in PTC devices this is not

**Figure 17: The Four-Point Bend Test Arrangement**



as important a property as strength or fracture toughness. However it was deemed necessary for this full mechanical study. An indenting load of 5kg was used throughout.

The diamond indenter was also mounted in the Lloyd 6000R testing machine to act as a crack initiator. The sharp edges of the Vickers indent cause small radial cracks to initiate at the corners under loading which are extended as the load is increased (Figure 9). The length of these cracks was estimated with the aid of a red dye and accurately measured using Scanning Electron Microscopy, and the maximum load was noted. Previous research work which is catalogued in Section 2.3.3, describes the formula used for the calculation of the fracture toughness of a material.

The Lloyd machine was used in preference to a standard hardness testing device because the maximum load, rate of loading and time under load could easily be altered and accurately measured over a wide range of values. Following the initial assessment of this form of testing a loading rate of 0.10mm/minute was used. Initial tests revealed problems with cracking of the specimens due to the large bending moments because of the uneven ceramic surfaces. This problem was solved by mounting the disc specimens in polyester resin. The blocks were then polished in the normal way to reveal the ceramic surface to be indented.

#### 4.2.4 Testing of Unsintered Compacts

The density of the Barium Titanate discs was measured both prior to and after sintering. Measurements were made prior to firing to assess the success of the pressing process. This process is dependant on the powder properties such as granule size, agglomerate strength, the preparation route used and the level of impurities or additives present.

The strength of the green pellets was measured using the diametral testing technique described earlier (Section 2.3.2). Concave loading anvils were again used but the radius of curvature was increased to 7.5mm to take account of the slightly larger pellets of 6.5mm radius. The parameters mentioned above have an effect on the "green" strength and in a production process which involves the handling of the unsintered pellets a high strength is desirable to limit wastage.

#### 4.2.5 Scanning Electron Microscopy

Mention has already been made of the uses of scanning electron microscopy in looking at fractures surface for assessing the mode and point of initiation of failure. However, the sizes of surface pores and cracks, their distribution and frequency, and the size of the grains within a material were also investigated due to their influence on both mechanical strength and

electrical performance. The Cambridge Instruments S600 microscope was used throughout.

## 5.0 -- RESULTS

### 5.1 -- Part I. : Initial Mechanical Tests

The sample groups used in this part of the study are shown in Figure 18. It can be seen that a number of preparation techniques were investigated.

Figures 19 & 20 show the Porosities and values of Ultimate Tensile Strength of the sintered materials referenced above. The values of porosity were obtained from mass/volume calculations and values of maximum possible density (at zero porosity) referenced in Appendix I . The Ultimate Tensile Stresses carried by the materials were obtained from Diametral Compression of 11mm pellets between curved anvils.

Figure 19 shows that porosities of between 2.5 and 9.0% were encountered with the lower values for the calcined laboratory prepared material. Increase in the pressing pressure to form the "green" pellet showed a small decrease in the porosity of the sintered material. Addition of the binder prior to milling resulted in little change in porosity but when no binder was used the porosity showed an increase. The values of strength displayed in Figure 20 show lower values when the commercially available Titanate was used and also when higher pressing pressures were employed. A slight decrease in strength was noted when no binder was used.



Figure 18

Sample Group	Pressing Pressure (MPa)	Commercial BaTiO <sub>3</sub>	Laboratory BaTiO <sub>3</sub>	Milling Time 12hrs	Milling Time 24hrs	Binder Used	Binder added during Milling
1	70	*		*		*	
2	140	*		*		*	
3	280	*		*		*	
4	70	*			*	*	
5	70		*	*			
6	210		*	*			
7	70		*	*		*	
8	70		*	*		*	*

Figure 19: Values of Porosity for sintered material investigated in Part I of the Study

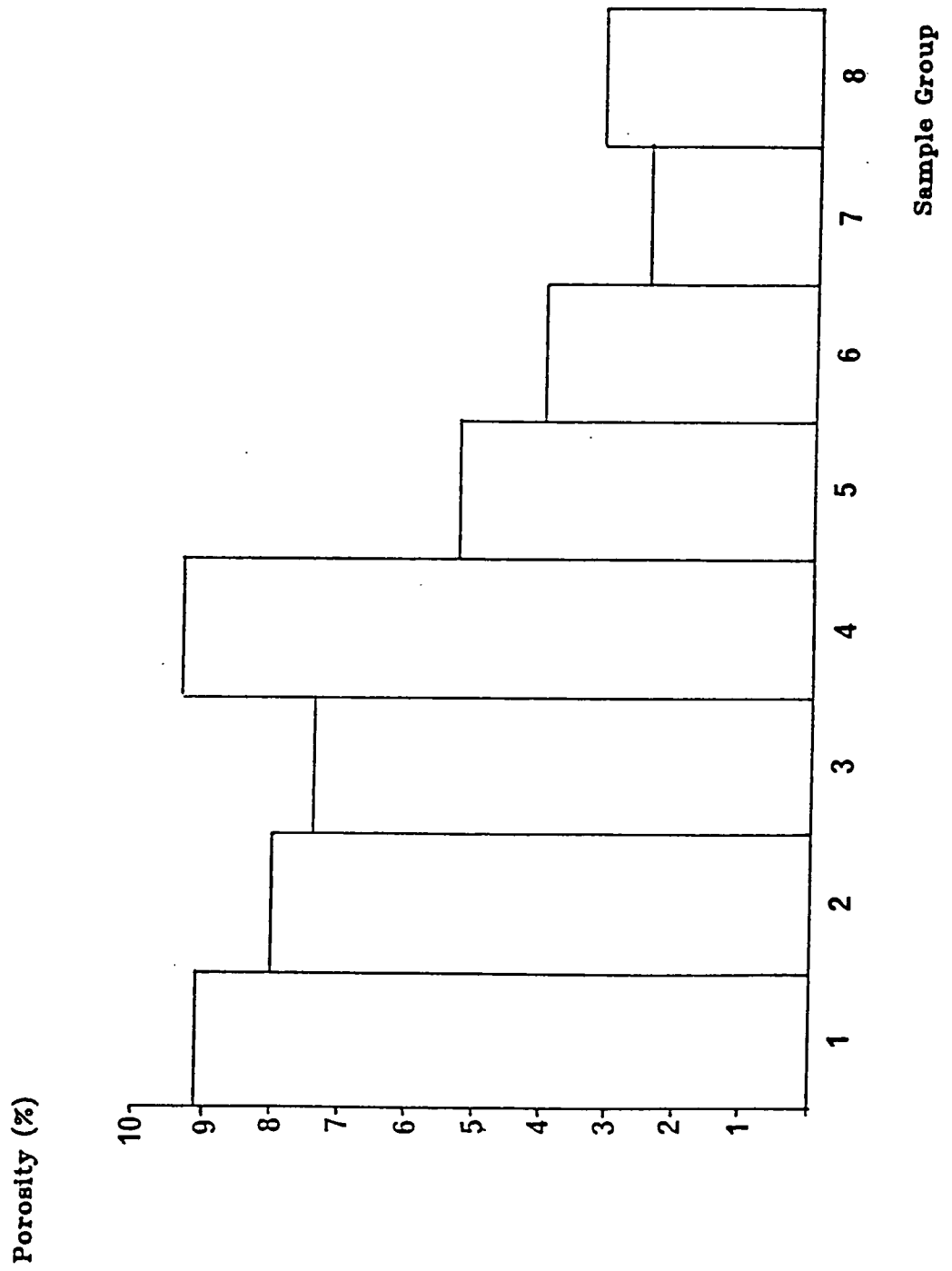
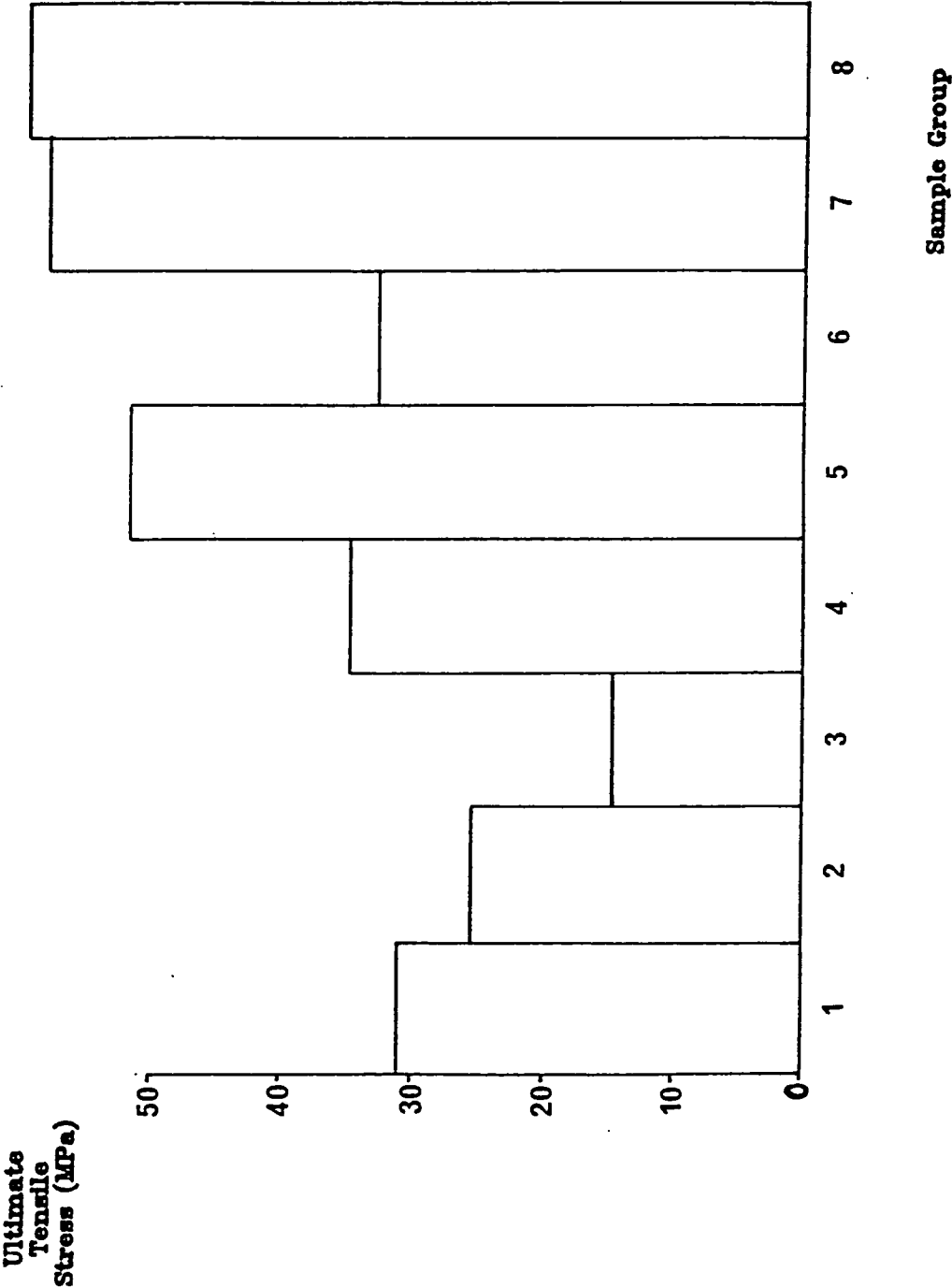


Figure 20: Values of Ultimate Tensile Stress obtained  
by Diametral Compression of Sintered material  
investigated in Part I of the Study



## 5.2 Part II : Mechanical Tests on Samples Sintered in Different Gaseous Atmospheres

There were four main sample groups investigated in this part of the research work. The compositions of each of the Mixes are included in Section 3.3.

Initial stages of the work were to look at how each of the groups behaved under standard laboratory preparation techniques prior to changes in the method of preparation.

Figure 22 shows the "green" (as pressed) and fired porosities of pellets of each material. It can be seen that the green porosities are similar over the range of Mixes with a spread of results of only approximately 8% from an average value of 46% porosity. However following sintering the spread is much greater with Mix 2 indicating a very low porosity of 1.5% and Mixes 3 & 4 porosities up to 20%. The addition of the Binder prior to the second milling stage seemed to produce a lower porosity in the sintered material than the standard laboratory technique, reductions of 35% in pore volume being typical. The material pressed and fired on the production facility at Elmwood Sensors Ltd. also showed improved porosity over the laboratory prepared material. The Cookson material, which contained a greater percentage of impurities than the standard Barium Titanate also showed reduced porosity.

Figure 21

Sample Group	Mix Used	
1	1	
2	2	
3a	3	Addition of Binder prior to Milling
3b	3	Addition of Binder as normal
3c	3	Cookson "low purity" BaTiO <sub>3</sub> used
4a	4	Pellets pressed and fired at Durham
4b	4	Pellets pressed at Elmwood Sensors and fired at Durham
4c	4	As 4b but two stage sintering with the "Green" pellet tested with Binder removed
4d	4	Samples produced at Elmwood Sensors

Figure 22: Porosity in "green" and sintered pellets for the Mixes used in Part II of the Study

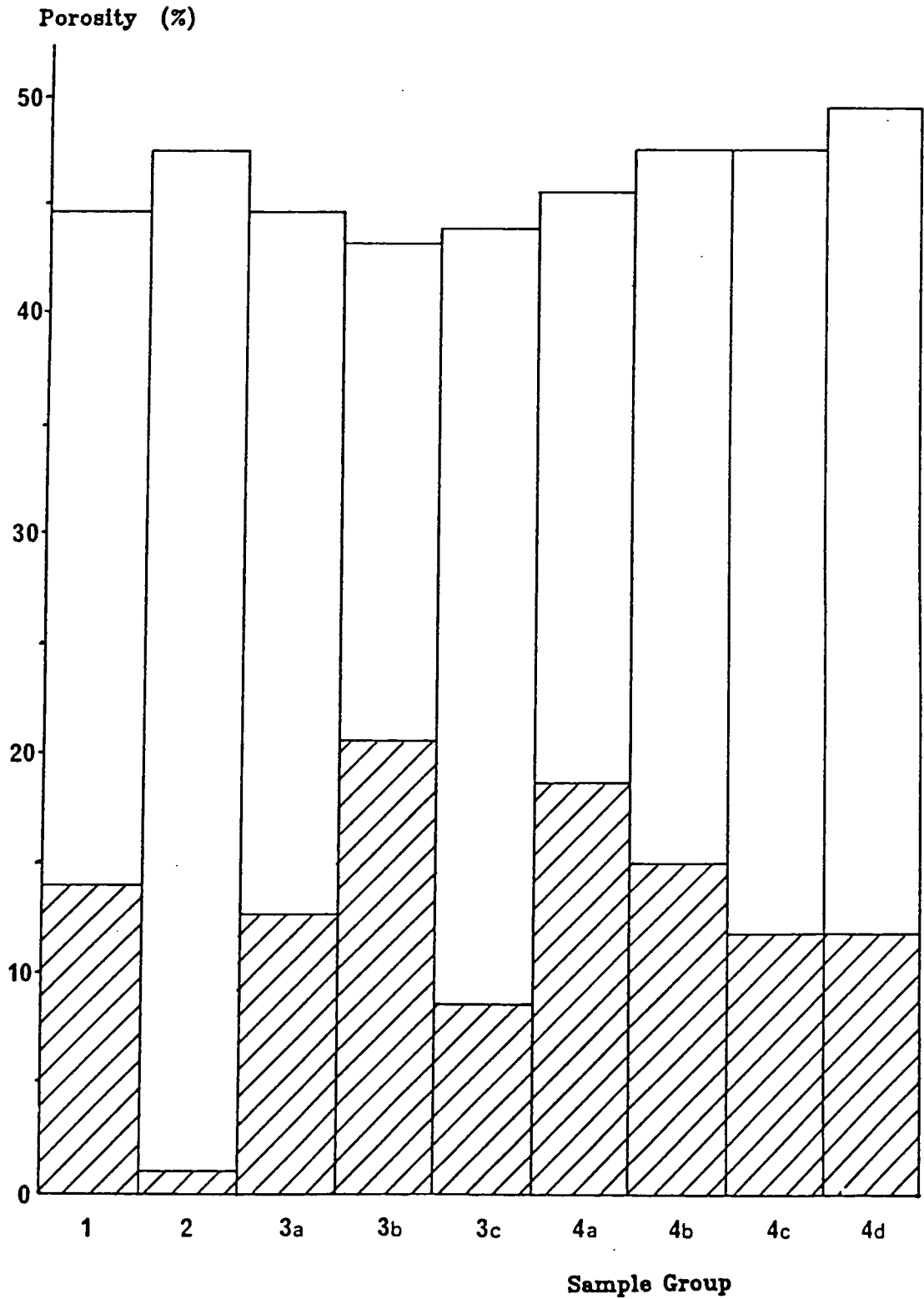


Figure 23 shows the strength of the pellets in the "green" state obtained from diametral compression of the pills between curved loading anvils. Addition of the binder prior to milling shows an increase in strength of the pressed pellet. The Elmwood prepared powder, in particular the Binder and Die Lubricant used and their method of addition, produced a very strong pill. This allowed easy transportation between press and furnace.

The effect of the binder on pill strength was investigated by burning off the binder from the pills at 500°C and then strength testing the samples under Diametral Compression. A decrease in strength of 80% was recorded.

Figure 24 indicates the variations in diametral compressive strength for the sintered pellets. The highest values were obtained for Mix 2, which contained the laboratory prepared  $\text{BaTiO}_3$ . The Elmwood production pressing and sintering stages were shown to be beneficial in producing stronger pellets. Addition of the Binder prior to milling led to a 100% increase in strength over material prepared in the standard way.

Further investigations were conducted with Mix 4 which involved pressing pellets over a range of pressures. Figure 25 shows the results of this short study. Porosity decreased with increasing pressing pressure, however there were incidents of cracking at the higher pressures (>200MPa)

Figure 23: Ultimate Tensile Stress for the "green" pellets of the Mixes used in Part II of the Study

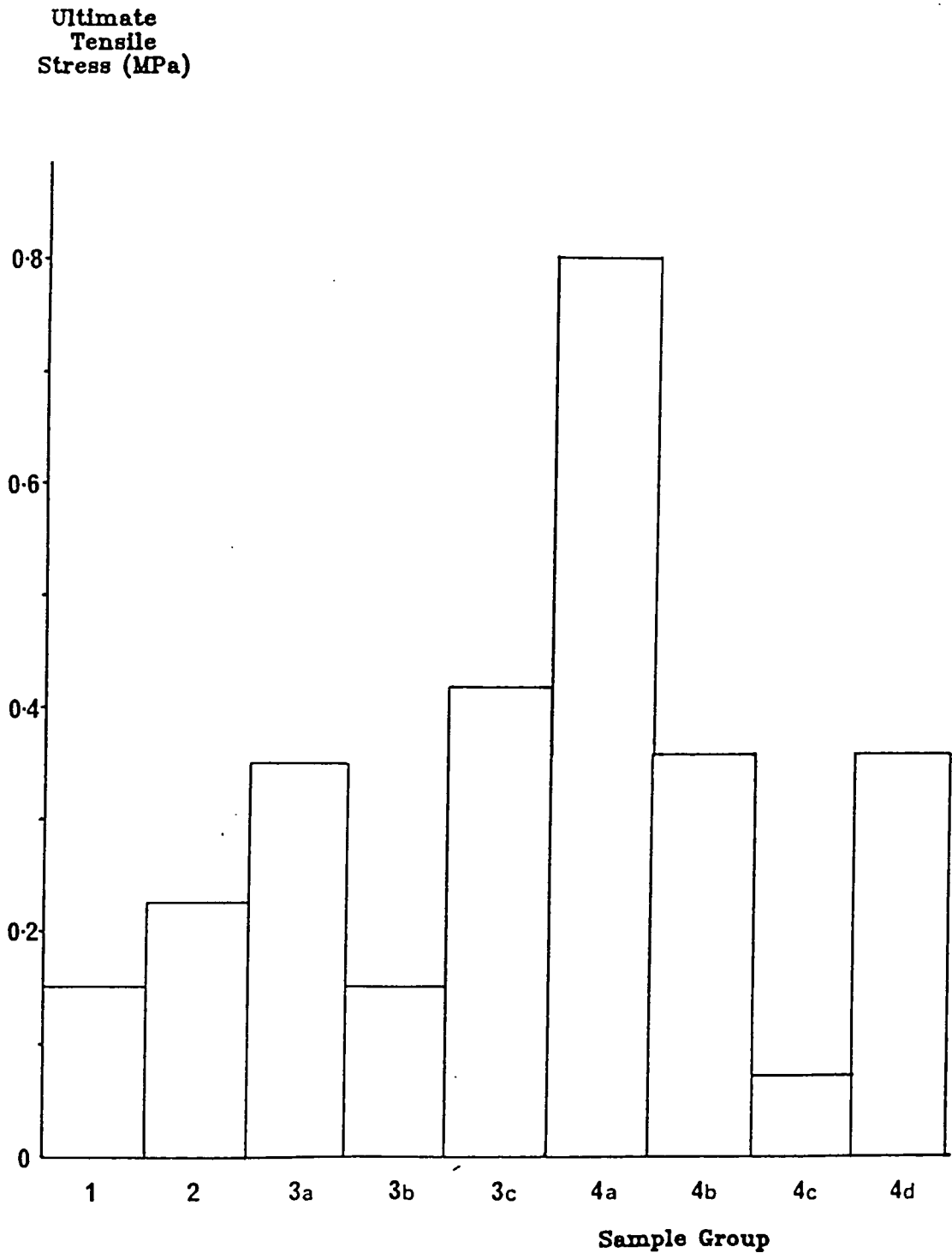




Figure24: Ultimate Tensile Stress for the sintered pellets of the Mixes used in Part II of the Study

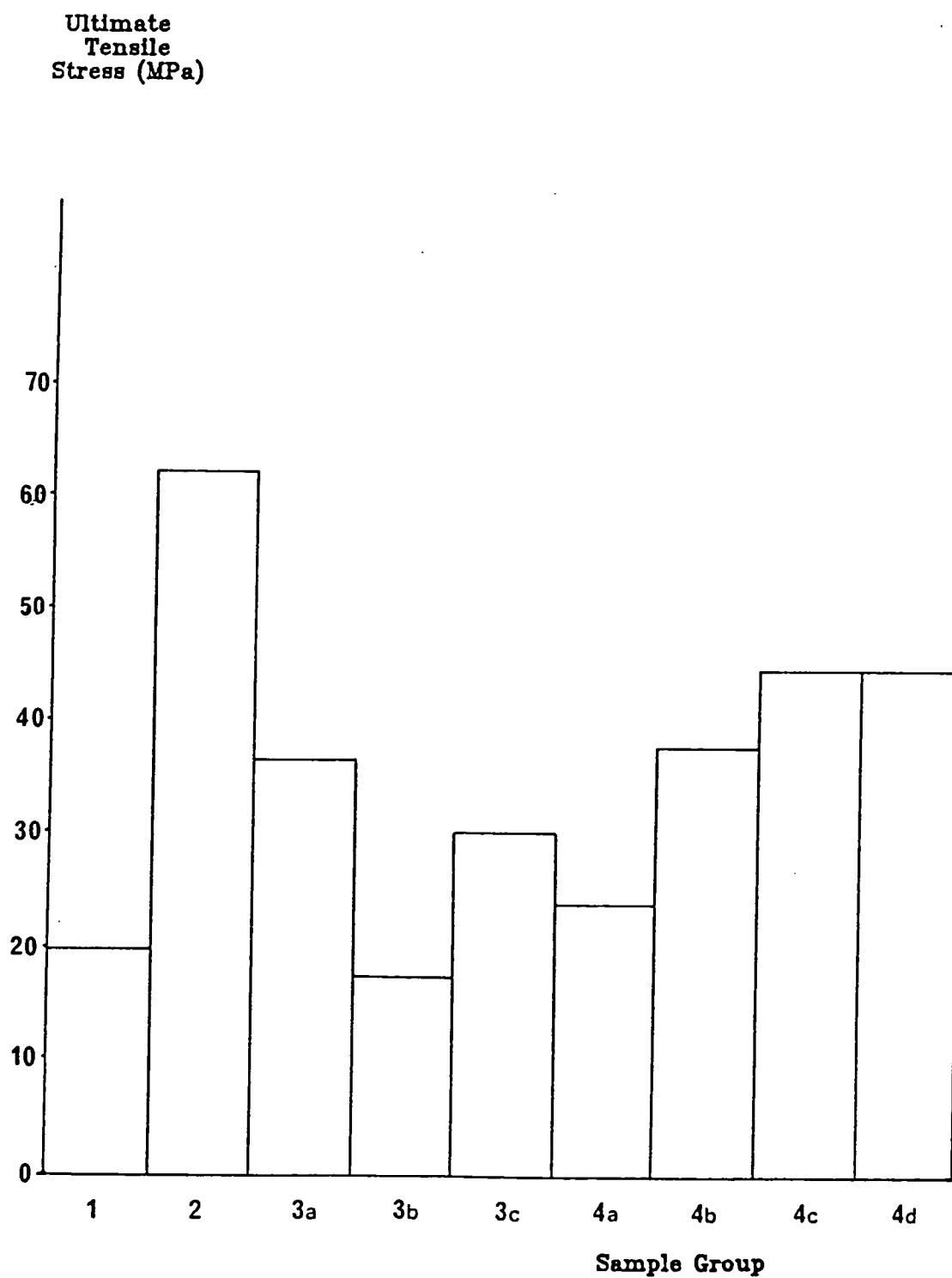
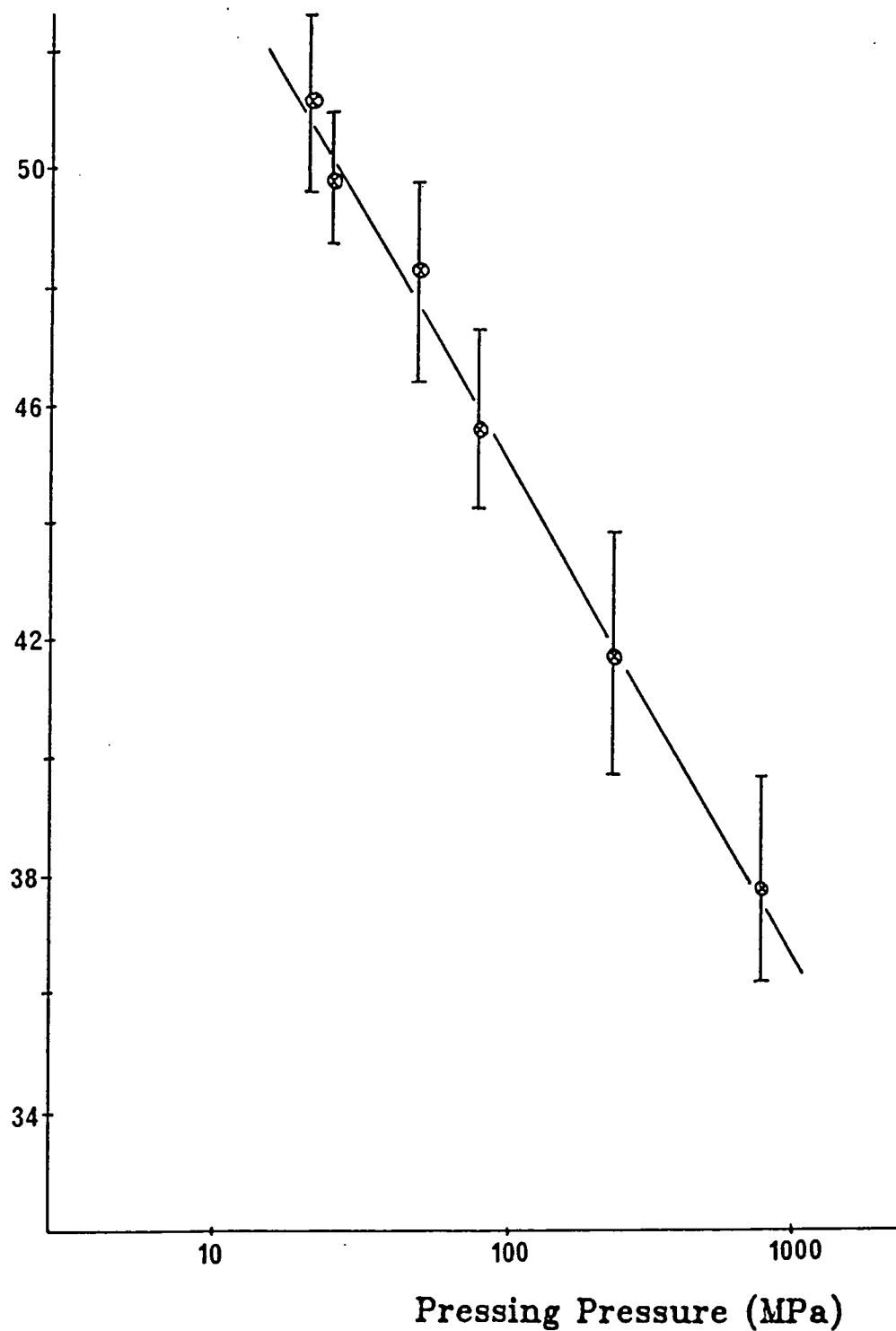


Figure25: A Plot of Porosity in the "green" pellet  
against Pressing Pressure for Mix 4

Porosity (%)



The effects of multiple sintering were also investigated. At Elmwood if a pellet does not satisfy the required electrical criteria required it is normally sintered a second (or third) time and retested. The diamteral compressive strength of pellets which had been sintered numerous times was measured as was the porosity. Pellets prepared and pressed at Elmwood Sensors Ltd. were used for the study.

	Sintered			Elmwood
	Once	Twice	3 times	Sinter
Diametral Comp.				
Strength (MPa)	34.8	35.3	36.1	44.5
Porosity (%)	15.0	15.4	15.8	12.0

A slight increase in porosity and strength was noted with repeated sintering. However the improved strength of pellets sintered in the Elmwood production furnace when compared with those sintered in the Durham tube furnace can be clearly seen.

The major study of Part II of the Programme investigated the response of the powders to sintering atmospheres ranging from 100% O<sub>2</sub> to 100% N<sub>2</sub>. Each powder was pressed into three pellet sizes: 39mm, 13mm, and 5.1mm diameters which were sintered together. The sintering atmospheres used are displayed in Figure 26.

Figure 26 : The sintering atmospheres used for  
each of the Mixes

Mix	Group	Atmosphere
1	1	100% N <sub>2</sub>
	2	80% N <sub>2</sub> 20% O <sub>2</sub>
	3	60% N <sub>2</sub> 40% O <sub>2</sub>
	4	40% N <sub>2</sub> 60% O <sub>2</sub>
	5	20% N <sub>2</sub> 80% O <sub>2</sub>
	6	100% O <sub>2</sub>
2	1	100% N <sub>2</sub>
	2	80% N <sub>2</sub> 20% O <sub>2</sub> (1320°C)
	3	80% N <sub>2</sub> 20% O <sub>2</sub> (1400°C)
	4	60% N <sub>2</sub> 40% O <sub>2</sub>
	5	40% N <sub>2</sub> 60% O <sub>2</sub>
	6	20% N <sub>2</sub> 80% O <sub>2</sub>
	7	100% O <sub>2</sub>
3 & 4	1	100% N <sub>2</sub>
	2	80% N <sub>2</sub> 20% O <sub>2</sub>
	3	60% N <sub>2</sub> 40% O <sub>2</sub>
	4	40% N <sub>2</sub> 60% O <sub>2</sub>
	5	20% N <sub>2</sub> 80% O <sub>2</sub>
	6	100% O <sub>2</sub>

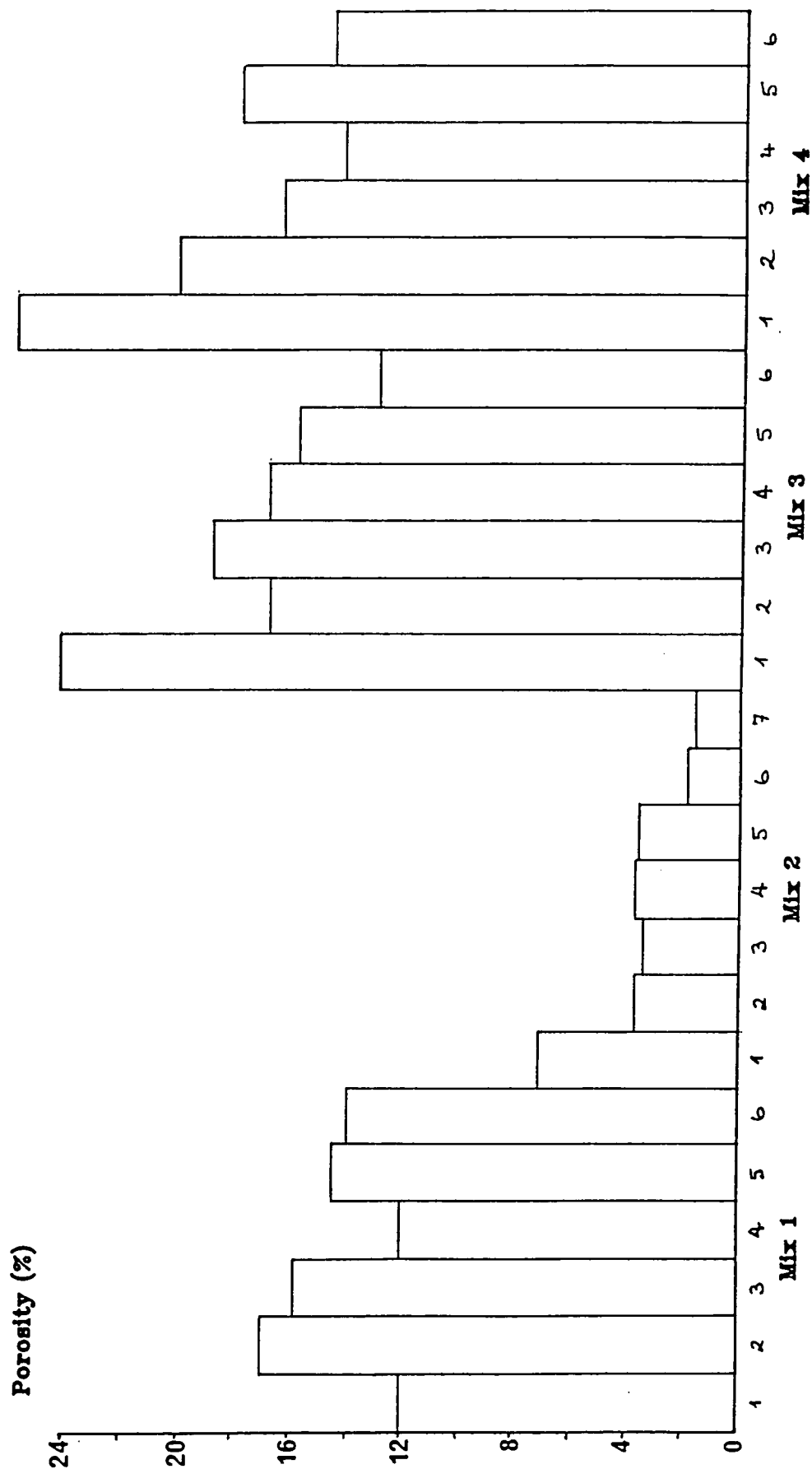
The fired porosities of all of the pellets were measured using the mass/volume technique, and the results are displayed in Figure 27. It can be seen that for the 13mm pills there was an overall reduction in porosity with increasing oxygen partial pressure, for all of the mixes. Mixes 3 and 4 showed similar porosity values. However, the values of porosity were high ranging from 27 to 16%. Mix 1 showed porosity values of approx 14% and Mix 2, of approx 3%. The larger (39mm) and smaller (5.1mm) pellets (Figures 28 & 29 respectively) showed similar porosity values, although porosity did not appear to be affected by the sintering atmosphere, except at low oxygen partial pressures, where very high values of porosity were noted.

Figure 27 displays the values of strength obtained from Diametral Compression and Four-Point Bend Tests.

The values obtained from the beam test were on average twice those obtained for diametral compression specimens. Mix 1 did not seem to be affected by the sintering atmosphere and the values of 23MPa under Diametral Compression and 42MPa under Four-Point Bending were consistent. Mix 2 showed small changes in strength with the highest values obtained at conditions close to Atmospheric. Four-Point Bending recorded values of 93MPa, with 70MPa for Diametral Compression.

Mixes 3 and 4 showed similar values with Mix 4 being marginally stronger. With 0% O<sub>2</sub> the values of Ultimate Tensile Stress

Figure27: Values of Porosity for 13mm Pellets  
sintered in different gaseous atmospheres



**Figure28: Values of Porosity for 39mm Pellets  
sintered in different gaseous atmospheres**

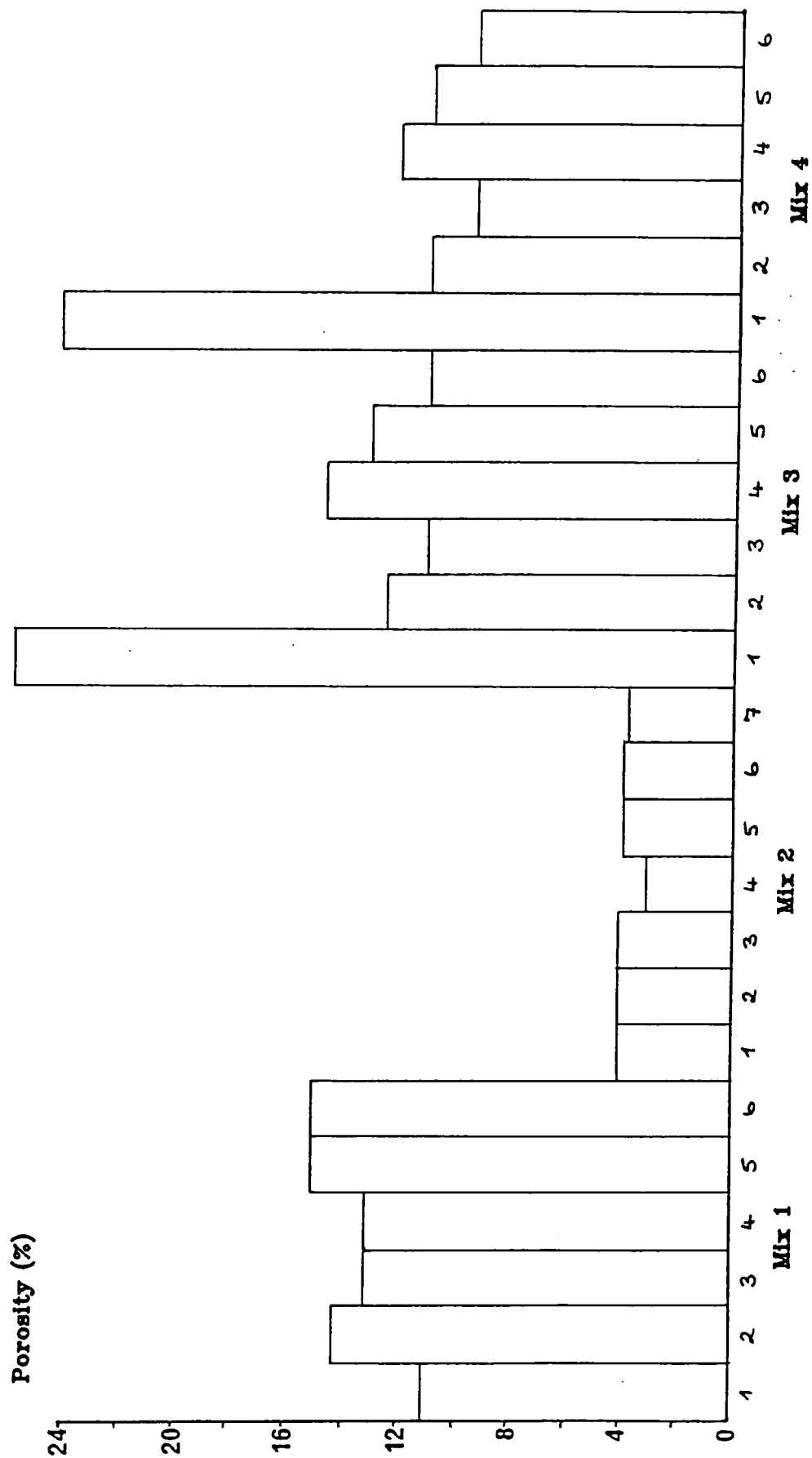


Figure 29: Values of Porosity for 5.1mm Pellets  
sintered in different gaseous atmospheres

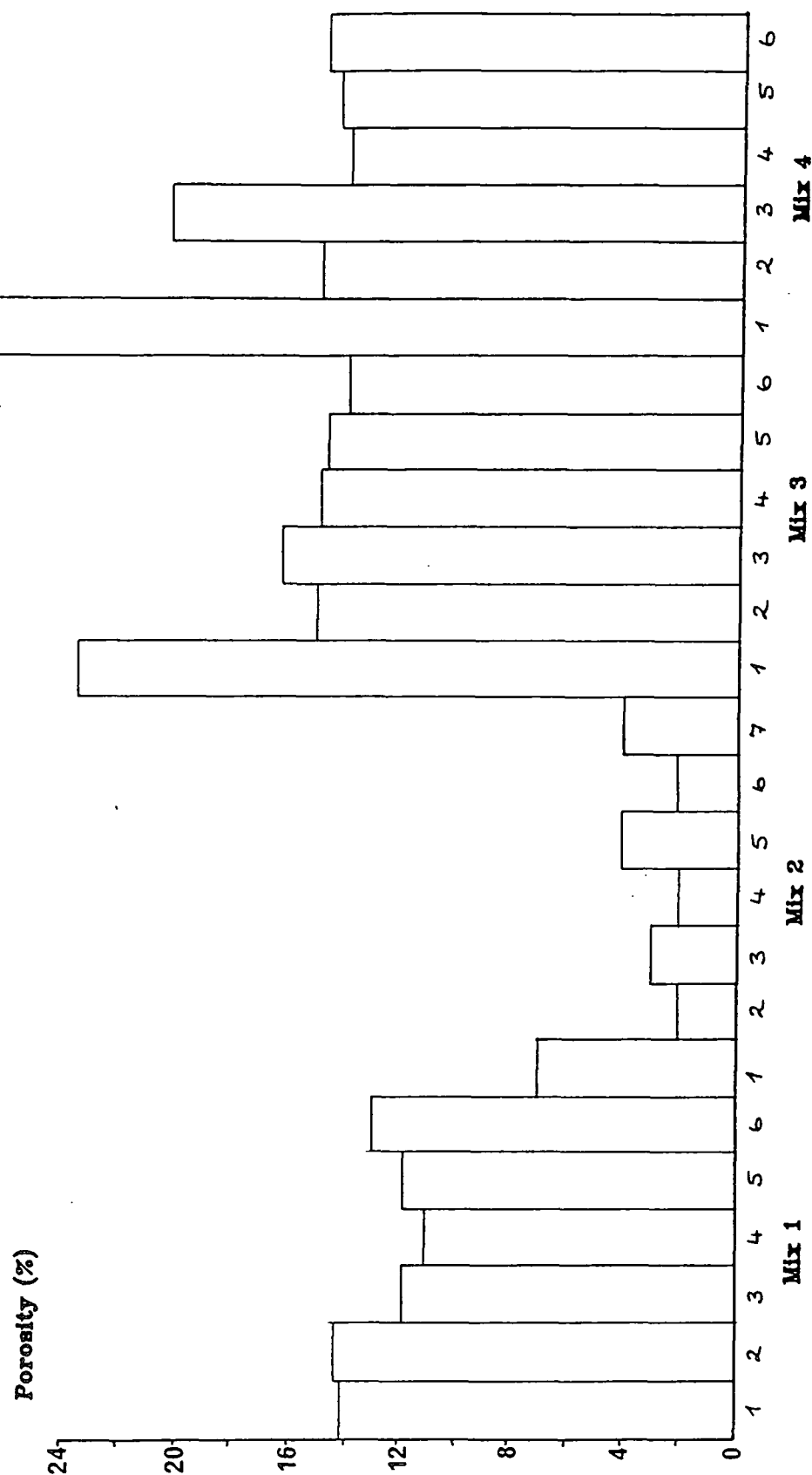
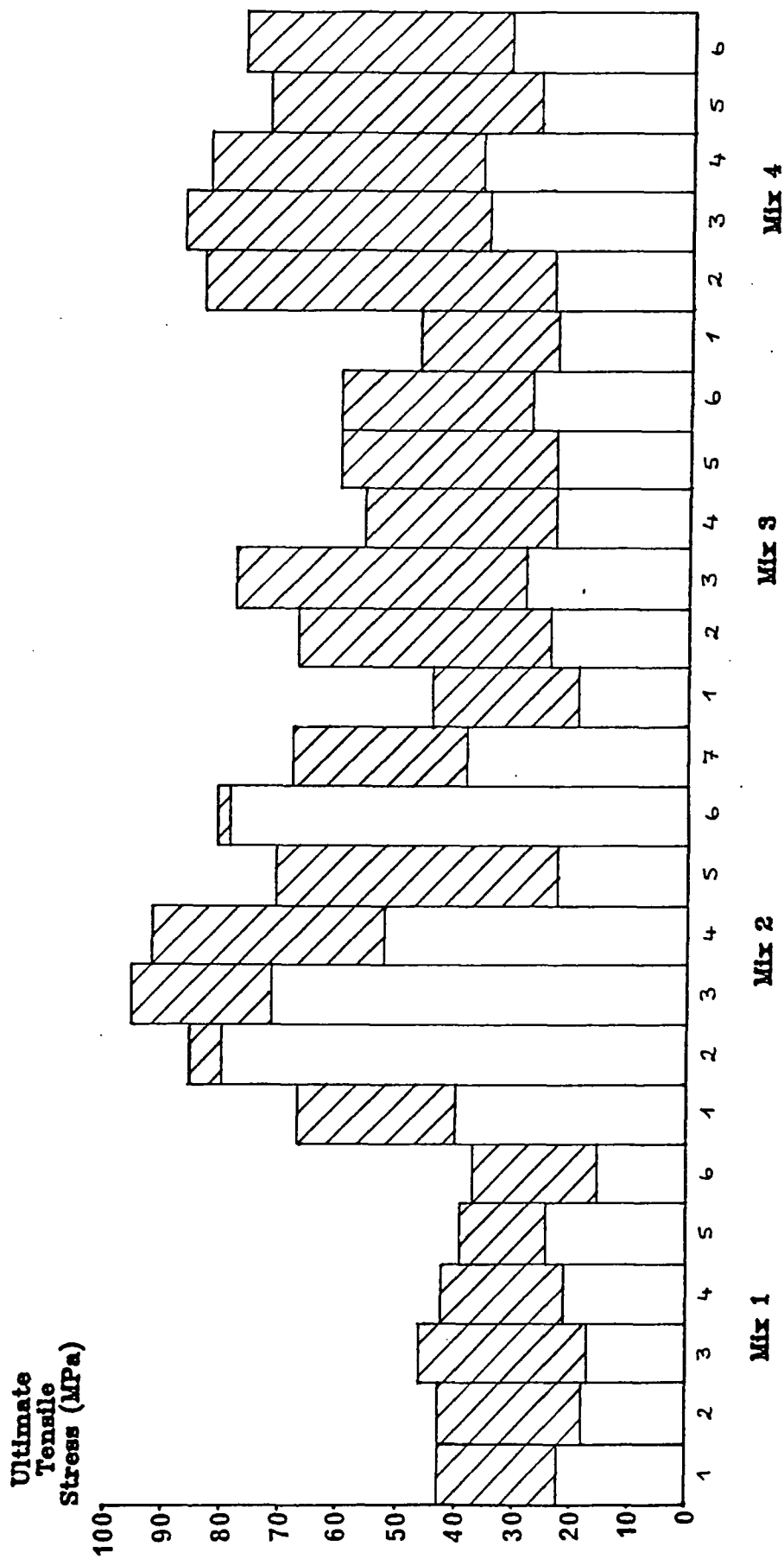




Figure30: Values of Ultimate Tensile Stress obtained from  
Diametral Compression and Bend Tests on specimens  
sintered in different gaseous atmospheres



were the lowest at 48MPa and 25MPa for Beam and Disc Tests respectively. However, values of 83MPa and 35MPa were measured for the two techniques at 40% N<sub>2</sub> and 60% O<sub>2</sub> sintering atmosphere.

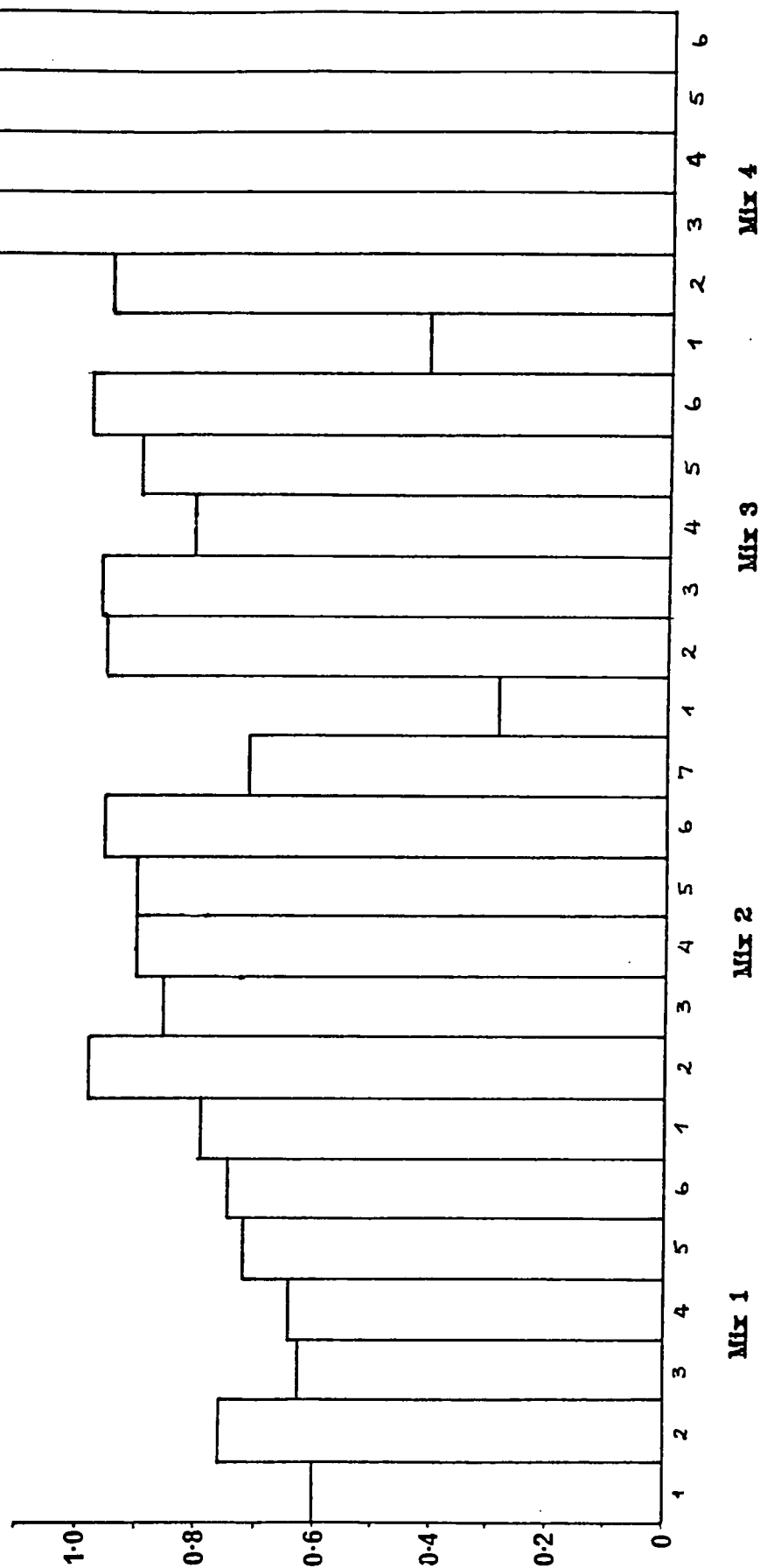
Figure 31 shows the results of fracture toughness obtained from the Four-Point Bend Test on a Notched Beam. The values of Fracture Toughness were similar to those which had been previously measured for pure Barium Titanate Dielectric material.

Mix 1 showed the lowest average values of fracture toughness with a trend towards increasing toughness with oxygen partial pressure. The range of toughness values was limited, however, from 0.6 to 0.75 MPam<sup>1/2</sup>. The highest fracture toughness values were obtained for samples sintered in flowing air.

Mix 2 showed marginally higher toughness values with a similar trend and the highest value obtained for air (80% N<sub>2</sub> 20% O<sub>2</sub>) sintered samples This Mix showed a much higher value of strength than Mix 1 and the fracture toughness were lower than expected.

Mix 3 showed similar fracture toughness values to Mix 2 with values of 0.9 MPam<sup>1/2</sup> being typical for all sintering atmospheres containing more than 20% oxygen. However, a very low value of 0.3 MPam<sup>1/2</sup> was obtained for nitrogen sintered

Figure31: Values of Fracture Toughness obtained  
from Notched Four-Point Bend Tests of Beams  
sintered in different gaseous atmospheres



samples. Low values were also measured for the samples of Mix 4 sintered in Nitrogen. Mix 4 showed the highest values with figures of  $1.3 \text{ MPam}^{1/2}$  recorded at sintering atmospheres containing more than 40% Oxygen. The value obtained when sintering in flowing air was approximately the same as for Mix 3 at  $0.95 \text{ MPam}^{1/2}$ .

Figure 32 shows the values of toughness obtained from the bend tests and also using the Vickers Indentation Technique. The Vickers Tests were conducted at a load of 20kg and the cracks originating from the corners of the indents were estimated with an optical microscope (Figure 33).

During the initial development of the technique the crack lengths were measured at different loads and it was discovered that the cracks required a minimum load of approximately 9kg with Mix 4 sintered in air to propagate from the corners of the indents.

The maximum lengths of the cracks had to be limited to 1.0mm as there were problems with the cracks propagating through the depth of the material being affected by the lower surface of the ceramic disc. This was seen as unstable crack growth in early tests in samples loading to 50kg.

The results obtained from the Vickers Indentation technique were 50 - 100% higher than those obtained from Notched Four-

**Figure 32: Values of Fracture Toughness obtained from Notched Four-Point Bend Tests of Beams and Vickers Indentation Techniques**

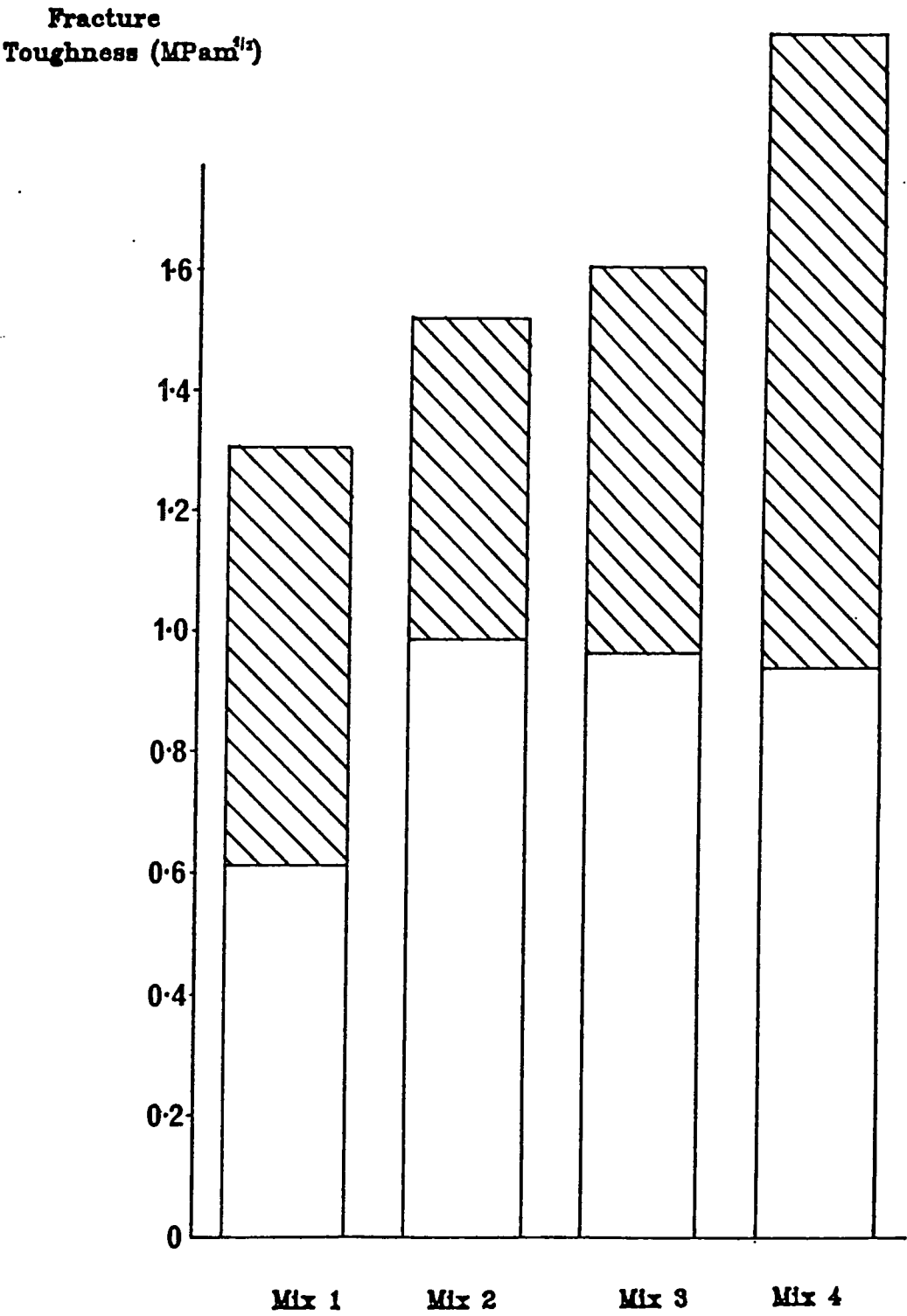
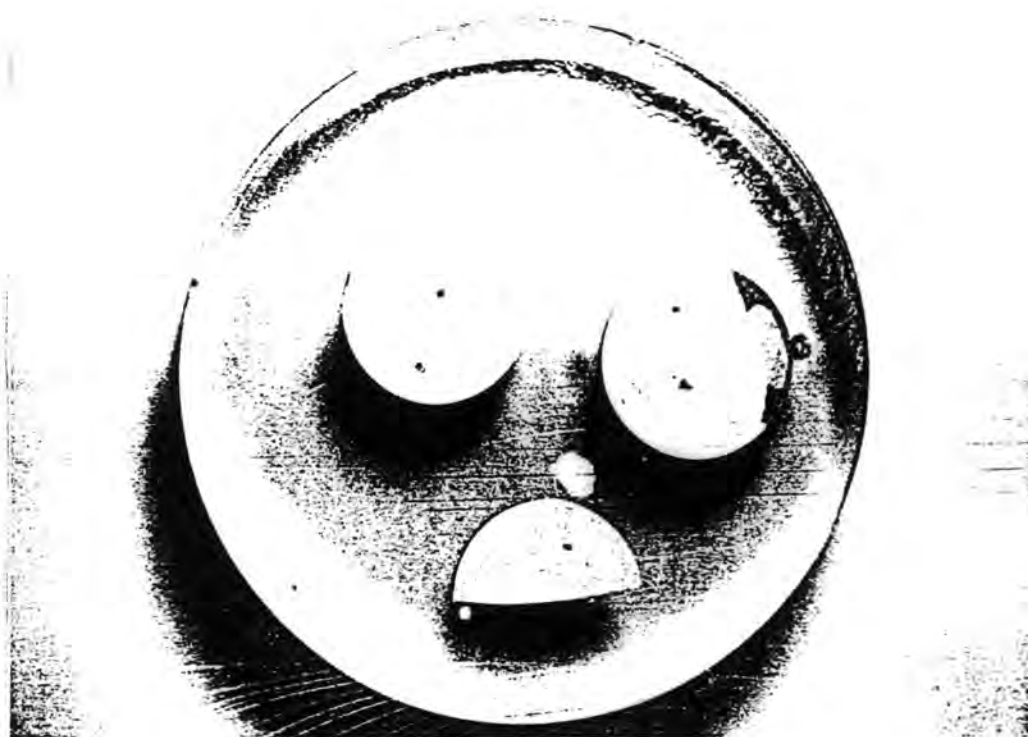


**Figure 33 : The Vickers Indents showing Cracking  
and mounting of the samples in polyester resin**



Point Bend Tests using the formula suggested by Evans & Charles (Section 4.2.3). This leads to toughness values ranging from  $1.3 \text{ MPam}^{1/2}$  for Mix 1 to  $2.0 \text{ MPam}^{1/2}$  for Mix 4. These values were obtained from averaging the results of 5 samples of each Mix. However, results scatter was higher than for Bend Tests at approximately  $\pm 15\%$  for all of the Mixes.

### 5.3. Electrical Characteristics of samples sintered in different gaseous atmospheres

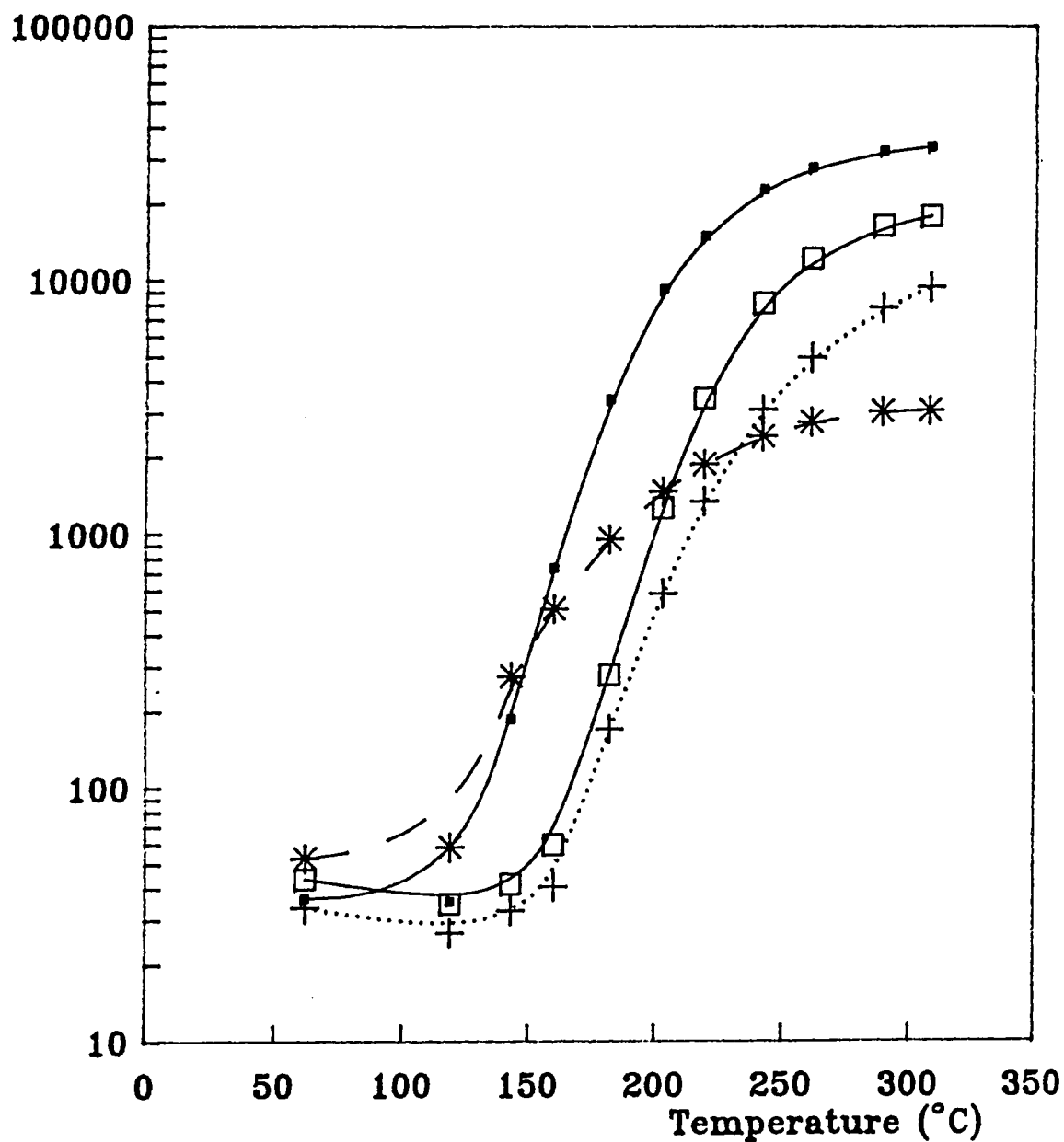
Figure 34 shows the Resistance-Temperature plots obtained for all the Mixes sintered in flowing air. Mix 1 showed the largest Resistance change of three orders of magnitude and a switching temperature of  $145^{\circ}\text{C}$ . Mix 2 containing laboratory prepared Barium Titanate showed the smallest resistance change and the shallowest gradient. A switching temperature of approximately  $150^{\circ}\text{C}$  was recorded. Mixes 3 & 4 showed similar R-T characteristics with Mix 4 showing a slightly larger PTC effect. The switching temperature of both materials was about  $180^{\circ}\text{C}$ . This was higher than the other two Mixes because of the addition of Lead Titanate to Mixes 3 & 4.

The electrical characteristics following sintering in a 100%  $\text{N}_2$  atmosphere are shown in Figures 35 & 36. Figure 35 shows the response of the samples directly after firing and Figure 36 shows similar samples after being annealed in air for 120 minutes at  $1100^{\circ}\text{C}$ . All of the samples show greatly improved properties following annealing. Mix 4 showed the steepest gradient and a total resistance change of close to three orders of magnitude. Mix 3 was very similar and the switching temperature was unchanged at  $180^{\circ}\text{C}$ . Both of these Mixes showed a decreased Switching Temperature of  $165^{\circ}\text{C}$  after sintering in Nitrogen. Mix 1 again showed a switching temperature of  $145^{\circ}\text{C}$  but the resistance change was reduced from the air sintered



Figure 34: Resistance-Temperature Plots for  
MIXES 1,2,3 & 4 Sintered in 80% N<sub>2</sub> 20% O<sub>2</sub>

Resistance (ohm)



—■— MIX 1    \* MIX 2    ·+· MIX 3    —□— MIX 4

**Figure 35 : Resistance–Temperature Plots for  
MIXES 1,2,3 & 4 Sintered in 100% N<sub>2</sub>**

Resistance (ohm)

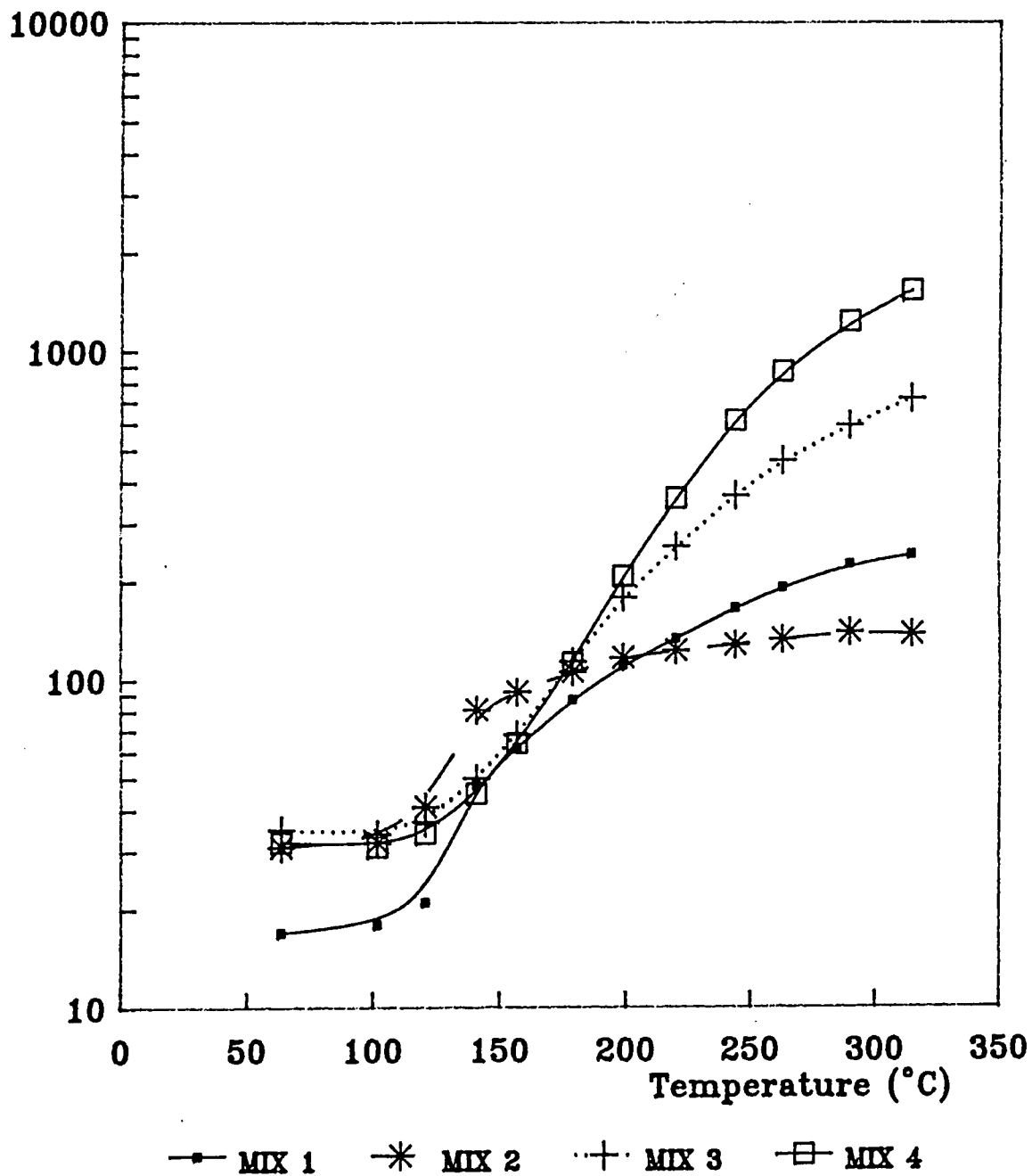
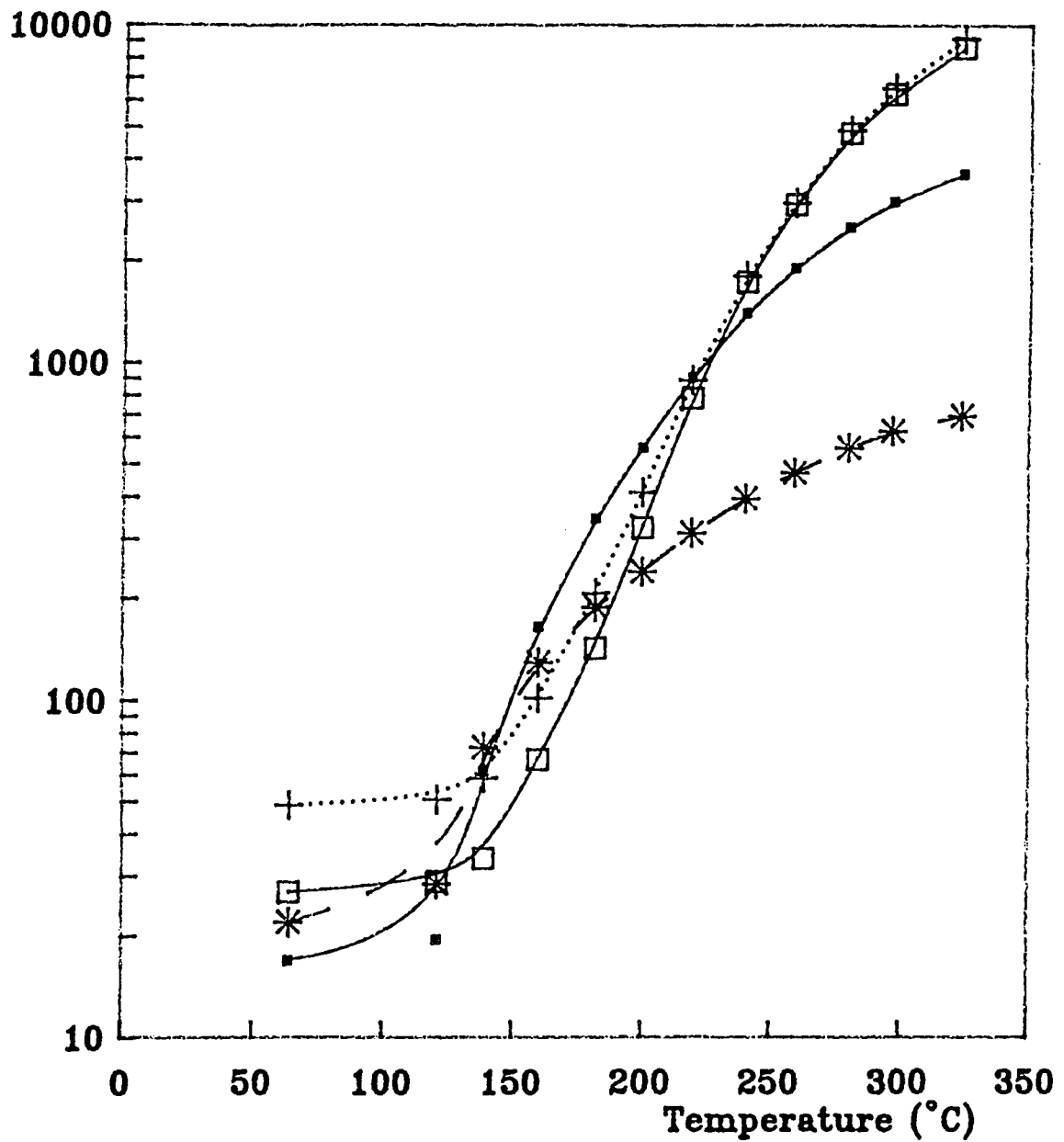


**Figure 36 : Resistance-Temperature Plots for MIXES 1,2,3 & 4  
Sintered in 100% N<sub>2</sub> and Annealed in Air**

Resistance (ohm)



—■— MIX 1    \* MIX 2    ·+· MIX 3    —□— MIX 4

samples at two orders of magnitude. Mix 2 again showed only a limited PTC effect of one order of magnitude.

Figures 37 to 40 show that at higher concentrations of oxygen similar results to those from samples sintered in air were recorded. The switching temperature of all the mixes seemed consistent throughout with a small decrease at very high percentages of oxygen (80%+) for Mix 1. Mix 2 showed slightly increased changes in resistance at 100% oxygen with a maximum value of close to two orders of magnitude attained. Mix 1 showed very similar resistance changes to Mix 4 at higher oxygen concentrations with Mix 3 having slightly smaller changes in resistance. The maximum change in resistance was three orders of magnitude which was achieved by Mix 4 at all of the sintering atmospheres investigated.

Samples which had been fired at the production furnace at Elmwood Sensors Ltd. were compared with those fired at Durham in the Tube Furnace and samples fired in a Vacuum Furnace at Bradford University (Figure 41).

The Durham Furnace produced samples with the largest PTC effect with the samples prepared at Elmwood showing a resistance change half an order of magnitude less. The samples also showed a switching temperature 10°C less than the production furnace with a switching temperature of 170°C being recorded. Mix 3 which was sintered at Durham showed a smaller PTC effect

**Figure 37: Resistance-Temperature Plots for  
MIXES 1,2,3 & 4 Sintered in 60% N<sub>2</sub> 40% O<sub>2</sub>**

Resistance (ohm)

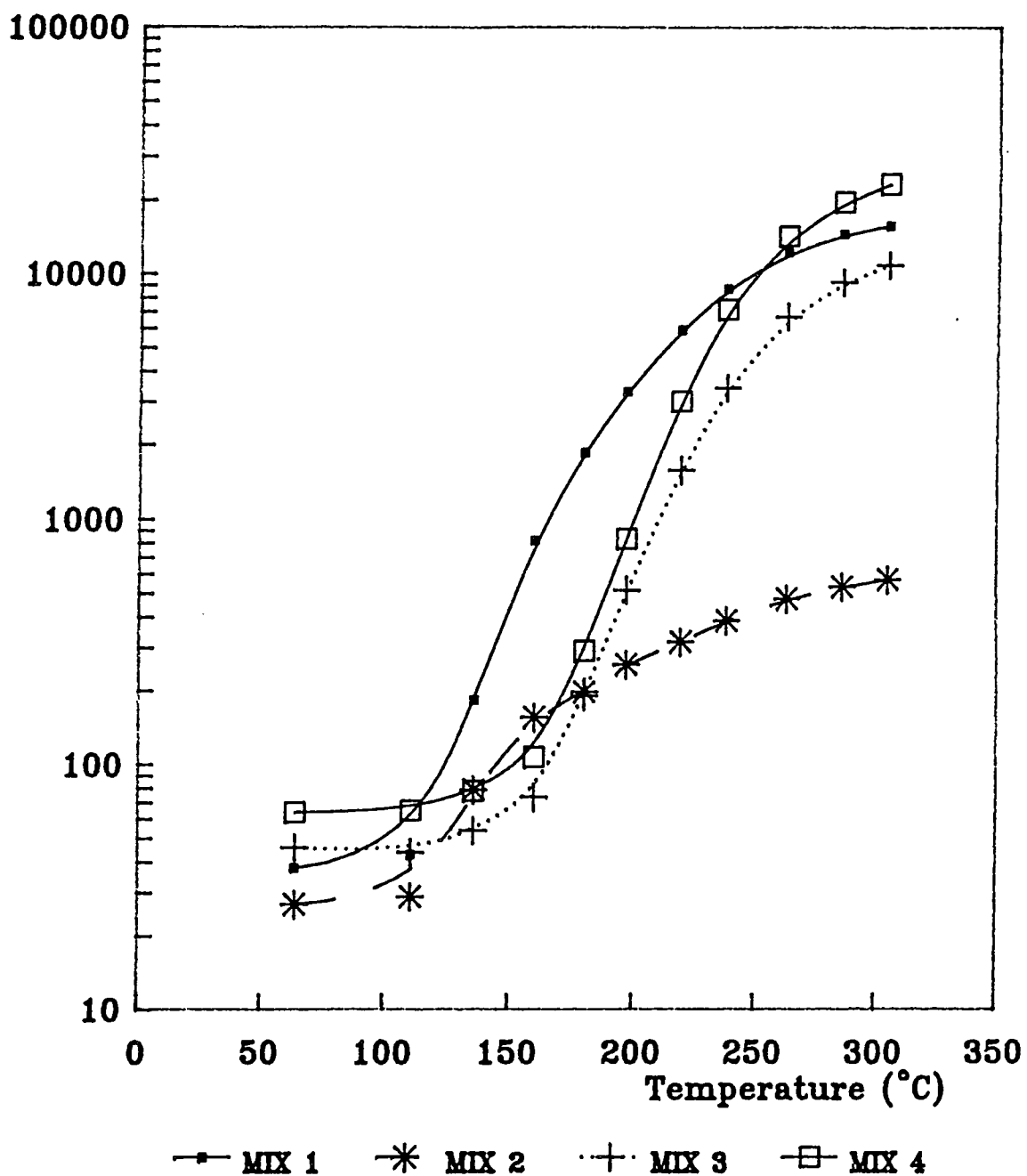


**Figure 38: Resistance--Temperature Plots for  
MIXES 1,2,3 & 4 Sintered in 40% N<sub>2</sub> 60% O<sub>2</sub>**

Resistance (ohm)

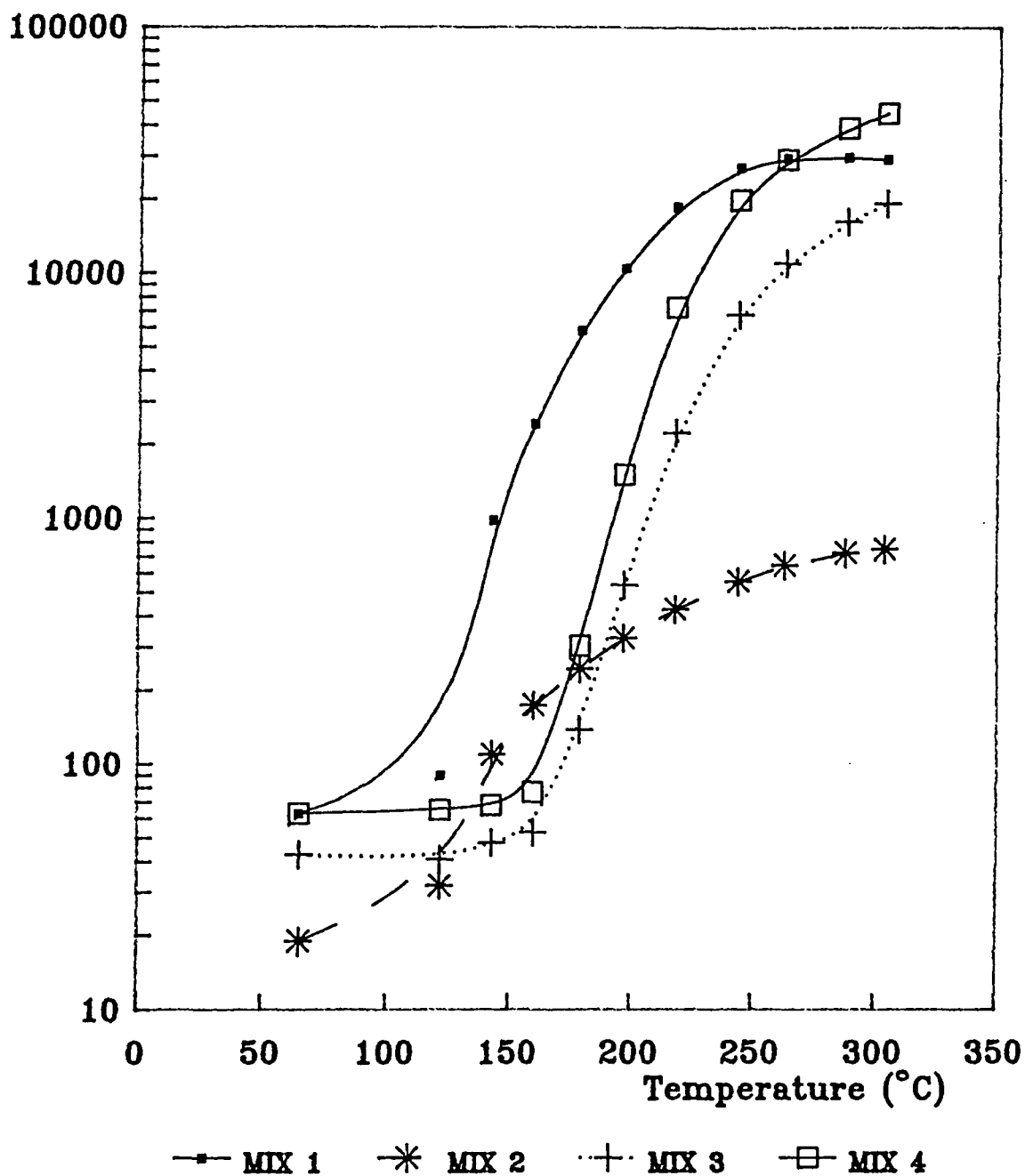
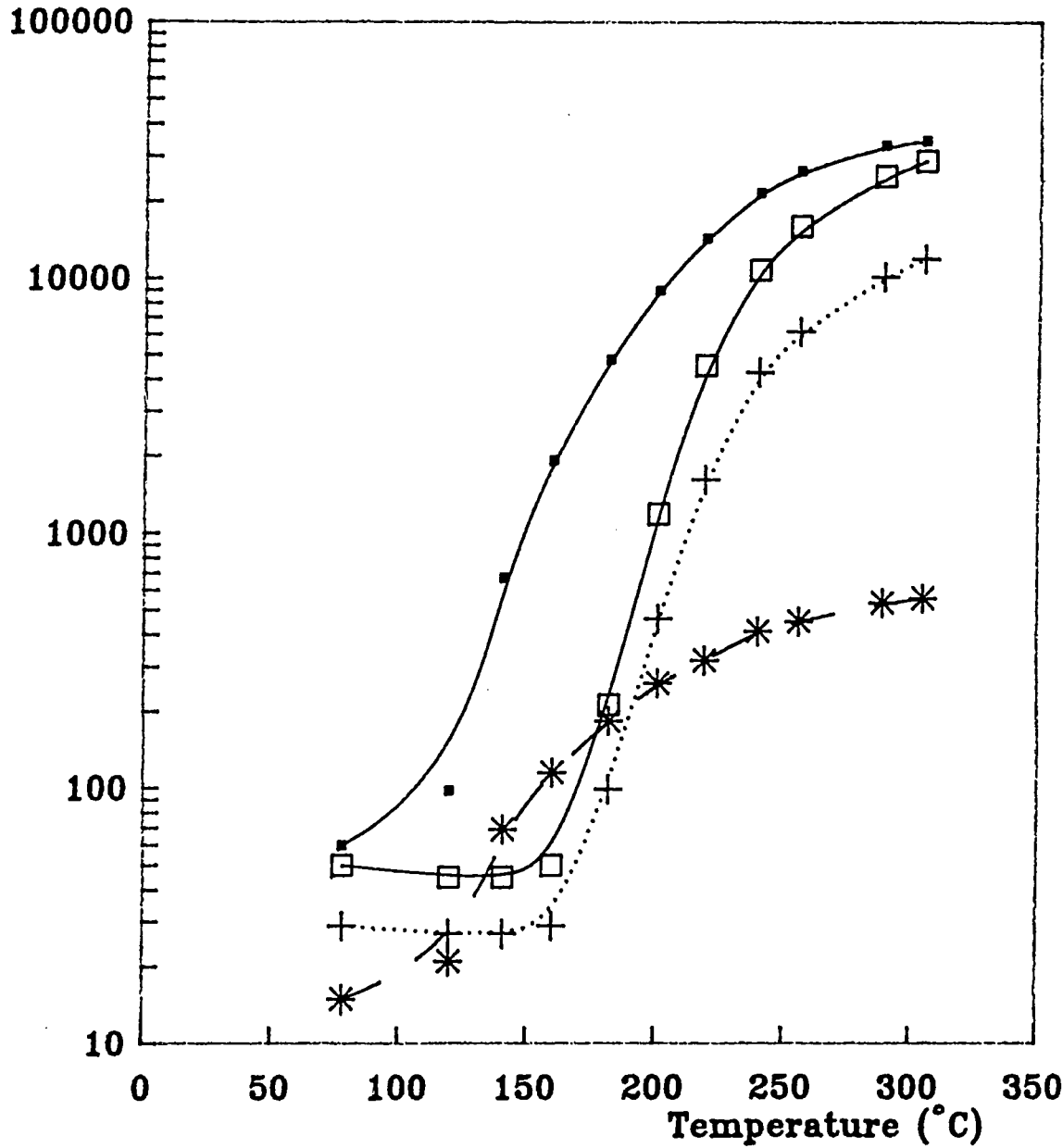


Figure 39: Resistance-Temperature Plots for  
MIXES 1,2,3 & 4 Sintered in 20% N<sub>2</sub>80% O<sub>2</sub>

Resistance (ohm)



—■— MIX 1    \* MIX 2    ·+· MIX 3    —□— MIX 4

**Figure 40 : Resistance-Temperature Plots for  
MIXES 1,2,3 & 4 Sintered in 100% O<sub>2</sub>**

Resistance (ohm)

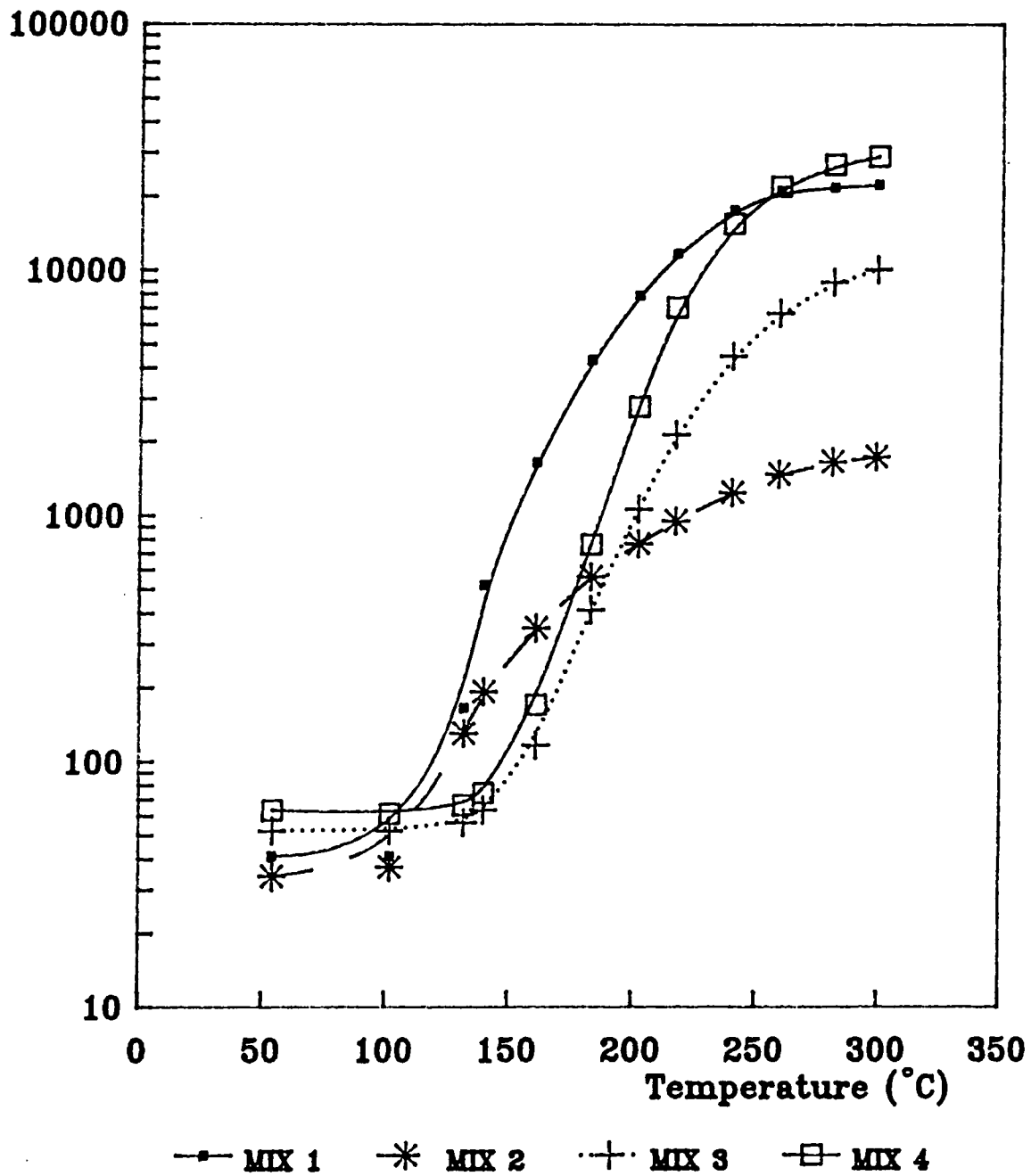
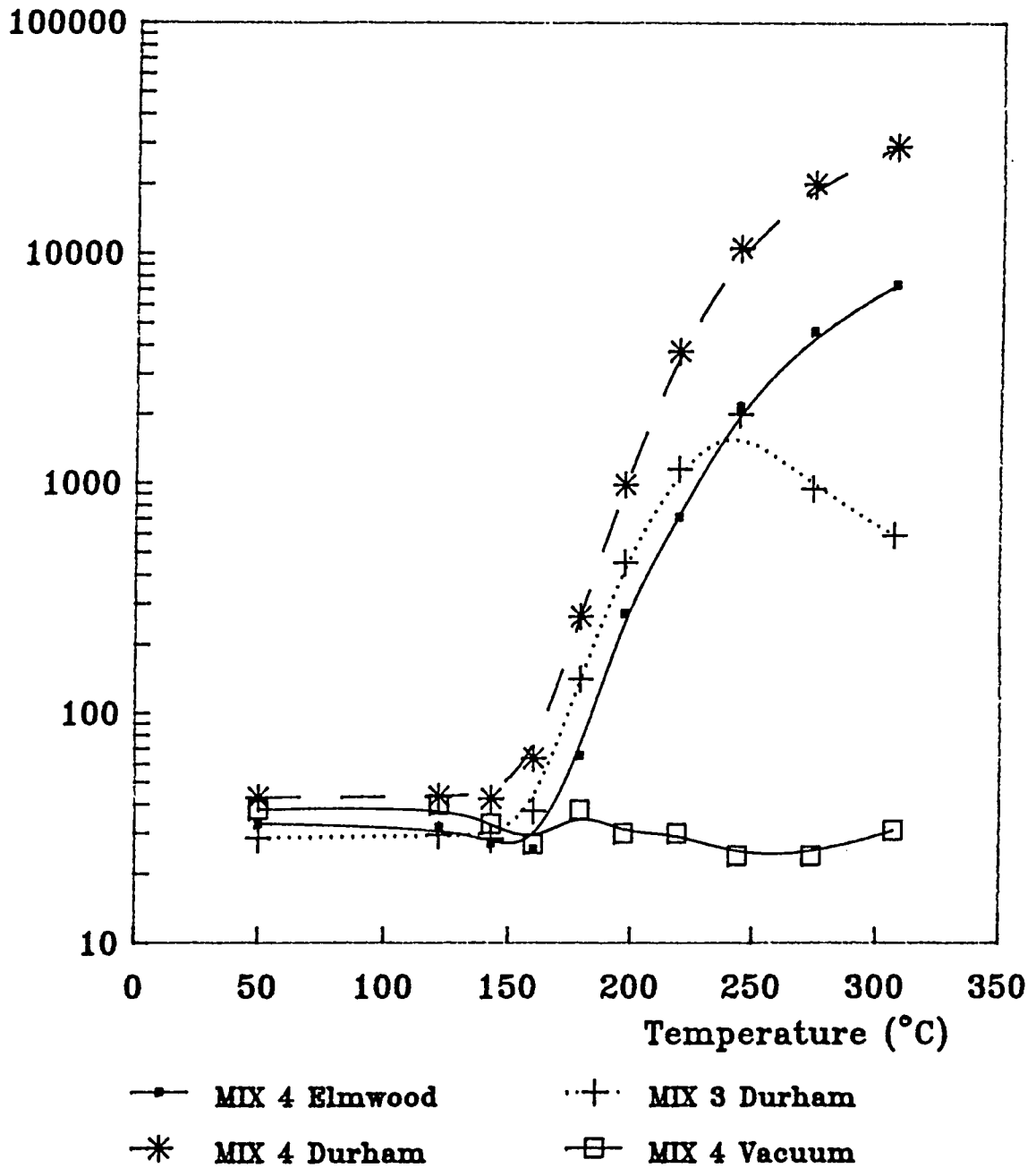




Figure 41: Resistance-Temperature Plots for MIXES 3 & 4 Sintered in Different Furnaces

Resistance (ohm)



than the two combinations above and less than when flowing air was used (as opposed to static air). An NTC effect (reduction in resistance with increasing temperature) was observed with Mix 3 sintered in static air at Durham.

The samples sintered in the Vacuum Furnace showed no PTC effect at all, possibly due to the non-oxidising atmosphere.

#### 5.4. Microstructure

The microstructure of all of the pellets used in the study was viewed under the Scanning Electron Microscope. The grain sizes were measured as accurately as possible and the shapes of the grains were assessed (Figures 42 to 45). Mix 1 seemed to have a large proportion of small grains as well as the largest spread of grain sizes when sintered in all of the atmospheres. Mix 2 showed very consistent angular grains of between 5 & 10 $\mu$ m diameter at all of the gaseous partial pressures. Mixes 3 & 4 had very similar grain sizes although at low oxygen partial pressures there were instances of small grains and a large spread of grain sizes.

Figure 42 : The Effect of Sintering Atmosphere on Grain Size & Shape

Material	Sintering Atmosphere	Grain Size (um)	Grain Shape (see key)
Mix 1	100% N <sub>2</sub>	1-5	*
	80% N <sub>2</sub> 20% O <sub>2</sub>	4-10	*
	Air	2-10	**
	60% N <sub>2</sub> 40% O <sub>2</sub>	0.5-10	**
	40% N <sub>2</sub> 60% O <sub>2</sub>	0.5-10	**
	20% N <sub>2</sub> 80% O <sub>2</sub>	2-10	**
	100% O <sub>2</sub>	2-9	**
Mix 2	100% N <sub>2</sub>	5-12	***
	80% N 20% O <sub>2</sub>	2-10	***
	Air	4-10	***
	60% N <sub>2</sub> 40% O <sub>2</sub>	4-10	**
	40% N <sub>2</sub> 60% O <sub>2</sub>	4-10	**
	20% N <sub>2</sub> 80% O <sub>2</sub>	5-10	**
	100% O <sub>2</sub>	5-10	**
Mix 3	100% N <sub>2</sub>	5-10	*
	80% N <sub>2</sub> 20% O <sub>2</sub>	1.5-10	****
	Air	6-10	****
	60% N <sub>2</sub> 40% O <sub>2</sub>	4-10	***
	40% N <sub>2</sub> 60% O <sub>2</sub>	4-10	***
	20% N <sub>2</sub> 80% O <sub>2</sub>	2-9	***
	100% O <sub>2</sub>	4-12	***
Mix 4	100% N <sub>2</sub>	1.5-10	*
	80% N <sub>2</sub> 20% O <sub>2</sub>	4-10	***
	Air	1-15	***
	60% N <sub>2</sub> 40% O <sub>2</sub>	4-10	****
	40% N <sub>2</sub> 60% O <sub>2</sub>	5-8	****
	20% N <sub>2</sub> 80% O <sub>2</sub>	3-10	***
	100% O <sub>2</sub>	4-9	***

Grain Shapes:

- \* Spherical grains
- \*\* Slightly Angular grains
- \*\*\* Angular grains
- \*\*\*\* Very Angular grains

**Figure 43: The Microstructure of the Mixes sintered in air**



4 $\mu$

**Mix 1**



10 $\mu$

**Mix 2**



10 $\mu$

**Mix 3**



4 $\mu$

**Mix 4**

**Figure 44: The Microstructure of the Mixes sintered  
in 100% Nitrogen**



100μ

**Mix 1**



4μ

**Mix 2**



100μ

**Mix 3**



4μ

**Mix 4**

**Figure 45: The Microstructure of the Mixes sintered  
in 100% Oxygen**



4μ

**Mix 1**



10μ

**Mix 2**



10μ

**Mix 3**



10μ

**Mix 4**

## 6.0 DISCUSSION

### 6.1 Part I of the Study

In general the strengths of the pellets prepared from commercially available Barium Titanate (sample groups 1-4) were approximately half of those of the calcined material (Figure 20), whilst it was discovered that on average the amount of porosity in the latter material was half that for the commercially available Barium Titanate (Figure 19). With reference to the lower mechanical strength this can be explained in terms of the increased porosity.

Comparisons of the maximum stresses between sample groups also allows the effect of pressing pressure to be investigated. The results show an increase in strength as the pressing pressure decreases. Very low pressures (under 70MPa) were also investigated but the pellets had so little strength in the unsintered (green) state that moving them to the furnace without incurring damage became extremely difficult. It was also discovered that shrinkage in the furnace was greater with the pellets pressed at lower pressures, thus leading to slightly higher densities in the fired pellets.

The effect of addition of binder to the pellets was also investigated. During early testing of the groups prepared from commercially available material it was noticed that blisters

were more likely to occur within the pellets when a binder was present. The reason for this is probably that concentration of the binder occurs in certain regions, for example cracks, and during sintering the gases produced cannot escape because of the closed pore network, and hence expand the cracks to form blisters.

Comparison of the strengths from groups 6 and 8 showed that there was an increase upon addition of the binder, however density changes were small. This increase in strength seems to be because with a binder a continuous void system is produced in the green state, consisting of many small holes linked with minute channels. This arrangement allows the liquid phase produced during sintering to flow more easily through the material eventually blocking the channels to form a closed pore system. However, with no binder present larger and potentially more damaging voids are present in the green state, which cannot be filled with the liquid phase because of the absence of channels between pores. This was suggested following mechanical testing which showed a higher scatter of results when no binder was used compared with the binder containing samples. Failure is often initiated at a particularly large or damaging crack or defect. A continuous void system provided by a binder ensures that a particularly large void is less likely to occur and so failure loads are dictated more by the properties of the material and not the size of any one void leading to more consistent results.



The reasons for the blistering of ceramics are still not yet fully understood and some researchers have suggested it may be due to large seed grains (Zajc & Drofenik, 1989). However, for the size of blisters encountered under certain conditions during this study, the addition of the binder would seem to be an important consideration.

Investigation into the porosities of the pellets cannot give an indication of which void system is present. However, most of the high strength mixes showed low porosities (less than 6%) and lower strength mixes higher porosities (in the region of 10%). Although this does not, at first, seem a large difference in porosity it represents an 80% increase in the volume of voids in the weaker samples.

It should be noted that sample groups 1, 2 & 3 showed the converse. This was because although higher pressing pressures produce a decrease in both green and sintered porosity the pore volume tends to be concentrated in damaging radial cracks originating at the circumference of the pellet. These cracks have been observed by other workers at high pressing pressures (Youshaw et al, 1982) and were observed to be a contributory factor in the failure of sintered discs under diametral compression in this work.

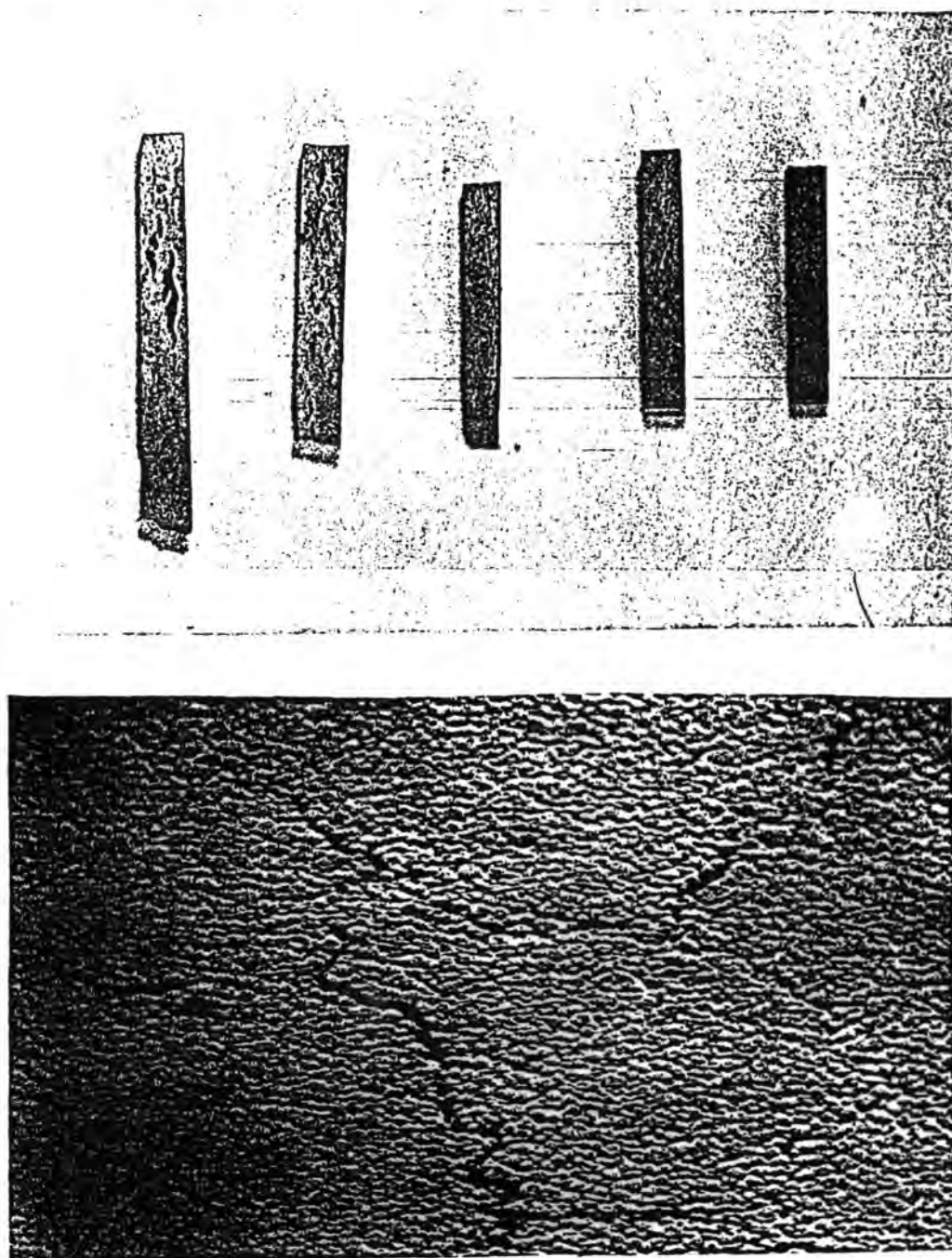
The preparation of sample group 8 involved addition of the binder directly after the calcining reaction and prior to the

second stage of milling to investigate the effects this may have on strength. The results showed little change in strength and suggest that addition of the binder followed by milling encourages better coating of each grain. One advantage of addition of the binder at this stage is that a reduction in the preparation time of the PTC of up to 8 hours can be obtained.

The Scanning Electron Microscope (SEM) was used quite extensively to look at fracture surfaces to decide whether inter- or trans-granular failure had occurred during diametral compression testing. The latter was found to be more common indicating that the liquid phase was bonding the grains well. However, in some samples both modes of failure were observed, usually inter-granular close to the initial stress concentrator or crack and trans-granular when the crack front has attained a higher speed and follows a shorter path. Blistering of the pellets was also investigated and found to occur in conjunction with large sub-surface cracks (Figure 45(b)). The cracks, which may have been present in the green state, were probably expanded during sintering by a combination of gases and the liquid phase to form the blisters. The size of the blisters seemed to be dependent on both the size of the initial crack and its distance from the surface of the pellet.

The size of the grains found within the pellets was fairly consistent between the mixes used in Part I, with a range of 5-20 $\mu$ m in diameter. The material prepared from commercial Barium

**Figure 45(b) : Blisters and their effects, showing cracking**



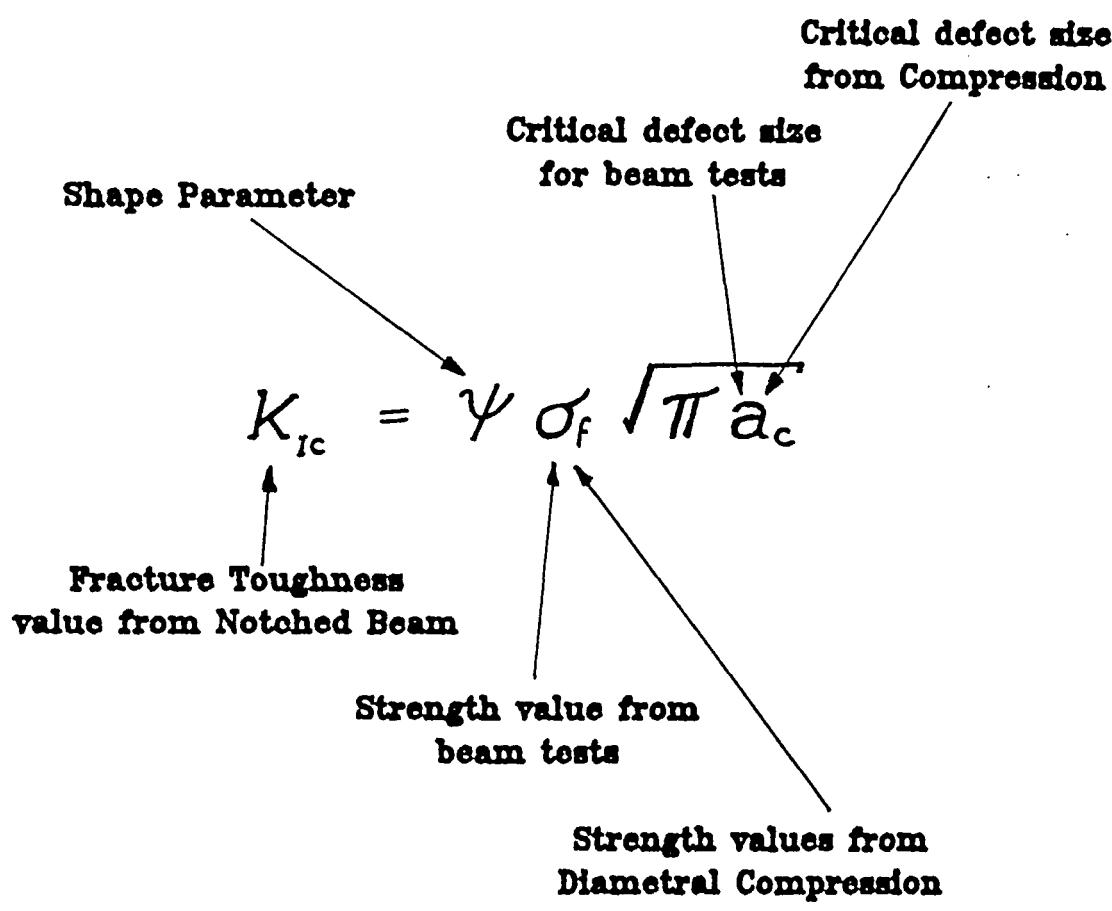
Titanate showed a number of voids up to  $40\mu\text{m}$  in diameter and cracks  $50\mu\text{m}$  in width and  $500\mu\text{m}$  in length were not uncommon (Figure 45(b)). The laboratory prepared barium titanate yielded a larger number of much smaller voids in the region of  $5\text{-}10\mu\text{m}$  in diameter and large cracks were almost nonexistent.

## 6.2. Mechanical Studies of Part II of the Project

From the results of the study on Barium Titanate PTC materials it was possible to calculate the critical defect sizes which caused failure for the Four-Point Bend and Diametral Compression specimens using equation (c). This is shown with the calculated values in Figure 46. It can be seen that the lowest value of the critical defect size for both forms of strength testing is  $40\mu\text{m}$  which compares with grains sizes of the order of  $5\text{-}10\mu\text{m}$ . The critical defect size for the diametral compression tests was much larger than for bending and this will be considered later. Thus, theories that failure is initiated in ceramic components because of individual grain inadequacies seem unjustified for this material in the light of this research. It suggests that extensive preparation to ensure small ( $<5\mu\text{m}$ ) and very regular grains may not provide benefits in mechanical properties.

Failure appears to be initiated at a large pore or crack which can be internal or at the surface (recalling that surface flaws are twice as damaging as internal ones of the same dimensions). Abnormal grain growth was not apparent in any of the materials prepared under standard laboratory conditions. This was confirmed by the results obtained from the mechanical studies.

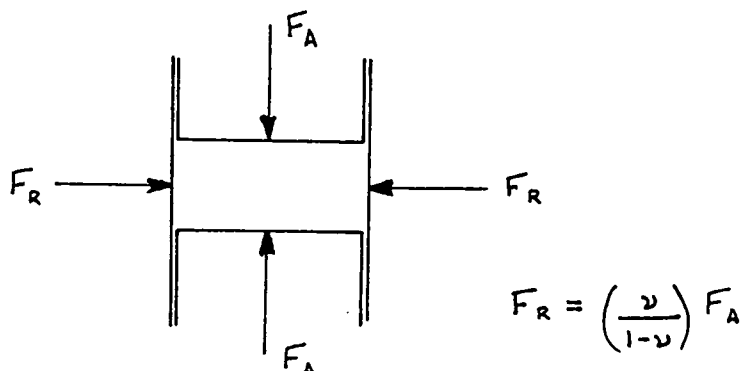
FIGURE 46



Material	$\sigma_f$ (4-pt) (MPa)	$\sigma_f$ (Comp.) (MPa)	$K_{IC}$ (MPa $m^{1/2}$ )	$a_c$ (4-pt) ( $\mu m$ )	$a_c$ (Comp.) ( $\mu m$ )
Mix 1	43	22.5	0.6	62	226
Mix 2	85	79.5	0.97	41	47
Mix 3	67	23.5	0.95	64	520
Mix 4	84	24.5	0.92	38	449

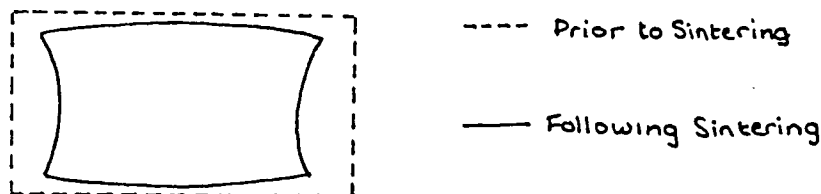
The pressing of pellets has been discussed in detail in section 2.4.3 and the non-uniform pressures that the powders are subjected to and the subsequent density variations within the compact have been mentioned. During sintering there are mechanisms which promote densification of the compacts and this leads to shrinkage in both the axial and radial directions. The degree of shrinkage depends on the density of the material prior to firing and this is why the shrinkage is uneven.

The forces to which a compact is subjected are shown in Figure 47.



If the material acted as a fluid (eg. hydrostatically) the value of  $\nu$  would be 0.5 and so axial and radial forces would be equal. However for most powders a value of 0.25 is more usual although this can be raised towards 0.5 by "wet" pressing or the addition of a binder or die lubricant. Therefore the radial force is expected to be only one third of the axial force. From this information a sample which is most porous around its circumference could be expected leading to greater

shrinkage in the radial direction (Figure 48).



The values of shrinkage were calculated for the Mixes used in Part 2 of the study which were pressed using the 13mm die and a load of 1.0 tonne which corresponds to an average pressure of 70MPa over the axial surfaces. The samples were then sintered in the tube furnace to 1320°C in an air atmosphere.

All quantities in %

Mix	Pressed Porosity	Radial Shrinkage	Axial Shrinkage	Fired Porosity
1	43.7	16.2	8.2	87.4
2	47.8	19.2	19.2	99.0
3	44.6	14.8	12.4	87.0
4	45.6	14.8	8.9	82.3

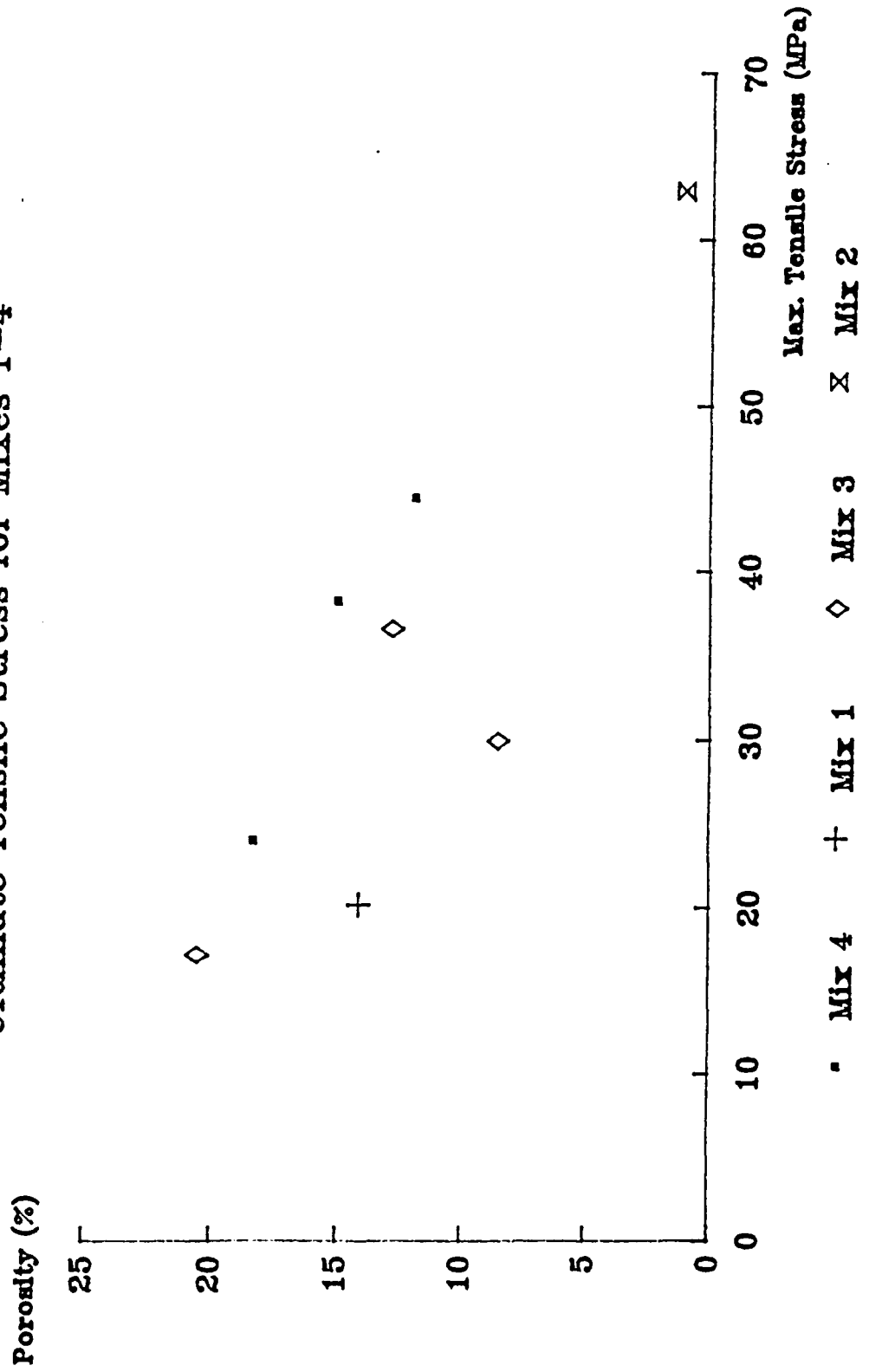


It can clearly be seen that the samples (Mix 2) which attain a high fired density have similar shrinkage in both axial and radial directions. The three other materials show radial shrinkages greater than the corresponding axial shrinkages as is described above.

The sintered pellets showed a large range of porosity values. The porosity in all cases had decreased from that of the "green" values due to the densification regimes operating during sintering. The extremely low porosity exhibited by Mix 2 shows that the utilisation of a calcined Barium Titanate produces much more powerful densification reactions. It was unfortunate that the length of the study could not be extended to include work on combinations of laboratory and commercially prepared Barium Titanate. The densification of pellets fired in the production furnace was higher than those sintered at Durham. This indicates that the time spent above a certain temperature is important in providing a dense ceramic (Figure 14) and is an obvious area for future research.

The measurement of the Strength by Diametral Compression proved successful with consistent results for each of the sample groups. Mix 2 showed the highest value but the porosity of this mix was very low and so, if sintered strength against porosity is plotted, it can be seen that the relative strengths of the materials accounting for the values of porosity (Figure 49). Mix 1 and Mix 3 (with low purity  $\text{BaTiO}_3$ ) showed values of strength below the trend line and so this leads to

Figure 49 : The Effect of Porosity on  
Ultimate Tensile Stress for Mixes 1-4



the conclusion that they are inherently less strong than the other materials if porosity and its detrimental effects on strength can be discounted. Mix 2 also showed a value of strength below the trend line and this may be a reflection of its low Fracture Toughness value of  $0.95\text{MPam}^{1/2}$ .

The increase in strength following multiple sintering is likely to be due to the diffusion of liquid phase throughout the pore network providing a more uniform structure with each subsequent firing. The porosity tended to increase slightly, owing to the removal of liquid phase by vaporisation from the material, with each subsequent firing.

The reduced porosity values obtained when Cookson "low purity" material was used can be interpreted as being due to the increased liquid phase formed in part from the impurities in the base materials. This accounts for almost 2% of the mix by mass and represents an approximate doubling of the liquid phase material. However, the failure load of this material was not as high as the low porosity indicated above. Failure of the material was often along the liquid phase which was seen on micrographs to be thicker than normal (Figure 50). Failure was thus highly dependent on the bonding of the impurities which make up the liquid phase.

Figure 50 : The Microstructure of the material made  
from Cookson "low purity" Barium Titanate



2μ



10μ

The wide variation in fired porosity for the four Mixes has previously been explained but the porosity changes with sintering atmosphere were also substantial.

Many of the Mixes showed increased porosity when a pure Nitrogen atmosphere was employed. In most of the pellets investigated the grains were spherical following sintering without oxygen which leads to inferior packing compared with that obtained with slightly angular grains. This suggests that the mechanism for forming angular grains is related to oxygen partial pressure during sintering.

The values of porosity between the pellet sizes seemed consistent even though the pellets had differing aspect ratios (diameter/thickness). The pressures generated during pressing are highly dependent on the aspect ratio. The dimensional changes of the smallest pellets (5.1mm pressed diameter) were most noticeable and required a great deal of subsequent polishing to obtain a shape suitable for density and electrical measurements. The changes of shape of the larger two pellets sizes were not as noticeable for all of the Mixes but some did show a slight decrease in radius at the centre thickness. This is due to the high densification of this region caused by low packing densities of the particles during pressing.

Fracture strength of all of the materials was measured using both Diametral Compression and Beam Tests. The results

obtained from the beam tests were always larger in magnitude, in some cases by as much as 100%, than the results from the tests loaded indirectly in compression. There are a number of reasons for this discrepancy.

In the beam tests considerable sample preparation was necessary which involved polishing and lapping of the surfaces to remove stress concentrators and surface stresses caused by the actions of sintering and machining, and thus lowering the number of stress concentrators acting.

The diametral tests can be susceptible to non-uniform loading contacts which were present on a number of samples following the dimensional changes occurring during the sintering process. Loading over a small area induces local failure and areas from which cracks may propagate and cause premature sample failure.

In the diametral test the stress is constant at its maximum value over a much greater surface area than for the four-point bend test. As surface pores are twice as damaging as internal pores of the same dimensions and that failure is almost always initiated from a pore, crack or other stress concentrator the increases in stressed area raises the probability of a large pore and so increases the likelihood of lower failure stresses in the diametral compression technique. In many of the in-service conditions to which PTC thermistors are subjected the values of strength required are when the maximum stress is

acting on the whole sample and thus diametral compression should give more representative results for PTC materials. However, with standard diametral compression techniques there is still a great deal of material which is not under the maximum stress value. To investigate this a short study was done which involved loading discs of Mix 1 over eight diameters ( $45^\circ$  between each) to a stress value of 50% of the average maximum value attained for that material to investigate failure originating from the largest pore. This resulted in failure of 40% of the samples indicating that the compression technique of measuring ultimate tensile stress can give overestimates. This study may have been influenced by cracking following loading prior to the one which caused ultimate failure however previous work has shown that the load would have to have been applied for a long duration to propagate cracks.

The Fracture Stress results for Mix 2 showed that for materials of low porosity the results from the two methods of testing are similar.

In many of the tests the values of strength were especially low for samples sintered in pure nitrogen. This is a reducing atmosphere which gives rise to problems with the dopant displacing Barium in the lattice which has been found to influence the electrical properties greatly. The liquid phase materials, especially silicon which is added in nitrate form may have trouble forming the phase in a reducing atmosphere

thus leading to a weaker structure. It is also possible that the Calcium and Lead Titanates require an oxidising atmosphere to filter into the Barium Titanate framework and the lack of oxidant may lead to areas of different properties and hence weakening of the structure. This was suggested by the electrical R-T plots which showed a lower switching temperature in the nitrogen only atmosphere compared with the other gaseous mixtures.

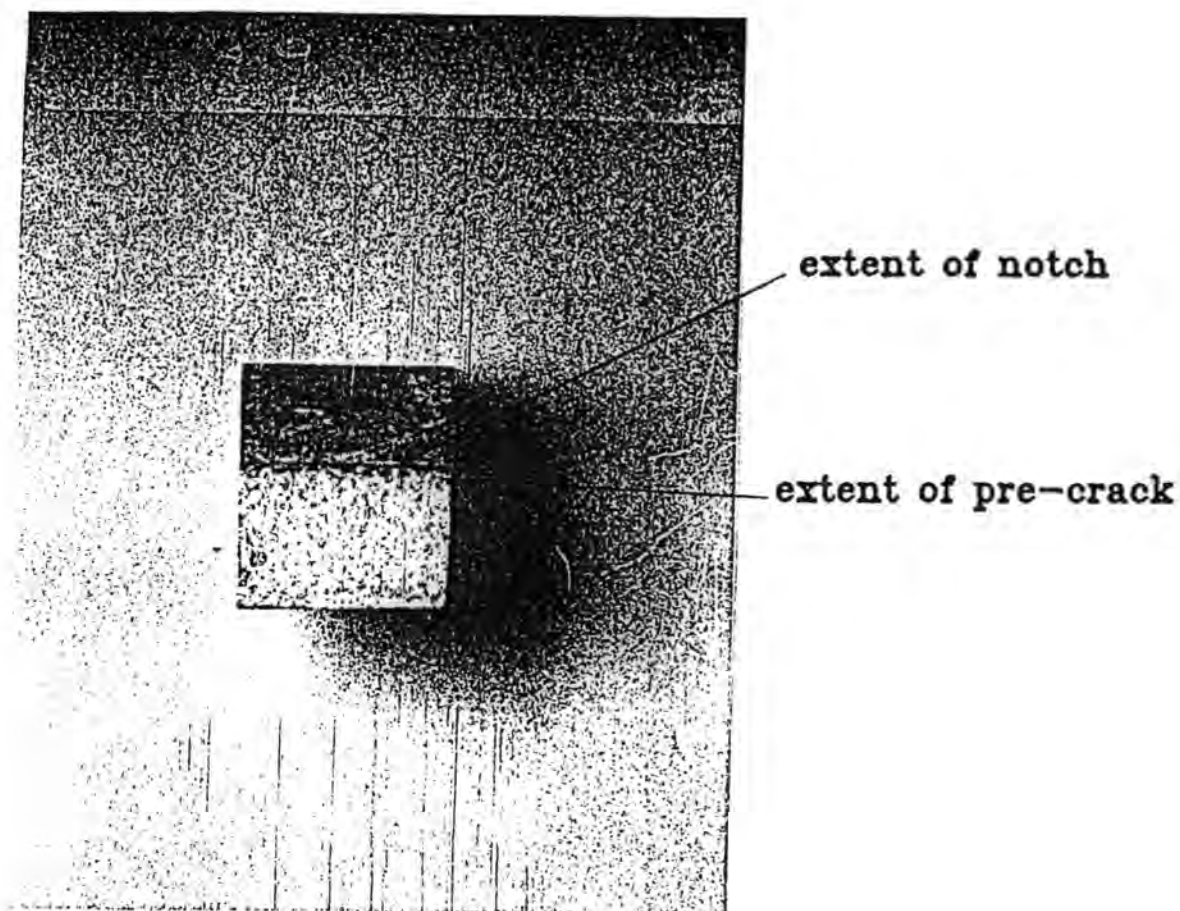
The Fracture Toughness values obtained from the Four-Point Bend Tests on the notched beams provided consistent results with a points scatter of only about 12% for each of the mixes.

Beams made from a model brittle material, PMMA (polymethylmethacrylate) were initially used to assess the degree of precracking required. Preliminary results suggested that the act of machining was sufficient to induce the required stress concentrator (Figure 51). PMMA has a similar fracture toughness value to Barium Titanate at about  $1.3\text{MPam}^{1/2}$  and so these tests were deemed to be relevant. The extent of the pre-cracking was also measured for the Barium Titanate beams after failure illuminating the cracks with dye and similar results were obtained.

The change in the fracture toughness with sintering atmosphere showed a similar trend to the results of ultimate tensile stress. However Mixes 3 & 4 showed particularly low values for



**Figure 51 : The pre-cracking caused by the action of machining a notch in a PMMA beam**



the nitrogen sintered samples. This tends to confirm the above suggestion that the Calcium and/or Lead are unable to diffuse into the structure reducing the mechanical properties. Mixes 1 & 2 showed a decrease when the nitrogen atmosphere was used but the change was not as great as the other two Mixes. Neither Mix 1 nor 2 contained Calcium or Lead.

The Vickers Indentation Test gave values of Fracture Toughness between 50 and 100% higher than the notched beam tests. These results made use of the empirical formula derived by Evans and Charles which was originally obtained from experimental tests on Silicon Carbide and Alumina Ceramics. Barium Titanate exhibits a value of Fracture Toughness of less than half that of the above materials and this could be a reason for the poor correlation of the results between the tests. However a number of other possibilities exist. In the papers which have been referenced there is no indication of the degree of penetration of the cracks through the material which can be tolerated. The samples of Barium Titanate exhibited crack/thickness ratios of between 0.20 & 0.35 under Vickers Indentation. The effect of the lower surface on crack propagation may be to provide a barrier to further extension of the cracks and hence lead to higher toughness values. It is also likely that the Four-Point Bend Tests may be affected by the pores within the material. The tests carried out by Evans & Charles on ceramics made use of materials of low porosities (<3%). The use of higher porosity materials (such as the PTC Mixes 1,3 & 4) would have

tended to reduce the values obtained from the bend tests but leave the indentation tests largely unaffected.

However, during early studies it was noticed that no cracks seemed evident at loads below 9kgf for the Titanate samples. This was not evident in the experiments of the other researchers as the formulae do not specify a value for the minimum loads. The fact that Barium Titanate required a measurable load to initiate cracks from the corners of the diamond indenter which is only a stress concentrator means that the loads required to drive the crack was only about 55% of the values used in the calculations. In Evans & Charles' formula fracture toughness is related to Hardness<sup>0.6</sup>. This corresponds to an identical relationship to load which equates to a reduction in fracture toughness of approximately 40% if the load required to extend the crack is used. This would bring the values of fracture toughness obtained from the two techniques much closer together.

It was discovered that cracks present in the "green" sample are largely unaffected by the sintering process and reveal similar sized pores in the fired component. This can be used to assess fracture toughness values for the "green" state.

Failure of "green" pellets is dependent on fracture toughness as a crack initiated at a pore or other stress concentrator grows and causes failure. The porosities of all of the "green"

pellets were in the region of 45%, much higher than for the sintered samples, and so it can be expected that toughness plays an important role. The fracture toughness of the pressed pellets was calculated using the data obtained from sintered samples of the same Mix.

The results show a large variation in fracture toughness. However considering the properties of a powder which presses well these results may be explained.

A successful pressing process depends on powder agglomerate size and hardness as well as the characteristics of the die. It is required to compress the agglomerates breaking them into small grains which conform in shape to each other instead of crushing the material into a very fine and highly porous powder. A softer agglomerate tends to be preferable and also tends to be broken into a range of grain sizes which should provide better packing than hard agglomerates.

The advantage of the die lubricant was apparent by the 100% strength increase in strength and fracture toughness. However the change which occurred when the binder was added during the milling stage was startling. This simple action which has the added advantage of reducing laboratory preparation time provides a more even coating of each grain and not just each agglomerate and resulted in a 150% strength increase.

The pressing process at Durham which relied on slow compaction lead to an increase in strength over the Elmwood shock compacted pellets. The use of a high rate tends to lead to crushing in some of the grains and a degree of fusion but there are frequent sites of loosely bonded material and large damaging pores. A slower compaction rate allows for re-organisation of the material prior to breakdown of the agglomerates, allows for air to be more effectively dispelled and reduces the incidences of crushing of the grains.

Mixes 1 and 2 were both observed to contain harder agglomerates (possibly due to the absense of the Lead and Calcium Titanates) and the effect of this was observed in the reduced "green" strength and fracture toughness of both Mixes. The Cookson "low purity" material showed an increase in strength compared with the "high purity" material. It is likely that the impurities contribute to the softer agglomerate which is pressed more successfully.

### 6.3 Electrical Testing

The description of the electrical properties of PTC devices must not be restricted to which material shows the largest resistance change. In Section 1 the applications in which PTC materials are used depend on a number of parameters. For example if a device was required to measure temperature over a wide range of say 150 to 300°C then Mix 2 sintered in a 60% N<sub>2</sub> 40% O<sub>2</sub> atmosphere would be a good choice because of the constant gradient of the R-T Plot. However, the same characteristics would be of little use in a protection device.

The effects of the additives to Barium Titanate on the electrical properties were investigated by testing the materials following sintering in flowing air.

The effect of Lead Titanate was clearly seen by the difference in the switching temperatures of the Mixes. Lead Titanate has a Perovskite structure similar to Barium Titanate which shows a Cubic to Tetragonal transformation at its Curie Temperature. However, the Curie Temperature is 500°C above that of Barium Titanate and so by adding a proportion of Lead the Curie Temperature of the mixture can be raised.

Calcium Titanate acts as a grain refiner and as such more regular grains were expected from Mixes 3 & 4. Figure 42 & 43 show that there was more homogeneity in the grain sizes of Mixes

3 & 4 compared with Mix 1, but this was minimal. There was no measurable change in the PTC effect on addition of the Calcium Titanate.

Mix 1 contained a smaller amount of Holmium than Mixes 3 & 4 but the Resistance-Temperature Plots showed similar PTC effects between all of the Mixes over the range of sintering atmospheres. This suggests that the proportion of Holmium used in the production Barium Titanate Mix is unnecessarily large and the same PTC effects could be obtained with reduced amounts. This could represent a major saving as at present the Holmium accounts for about a third of the total material cost.

The results from the samples sintered in the 100% Nitrogen atmosphere show the importance of an oxidising atmosphere in the production of PTC devices. The performance of the materials after annealing in air was similar to those samples sintered in air revealing that the changes which occur when sintering takes place in pure nitrogen are reversible.

The oxidising atmosphere is required to allow the materials such as Holmium and Lead to infiltrate the Barium Titanate lattice. The effect of the Holmium in determining the extent of the PTC effect can easily be seen but the effect of the Lead Titanate is noticed as a slight lowering of the switching temperature. As these two materials are important in

determining the PTC effect a sample exhibits reducing atmospheres must be avoided.

Atmospheres with a higher proportion of oxygen than air were investigated but there seemed little change in the PTC effect. Thus it can be deduced that the air atmosphere is sufficiently oxidising to obtain the best PTC results for the Mixes investigated.



#### 6.4 FUTURE WORK

It would be beneficial to investigate the following areas of research to obtain a more accurate and comprehensive picture of Barium Titanate ceramics and their mechanical limitations.

1. Mechanical strength at elevated temperatures.
2. Strength degradation during temperature cycling (thermal fatigue).
3. Techniques to identify voids by non destructive testing.
4. Changes that can be made in the pressing process to reduce the residual stresses present after firing.
5. Quench testing of ceramics in liquid or gaseous media to determine the ultimate thermal stresses that could be tolerated. A variation of this technique could involve placing the sample into a warmer liquid, allowing strength to be investigated under both internal and surface loading. Potential advantages of this technique are that the stresses produced are constant over the surface (or internally) and so scatter of results should be low. Also, by using thermal testing, this more closely simulates the in service conditions of the pellets as temperature sensors, protection devices or heating elements. With this technique it will also be possible to test a number

of samples under exactly the same conditions improving the accuracy of sample group comparison. Should this technique prove successful it is possible that it could be implemented as a production line quality control test as crack growth without failure of the pellets is small and so degradation of the samples caused by the test is eliminated.

## 7.0 CONCLUSIONS

The stages of the production process of a Ceramic PTC were investigated to assess which were the most critical in the formation of a mechanically strong and tough PTC.

Milling time was found to be largely unimportant in terms of mechanical strength and the act of increasing milling time increases the contamination from milling vessel and media.

The use of Calcined laboratory prepared Barium Titanate significantly increased the strength and toughness of the Ceramic when compared with commercially available material. This was because of a large reduction in porosity with values of 2% being typical. However, the electrical properties of this material were found to be less impressive than other PTC materials.

Pressing pressures must be high enough to provide the "green" pellets with sufficient strength to allow easy movement between the Press and Furnace but must not be too high as to promote crack formation. Cracking of pellets is reduced by the use of a die lubricant and binder or increased moisture content within the powder. It was also found that a high aspect ratio, diameter/thickness, reduced the tendency for cracks within the "green" material. The formation of cracks at the higher

pressures lead to lower mechanical strength but lower porosities.

Making use of the milling stage for the addition of the binder to the mix was shown to produce a stronger compact and a much less porous and stronger sintered material. The Elmwood technique of binder and die lubricant addition resulted in fired pellets with porosities and strengths between the two techniques investigated in the research laboratories at Durham.

The Elmwood pressing technique resulted in weaker "green" samples but improved sintered strength and porosity and the samples sintered in the production furnace also showed improved mechanical properties and porosities over those sintered at Durham.

The low purity material showed similar mechanical properties to the high purity Barium Titanate but a lower porosity owing to the larger amounts of liquid phase present.

Diametral Compression was shown to give consistent results when concave loading anvils were used but lower values of Ultimate Tensile Stress than those obtained from Four-Point Bend Tests. The technique was also successfully applied to "green" pellets.

The use of the Vickers Indentor to measure Fracture toughness was investigated and comparisons with Notched Four-point Bend

Tests showed that the technique yielded consistent results. However, results were up to 90% higher using Evans and Charles' Formula (Evans & Charles, 1976) when compared with the bend tests. Values of  $2.1\text{MPam}^{1/2}$  for the Indentation and  $1.3\text{MPam}^{1/2}$  for the Bend Tests were measured for Mix 4 which compares with values of  $4.0\text{MPam}$  for Alumina, one of the toughest ceramic materials. During the Notched Beam Tests pre-cracking from the initial notch was investigated and found to be unnecessary due to the damage from the notch machining operation. From the Vickers Indentation Tests it was noted that at loads less than 9kgf little cracking was evident; a previously unrecorded phenomenon for ceramics.

The Sintering Atmosphere was found to have little effect on the mechanical or electrical properties at oxygen partial pressures above 0.2 bar. However, at lower oxygen partial pressures the PTC characteristics were subdued as were the mechanical strength and toughness especially for Elmwood Mixes 3 and 4. It was found that annealing in air restored the electrical properties to normal values of a three order of magnitude resistance change and a switching temperature of  $180^{\circ}\text{C}$  for Mixes 3 and 4.

## References

- Agbarakwe, U.B., Banda, J.S. & Messer, P.F. (1989) "Non Uniformities and Pore Formation", Materials Science and Engineering **A109** 9-16.
- Al-Allak, H.M., Parry, T.V., Russell, G.J., Woods, J. (1988) "Effects of Alumina on the electrical and mechanical properties of PTCR Barium Titanate Ceramics as a function of sintering temperature: Part 1 Electrical Behavior", J.Mat.Sci. **23** 1083-89
- Almond, E.A., Roebuck, B. & Gee, M.G. (1986) "Mechanical Testing of Hard Materials", Metals & Materials **February 1986** 76-82.
- Cook, R.F., Freiman, S.W., Lawn, B.R. & Pohanka, R.C. (1983) "Fracture of Ferroelectric Ceramics", Ferroelectrics **Vol 50** 267-272.
- Evans, A.G. & Charles, E.A. (1976) " Fracture Toughness determinations by indentation", J.Amer.Ceram.Soc. **59 [7-8]** 371-372.
- Fang, T.T. & Hsieh, H-L. (1989) "Effects of powder processing on the green compacts of high purity Barium Titanate", J.Amer.Ceram.Soc. **72 [1]** 142-145.
- Gerthson, P. & Hardtl, K.H. (1963) "Method for Proof of Inhomogenity of Conduction at Grain Boundaries", Z.Naturforsch **18a** 423-429.
- Goodman, G. (1963) "Electrical Conductivity Anomaly in Samarium-Doped Barium Titanate", J.Amer.Ceram.Soc. **46 January** 48-52.
- Heintz, J.M., Weill, F. & Bernier, J.C. (1989) "Characterisation of Agglomerates by Ceramic Powder Compaction", Materials Science and Engineering **A109** 271-277.
- Heywang, W. (1964) "Resistivity Anomaly in Doped Barium Titanate", J.Amer.Ceram.Soc. **47 October** 484-488.
- Heywang, W. (1971) "Semiconducting Barium Titanate",

J.Mater.Sci. **6** 1214.

Irwin, G.R. (1957) "Analysis of Stresses and Strains near the end of a crack traversing a plate", J.Appl.Mech. **24** 361.

Jonker, G.H. (1964) "Some aspects of Semiconducting Barium Titanate", Solid State Electronics **7** 895-901.

Kahn, M. (1971) "Preparation of small grained and large grained ceramics from Nb-doped Barium Titanate", J.Amer.Ceram.Soc. **Vol.54 No.9** 452-454.

Kamiya, N. & Kamigaito, O. (1989) "Thermal Fatigue life of glass subjected to air blast quenching", J.Mat.Sci. **24** 2461-66.

Kellett, B.J. & Lange, F.F. (1989) " Thermodynamics of Densification Part I: Sintering of simple particle arrays, equilibrium configurations, pore stability and shrinkage", J.Amer.Ceram.Soc. **Vol.72 No.5** 725-734.

Kuwabara, M., Suemura, S. & Kawahara, M. (1985) "Preparation of High Curie-Point Barium-Lead Titanates and their PTCR Characteristics", Am.Ceram.Soc.Bull. **64 (10)** 1394-1398.

Lankford, J. (1982) "Indentation Microfracture in the Palmqvist crack regime: Implications for fracture toughness evaluation by the indentation method", J.Mat.Sci.Letters **1** 493-495.

Lawn, B.R. & Swain, M.V. (1975) "Microfracture beneath point indentations in brittle solids", J.Mater.Sci. **10** 2016-2024.

Leiser, D.B. & Whittlemore (Jr), O.J. (1970) "Compaction Behavior of Ceramic Particles", Ceramic Bulletin **Vol.49 No.8** 714-717.

Long, W.M. (1960) "Forces developed during compaction of powders", Powder Metallurgy **6** 73-78.

Lubitz, K. (1982) "Development of the microstructure of semiconducting Barium Titanate Ceramics", Materials Science Monographs **Vol.14** 343-348.

Macleod, H.M. & Marshall, K. (1977) "The determination of density distributions in ceramics compacts using autoradiography", Powder Technology **16** 107-122.

- Matsuo, Y. & Sasaki, H. (1971) "Exaggerated Grain Growth in Liquid-Phase Sintering of Barium Titanate", J.Amer.Ceram.Soc. **Vol.54 No.9** 471.
- Matsuoka, T., Matsuo, Y., Sasaki, H. & Hayakawa, S. (1972) "PTCR Behavior of Barium Titanate with Nb & Mn Additives", J.Amer.Ceram.Soc. **55** 108.
- Michuie, M., Igarashi, H. & Okazaki, K. (1986) "Measurement of Internal Stress in PTC Ceramics", J.Amer.Ceram.Soc. **69** [1] 110-112.
- Morrell, R. (1989) "Mechanical Testing of Engineering Ceramics: Test Bars versus Components", Materials Science & Engineering **A109** 131-137.
- Nelson, K.E. & Cook, R.L. (1959) "Effect of contamination induced during wet milling on the electrical properties of Barium Titanate", Ceramic Bulletin **Vol.38 No.10** 499-501.
- Niihara, K., Morena, R. & Hasselman, D.P.H. (1982) "Evaluation of Fracture Toughness of brittle solids by the indentation methods with low crack-to-indent ratios", J.Mater.Sci.Letters **1** 13-16.
- Palmqvist, S. (1962) "Occurrence of crack formation during vickers indentation as a measure of the toughness of hard materials", Arch.Esienhuttenwes **33** 629-633.
- Rehme, H. (1966) "Detection of Barrier Layers in Barium Titanate by Electron Microscopy", Phys.Stat.Sol. **18** K101.
- Sauer, H.A. & Flaschen, S.S. (1956) "Positive Temperature Coefficient of Resistance Thermistor Materials for Electrical Applications", Proc. 7th Electronics Symp., Washington 41.
- Shirane, G., Jona, F. & Pepinski, R. (1955) "Some Aspects of Ferroelectricity", Proc. IRE **43** 1738-1746.
- Thompson, R.A. (1981) "Mechanics of Powder Pressing: I Model for Powder Densification II Finite Element Analysis of End-Capping III Model for Green Strength of Pressed Powders", Ceramic Bulletin **Vol.60 No.2** 237-251.



- Ueyama, T., Yamana, S. & Kaneko, N. (1987) "Sintering properties of Barium Titanate Green Sheets with high packing density", Japanese J.of App.Physics **26 Supp.26-2** 139-141.
- Van den Avyle, J.A. & Mecholosky, J.J. (1983) "Analysis of soldering induced cracking of Barium Titanate Ceramic Capacitors", Ferroelectrics **Vol. 50** 293-298.
- Westergaard, H.M. (1939) "Bearing Pressures and Cracks", J.Appl.Mech. **61** A49.
- de With, G. & Parren, J.E.D. (1984) "Surface Stresses in Modified Barium Titanate Ceramics", Proc.Brit.Ceram.Soc. **34** 99-108.
- Youshaw, R.A. & Halloran, J.W. (1982) "Compaction of Spray-Dried Powders", Ceramic Bulletin **Vol.61 No.2** 227-230.
- Xue, L.A. & Brook, R.J. (1989) "Promotion of Densification by Grain Growth", J.Amer.Ceram.Soc. **Vol.72 No.2** 341-344.
- Zajc, I. & Drofenik, M. (1989) "Grain Growth and Densification in Donor-Doped Barium Titanate", Brit.Ceram.Trans. **Vol.88 No.6** 223-226.

### General References

Bradt, R.C., Hasselman, D.P.H. & Lange, F.F. (Eds) (1978) "Fracture Mechanics of Ceramics Vol.3: Flaws and Testing and Vol.4: Crack Growth and Microstructure", Plenum Press, New York

Freiman, S.W. & Fuller, J.R. (Eds) (1981) "Fracture Mechanics of Ceramics, Rocks & Concrete", ASTM STP745 Baltimore.

Johns, D.J. (1965) "Thermal Stress Analysis" Pergamon Press, London pp.35-38.

Lawn, B.R. & Wilshaw, T.R. (1975) "Fracture of Brittle Solids" Cambridge Uni. Press, London Chapters 2, 3 & 6.

Liebowitz, H. (Eds) (1968) "Fracture Vol.I: Microscopic and Macroscopic Fundamentals & Vol.VII: Fracture of Non-Metals and Composites", Academic Press Inc., New York.

Manson, S.S. (1966) "Thermal Stress and Low Cycle Fatigue" McGraw-Hill New York pp.1-5 & 276-300.

Taplin, D.M.R. (Ed) (1978) "Advances in Research on the Strength and Fracture of Materials Vol.I: An Overview", Pergamon Press, New York.

Warke, W.R., Weiss, V. & Hahn, G. (Eds) (1976) "Properties Relating to Fracture Toughness", ASTM STP605 Baltimore.

## APPENDIX I

### Density Calculations of Doped Barium Titanate Ceramics

The density of pure Barium Titanate of zero porosity has been calculated by research groups to be  $6.01 \text{ g/cm}^3$ .

Barium Titanate when used as a PTC material requires small amounts of dopant to produce the PTC effect, materials such as Alumina which form the liquid phase and other Titanates to regulate the temperature at which the effect occurs. The Titanates produce the largest density change from the pure material owing to the large amounts often required to achieve the desired switching temperature. Barium (Ba) is effectively replaced in the structure by Lead (Pb), Strontium (Sr) or Calcium (Ca) which have differing atomic masses.

Element	Atomic Mass
Ba	137.3
Pb	207.1
Ca	40.2
Sr	88.0

The liquid phase materials are incorporated into the calculation by determining the amount of each used as a percentage of the total material mass, and the dopant is discounted because of the very small quantities used. The

calculations yield the following values of maximum theoretical density.

Part .I

All sample Groups	5.669 g/cm <sup>3</sup>
-------------------	-------------------------

Part .II

MIX 1	)	
	)	5.977 g/cm <sup>3</sup>
MIX 2	)	
	)	
MIX 3	)	
	)	5.817 g/cm <sup>3</sup>
MIX 4	)	